A review of Himalayan stratigraphy, magmatism, and structure

Aaron J. Martin (aaron.martin@ipicyt.edu.mx)

División de Geociencias Aplicadas, IPICYT, CP 78216, San Luis Potosi, S.L.P., MEXICO

Keywords: Himalaya; tectonics; suspect terrane; exotic terrane; Proterozoic Eon

ABSTRACT

The Himalayan Orogen consists of two rock packages that parallel the topographic trend of the mountain belt between the eastern and western syntaxes. To avoid confusion with appellations previously used to identify elevation, Cenozoic metamorphic grade, or Cenozoic structural position, in this paper I introduce new names for these rock packages: Himalayan Assemblage A and Himalayan Assemblage B. Inclusion in an assemblage signifies that there was physical contiguity between adjacent members of the assemblage at the time of deposition or intrusion. Assemblage A and Assemblage B may not have shared depositional or intrusive relationships prior to Early Cretaceous time.

Himalayan Assemblage A mostly consists of sedimentary rocks deposited on the northern margin of India; the depositional substrate for these strata is not exposed anywhere in the orogen. Assemblage A comprises three main groups of rocks divided based on age of deposition or intrusion: Paleoproterozoic to Early Mesoproterozoic, Late Carboniferous to Permian, and terminal Cretaceous to Pleistocene. The oldest rocks exposed in the Himalaya, ca. 1900-1800 Ma clastic deposits and the ca. 1880-1830 Ma granite and gabbro that intruded them, may have formed in a continental rift setting. This rift system established depositional strike toward the northeast, at a high angle to the strike of Cenozoic thrusts in the western Himalaya, with obliquity decreasing eastward. The succeeding Upper Paleoproterozoic to Lower Mesoproterozoic strata were deposited in a passive margin setting or, alternatively, in an epi-cratonic basin. Upper Carboniferous to Permian strata are called the Gondwana Group; these deposits are present only in the eastern half of the orogen. This package is dominantly clastic and probably was deposited in extensional basins related to the breakup of Pangea. Depositional strike of the Gondwana Group was likely between 25 and 50 degrees west of north. Upper

Paleocene to Pleistocene, dominantly clastic, strata were deposited in the Himalayan foreland basin. Along the central two-thirds of the orogen, depositional age uncertainties extend the possible depositional ages of the lowermost of these strata into the latest Cretaceous Period. If the lowermost strata of this package were deposited only in the Paleogene Period, they may be earliest Himalayan foreland basin strata, in contrast to current interpretations that formation of their depositional basin was unrelated to the Cenozoic Himalayan orogeny. Depositional strike paralleled the strikes of the Cenozoic Himalayan thrusts.

Between the syntaxes, most Pliocene to Holocene Himalayan thrust faults are contained in Assemblage A rocks. Most of these Pliocene to Holocene thrusts broke new paths through Assemblage A, they did not reactivate ancient high strain zones except possibly in the eastern Himalaya. The lack of reactivation in the western and central Himalaya may have resulted from unfavorable orientations of the ca. 1900-1800 Ma rift-related high strain zones relative to the direction of Cenozoic convergence. The Shillong Plateau is the only location between the syntaxes where deformation jumped far forward of the main thrust belt. There, the plateau-bounding Dauki Thrust is interpreted to have reactivated Cretaceous rift-related normal faults. The Dauki Thrust is broadly parallel to slightly oblique to nearby Paleoproterozoic normal-sense high strain zones. It is possible that these Paleoproterozoic normal-sense high strain zones were reactivated during both Cretaceous rifting and Cenozoic thrusting.

Salients and recesses in Himalayan frontal thrusts between the syntaxes have small amplitudes and wavelengths compared to their counterparts in many other Phanerozoic orogens. Three factors that contribute to these small map-view bends are: (1) The absence of a Mesozoic or Cenozoic magmatic arc and back-arc in the Himalayan foreland, in contrast to the northern Canadian Cordillera. (2) Unfavorable orientations of large stratigraphic thickness changes in the foreland, possibly except in the eastern Himalaya, in contrast to the Appalachian Orogen. (3) Unfavorable orientations of ancient high strain zones for reactivation, again possibly except in the eastern Himalaya, in contrast to the Appalachians.

Himalayan Assemblage B consists of Neoproterozoic to Pleistocene strata that were intruded by granite at ca. 880-800, 510-460, and 28-14 Ma. In northern Pakistan and northwestern India, granite also intruded at ca. 290-260 Ma, contemporaneous with deposition of Panjal Traps basalt in the western Himalaya. The possible depositional substrate for Assemblage B may be exposed only in a small area in northwestern India, where lowermost Assemblage B strata may have been deposited on the ca. 1850 Ma Baragaon granitic gneiss.

Himalayan Assemblage B satisfies all three parts of the definition of a suspect terrane: It has an internally consistent geologic history, its pre-Cretaceous geologic history differs significantly from the histories of neighboring rocks, and it is separated from neighboring rock packages by high strain zones. Himalayan Assemblage B may have been located north of western Australia from Neoproterozoic to Middle Jurassic time. During Late Jurassic to Early Cretaceous time, a system of left-handed transcurrent faults may have juxtaposed Assemblage B against rocks of the northern Indian Shield, including Assemblage A. The Miocene Main Central Thrust reactivated this transcurrent fault system and, between the syntaxes, continued to juxtapose Assemblage A and Assemblage B in its footwall and hanging wall, respectively. In this scenario, the Main Central Thrust does not repeat pre-Cretaceous stratigraphy because the footwall and hanging wall assemblages did not share depositional contiguity prior to the Early Cretaceous Epoch.

The Namche Barwa and Shillong Plateau/Mikir Hills areas have pre-Cretaceous geologic histories distinct from Assemblage A and Assemblage B and the pre-Cretaceous rocks of these two regions thus do not belong to either assemblage. The Namche Barwa and Shillong Plateau/Mikir Hills rocks were deformed, metamorphosed, and intruded in the Mesoproterozoic Era along with rocks of the Central Indian Tectonic Zone–Chhotanagpur Gneissic Complex–North Singhbhum Mobile Belt. The Namche Barwa and Shillong Plateau/Mikir Hills rocks additionally were affected by the late Ediacaran to Cambrian Kuunga Orogeny, as also recorded in the Eastern Ghats. Cambrian strata of eastern Assemblage A may have been deposited in a foreland basin in front of the Kuunga Orogeny, like similar-age deposits in the Shillong Plateau/Mikir Hills and Namche Barwa areas.

1. INTRODUCTION

Nearly 200 years of research has illuminated many aspects of Himalayan geology, and numerous summaries of this knowledge have been published over the past seventeen years (Hodges, 2000; Yin, 2006; Harris, 2007; Guo and Wilson, 2012; Hebert et al., 2012; Thakur, 2013; Bollinger et al., 2014; Dubey, 2014; Kohn, 2014; Acharyya, 2015; Dhital, 2015; Mukherjee, 2015; Bracciali et al., 2016; Chakraborty et al., 2016; 2017; Ding et al., 2017; Martin, 2017). This new review does not replicate these older synopses; instead, it seeks new insights into Himalayan tectonic evolution through comparisons with other Phanerozoic orogens. Although many aspects of Himalayan geology are quite similar to the tectonic features found in other Phanerozoic orogens, several key differences set the Himalaya apart. This review highlights three of these differences by addressing the questions listed in Subsections 1.2, 1.3, and 1.4 using a new integrated analysis of deposition, intrusion, and deformation.

Most interpretations of the Oligocene to Miocene tectonic evolution of the Himalayan Orogen focus on two major, if unusual, high strain zones (Figs. 1, 2, 3). At structurally high levels, geologists routinely interpret the South Tibet Detachment to consist of one or more normal-sense high strain zones (Herren, 1987; Cottle et al., 2007), even though the detachment repeats stratigraphy in many locations. Conversely, all workers interpret the Main Central Thrust (MCT) to be a foreland-vergent thrust (Webb, 2013; DeCelles et al., 2016), yet it does not repeat stratigraphy. These examples illustrate the types of tectonic issues I address in this review largely from the perspective of the stratigraphic and intrusive relationships within the two rock packages juxtaposed by the MCT.

1.1 A brief word on nomenclature

Current schemes for naming rock packages in the Himalayan Orogen are unwieldy because identical terms are used for four different concepts: elevation, structural position, metamorphic grade, and depositional or intrusive relationships. To avoid the confusion that results from using the same name for different classes of features, in this paper I use distinct names for these different concepts (Tables 1, 2). This subsection briefly states the terminology used throughout the article; Section 2 explains this naming system in detail.

The terms Low, Midlands, and High are used for modern elevation. Sub-, Lesser, Greater, and Tethyan Himalayan refer to Cenozoic structural position, with the addition that Tethyan Himalayan rocks reached lower Cenozoic peak metamorphic grade than did Greater Himalayan rocks. In this article I introduce new terms, Himalayan Assemblage A and Himalayan Assemblage B, to label rock packages that shared depositional or intrusive relationships that are still observable today.

1.2 Why are the bends in the Himalayan front so small?

Comparing the map-view topography of the entire Himalaya to either a topographic or a tectonic map of some other large Phanerozoic orogens highlights an unusual geologic characteristic of the Himalaya (Fig. 4). Whereas other Phanerozoic orogens typically contain foreland salients, recesses, or oroclines with map-view amplitudes up to 200-500 km and half-wavelengths up to 600-1200 km (ranges denote values from different orogens), the largest map-view bend in the front of the Himalaya between its syntaxes has an amplitude and half-wavelength of only about 20 and 160 km, respectively. Although not a bend in the frontal fault, there is a recess in interior high strain zones, including the MCT, in northwestern India (Figs. 2, 4C). This feature is the Kangra Recess. Like the frontal bends, the Kangra Recess is small, with an amplitude and half-wavelength of only 40 and 130 km, respectively. The front of the Shillong Plateau in the eastern Himalaya sits 180 km in front of the main part of the orogen between the eastern and western syntaxes (Figs. 1, 2, 4C, 5), but the frontal Himalayan thrust and the Dauki Thrust, which bounds the southern margin of the Shillong Plateau, apparently do not currently connect (Clark and Bilham, 2008; Islam et al., 2011; Berthet et al., 2014). This article examines causes of large salients and recesses in two other Phanerozoic fold-thrust belts and explains why these factors did not produce large bends in the Himalayan front between its syntaxes.

1.3 Why does robust evidence for inherited fault reactivation in the Himalaya indicate so little Cenozoic slip?

Reactivation of older structures inherited from a previous tectonic event is nearly ubiquitous in Phanerozoic orogens (references in Appendix D). In some orogens such as the Andes, Appalachians, and Atlas, inherited structures are a primary control on tectonic architecture across wide regions. In others such as the Alaskan and Canadian Cordillera, the magnitude of slip on reactivated high strain zones is minor and/or reactivation is limited to narrow sectors.

Along most of the Himalaya there is little evidence that reactivation of inherited high strain zones controlled the Cenozoic tectonic or depositional architecture. The clearest signal of renewed motion on pre-Cenozoic high strain zones comes from the foreland (e.g., Raiverman et al., 1994), but there the absence of outcrop and paucity of publicly available deep subsurface data means that robust high strain zone reactivation signatures such as sense-of-slip indicators or reversal of stratigraphic separation have not been documented in the peer-reviewed literature. Hindward of the Main Boundary Thrust, Cenozoic deformation mostly overprinted and obscured any pre-Cenozoic tectonic fabrics; consequently, such robust indicators of reactivation have not been found at structurally higher positions either. Instead, suggestions of reactivation of hinterland high strain zones mostly depend on inferences from stratigraphic correlations and regional tectonic analysis as well as interpretations of sediment provenance (e.g., Brookfield, 1993; DeCelles et al., 2000; Yin, 2006). The current paper surveys factors that promoted reactivation of ancient high strain zones in other Phanerozoic fold-thrust belts and assesses why these influences may not have been as effective at stimulating high strain zone reactivation in the Himalaya.

1.4 What was the pre-Cenozoic tectonic history of the lithotectonic units of the Himalaya?

Another difference between the Himalaya and most other orogens concerns the origins and positions of major tectonic blocks prior to orogeny. The location of the northern half of the Himalaya (Himalayan Assemblage B, Table 1) prior to Cenozoic collisional orogeny is poorly known (Fig. 6). Jain and Kanwar (1970) hypothesized that Neoproterozoic to Cretaceous Assemblage B strata were deposited at least 5000 km north of the northern margin of the Indian continent. In this model, Himalayan Assemblage B accreted to the northern edge of India during the Cenozoic Era as India drifted northward (see also Sinha-Roy, 1976). In contrast, other geologists postulated that Himalayan Assemblage B strata were deposited on or near the northern margin of India beginning in the Neoproterozoic Era (Wadia, 1919; 1939; Colchen et al., 1982; Searle, 1986; Brookfield, 1993; DeCelles et al., 2000; Gehrels et al., 2003; Myrow et al., 2003; DiPietro and Pogue, 2004; Yin, 2006; Yin et al., 2010a). Brookfield (1993) modified this scenario by arguing for approximately 1000 km of Late Jurassic-Early Cretaceous left-handed transcurrent motion of Assemblage B rocks relative to Assemblage A and cratonal India.

Regardless of their pre-Cenozoic origin, geologists additionally are uncertain how far north of their current position Assemblage B rocks were immediately prior to slip on Cenozoic Himalayan thrusts. When palinspastically restoring the location of Assemblage B, geologists are forced to use a minimum estimate of about 100 km north of its current location (relative to directly underlying Assemblage A rocks) based on the mapped distance of thrusting of Assemblage B over Assemblage A along the MCT (Schelling and Arita, 1991; Srivastava and Mitra, 1994; DeCelles et al., 1998a; 2001; Robinson et al., 2006; Yin et al., 2010a; Long et al., 2011a; 2012; Khanal and Robinson, 2013; Webb, 2013; Robinson and Martin, 2014; DeCelles et al., 2016). Reversing the minimum 100 km of MCT offset restores the southern edge of Assemblage B to a position directly adjacent to the northern limit of Assemblage A at the dawn of the Cenozoic Era. In contrast, Sinha-Roy (1976), Fuchs and Willems (1990), van Hinsbergen et al. (2012), and Huang et al. (2015a) advanced a modified version of the Jain and Kanwar (1970) model. The latter three articles argued that Assemblage B sat about 2500 km north of the northern edge of India at 66 Ma, not because Assemblage B strata initially were deposited that far north of the northern Indian margin as in the Jain and Kanwar (1970) model, but due to Cretaceous northward rifting of Assemblage B rocks away from India. The main support for this idea came from paleomagnetic results from supracrustal rocks that indicated that the paleolatitudes of Assemblage B and cratonal India were nearly identical at ca. 118 Ma, but Assemblage B was 2675 ± 700 kilometers north of cratonal India at ca. 66 Ma (values taken from the compilation of paleomagnetic data in van Hinsbergen et al., 2012). The Cretaceous northward rifting interpretation implies that Assemblage B restores much farther north than assumed in palinspastic reconstructions of the pre-Cenozoic geometry of the northern Indian margin based on the mapped distance of thrusting of Assemblage B over Assemblage A.

Unlike the Himalaya, in most other Phanerozoic continental mountain belts the pre-orogenic positions of major crustal blocks are known and motion of these blocks provides a framework for understanding the tectonic development of the orogen. For example, in the Appalachian Orogen it is now accepted that the Suwannee, Carolinia, Ganderia, Avalonia, and Meguma terranes formed near Gondwana in Neoproterozoic to early Ordovician time and accreted to the eastern margin of Laurentia during the Ordovician to Carboniferous periods (Pollock et al., 2012). Accretion of these terranes provides a foundation for understanding the early to middle Paleozoic tectonic evolution of the Appalachians. Exotic terranes likewise are recognized along strike in the Caledonian orogen (Pollock et al., 2012; Agyei-Dwarko et al., 2012; Augland et al., 2013) and Mexico (Keppie et al., 2012). Similarly, the locations of major crustal blocks prior to orogeny are well recorded in other major Phanerozoic continental orogens around the world (Appendix D). As in the Appalachians, interactions between blocks exerted first-order control on the tectonic development of these orogens. This paper examines evidence that Himalayan Assemblage B is a suspect terrane, and further, that it was exotic to India prior to Late Jurassic-Early Cretaceous time.

1.5 What was the structural history of the South Tibet Detachment?

The South Tibet Detachment is possibly a globally unique high strain zone (Figs. 2, 3). Most geologists interpret it as a system of gently hinterland-dipping high strain zones that accommodated top-to-the-hinterland extension (e.g., Powell and Conaghan, 1973; Seeber and Armbruster, 1981; Caby et al., 1983; Burg et al. 1984; Herren, 1987; Burchfiel et al., 1992; Searle et al., 1997; Cottle et al., 2007; Searle, 2010; Kellett and Grujic, 2012; Schultz et al., 2017; see also Corrie et al., 2012). The detachment separates Tethyan from Greater Himalayan rocks and in some locations it appears that the more metamorphosed footwall rocks are direct equivalents of the lower-grade hanging wall metasedimentary rocks. DiPietro and Pogue (2004) reached this conclusion for high-grade and lower-grade rocks in northern Pakistan and northwestern India, for example (see also Herren, 1987). In northeastern Pakistan, Greco et al. (1989) and Papritz and Rey (1989) related Greater Himalayan amphibolite and meta-clastic rocks to the Tethyan Himalayan Panjal Traps and Paleozoic clastic strata, respectively. In the Zanskar region, Honegger et al. (1982) similarly correlated Greater Himalayan amphibolite and marble with the Tethyan Himalayan Panjal Traps and Mesozoic limestone, respectively, and Searle et al. (1992) and Walker et al. (2001) supported the correlation between Greater and Tethyan Himalayan strata. The Panjal Traps were the protolith for eclogite in the northwestern Himalaya (Spencer et al., 1995; Luais et al., 2001; Kouketsu et al., 2017), supporting the link between the Panjal Traps and equivalents at higher metamorphic grade. Farther southeast in northwestern India, the lowermost Tethyan Himalayan unit, the Haimanta Group, is interpreted to be the protolith for the Greater Himalayan rocks (Myrow et al., 2003; Steck, 2003; Webb et al. 2011a; Webb 2013). In the Annapurna Range of central Nepal, South Tibet Detachment footwall meta-clastic Unit I and meta-carbonate Unit II are correlated with the hanging wall siliciclastic Sanctuary and carbonate Annapurna Yellow formations, respectively (Le Fort, 1975; Gehrels et al., 2003; Searle, 2010). McQuarrie et al. (2013) used detrital zircon U/Pb ages and other data to show that, in Bhutan, the stratigraphically upper Greater Himalayan metasedimentary unit and the lowest Tethyan Himalayan formations were deposited contemporaneously and received sediment from the same sources. These shared provenance and depositional histories suggest that the Bhutanese upper Greater Himalayan metasedimentary unit could be correlative with the Tethyan Chekha Formation and basal Pele La Group.

Slip on an extensional high strain zone that dips more gently than bedding repeats stratigraphic section across the high strain zone when viewed in the vertical plane, and this geometry is one possible explanation for the repeated stratigraphy across the South Tibet Detachment. However, except for the South Tibet Detachment, I cannot find a real-world example of such a geometry for extensional high strain zones with more than 10 km offset. That is, if the South Tibet Detachment were simply an extensional high strain zone, it would be the only known extensional high strain zone with more than 10 km offset that repeated stratigraphic section. Although Druschke et al. (2009) and Surpless (2010) mentioned stratigraphy repeated by normal faults in Nevada, western USA, both articles were describing the map pattern of similar stratigraphic units exposed in a horizontal section through multiple normal fault-bounded blocks. These faults omit stratigraphy in cross-sectional view (see cross-sections in Druschke et al., 2009, their Fig. 7 and Surpless, 2012, their Fig. 3).

Interpreting thrust-sense motion on the South Tibet Detachment provides a resolution to the uniqueness conundrum. Gehrels et al. (2003) suggested that the detachment was a thrust in late Cambrian to early Ordovician time that was reactivated as an extensional high strain zone during the Cenozoic Himalayan orogeny, whereas numerous other articles argued for initial foreland-directed thrusting during early stages of Cenozoic Himalayan development (McElroy et al., 1990; Gapais et al., 1992; Spring and Crespo-Blanc, 1992; Jain and Manickavasagam, 1993; Patel et al., 1993; Vannay and Hodges, 1996; Dezes et al., 1999; Vannay and Grasemann, 2001; Walker et al., 2001; Wiesmayr and Grasemann, 2002; Neumayer et al., 2004; Yin, 2006; Dubey, 2014; Finch et al., 2014; see also Powell and Conaghan, 1973; Searle et al., 1997). Seeber and Armbruster (1981) showed the South Tibet Detachment connected to the high strain zones of the Indus-Yarlung Suture in the central Himalayan hinterland and Caby et al. (1983) showed the

South Tibet Detachment joining the MCT in the up-dip, foreland direction in central Nepal. Yin (2006) combined these three ideas and proposed that following an initial stage of Paleogene foreland-vergent thrusting, the South Tibet Detachment reactivated as a hinterland-directed backthrust that branched from the MCT and was geometrically and kinematically tied to the hinterland-vergent Great Counter Thrust within the Indus-Yarlung Suture (Fig. 3C). I do not discuss the reactivation and backthrust interpretations for the South Tibet Detachment further in this paper because these ideas have received ample attention in recent articles (Webb et al., 2007; 2011a; 2011b; 2013; Corrie et al., 2012; Leger et al., 2013; Montomoli et al., 2013; Robyr et al., 2014; Cottle et al., 2015; He et al., 2015; 2016; Horton et al., 2015; Khanal et al., 2015a; Yu et al., 2015; Schultz et al., 2017; see also Burchfiel and Royden, 1985 and Mukherjee, 2013; note that Beaumont et al., 2001, Larson et al., 2010, and Larson and Cottle, 2014 also showed the structural top of the Greater Himalayan rocks as a backthrust in early stages of their tectonic evolution models, though none of these articles used the term explicitly).

2. DEFINITION OF TERMS AND GEOLOGIC FRAMEWORK

Throughout the article I use the general term “high strain zone” to refer to offset by both brittle and ductile processes because distinguishing deformation mechanisms is not important for the conclusions. All high strain zones, ductile and brittle, comprise a volume of strained rock (e.g., Childs et al., 2009; Platt and Behr, 2011; Rennie et al., 2013; Sullivan et al., 2013). I follow convention in drawing locations of high strain zones on maps and cross-sections at the approximate position of most intense strain. I do not show the boundaries of the volume of strained rock, unlike Searle et al. (2008; see criticism in Yin et al., 2010a; Webb et al., 2013; and Martin, 2017). All compass directions throughout the article are given using present-day orientations, though it is important to keep in mind that India as well as Himalayan Assemblage B rotated in map view over the 2000 M.y. covered in this review (Li et al., 2008; Seton et al., 2012; Kaur et al., 2013; Torsvik and Cocks., 2013). Repeated stratigraphic section is defined along a conceptual line that both is contained in the vertical plane and parallels a line that bisects the obtuse angle between bedding and the high strain zone. When discussing the South Tibet Detachment, I use the term "extensional high strain zone" instead of "normal-sense high strain zone" to exclude overturned thrusts (e.g., Balkwill, 1972). "Depositional dip" is the magnitude and direction of the gentle incline of beds at the time of deposition (i.e. prior to post-depositional deformation); the trend of the depositional dip thus is nearly identical to the direction of regional sediment transport. "Depositional strike" is the trend of a horizontal line perpendicular to the depositional dip and contained in a bedding plane.

The Main Frontal Thrust and the Indus-Yarlung Suture form the frontal and rear boundaries of the Himalayan Orogen, respectively (Fig. 2; Gansser, 1983). To the west, the boundary of the orogenic system is the left-slip Chaman Fault and to the east, it is the right-slip Sagaing Fault (Yin, 2006). Although the orogen extends beyond the Himalayan syntaxes, this review focuses on the part between the syntaxes. Like Yin (2006), I include the Shillong Plateau and Mikir Hills in the Himalayan Orogen because these uplands are kinematically and dynamically linked to the main part of the orogen (Fig. 2; Clark and Bilham, 2008; Yin et al. 2010b; Kumar et al., 2015).

Some of the first European geologists exploring the Himalaya recognized that rock type broadly correlates with elevation and distance from the mountain front (e.g., Fraser, 1821; Colebrooke, 1822; Calder, 1833; Cautley, 1840; Herbert, 1844 [map drawn 1826]). Elaborating on this idea, Strachey (1851) documented a *sine qua non* for tectonic understanding of the orogen: several generally hinterland-dipping belts of rocks with internally similar depositional age and metamorphic grade parallel the topographic front of the orogen in northwestern India (Figs. 2, 3). All subsequent studies of Himalayan tectonics followed this organizational scheme in some form (e.g., Medlicott and Blanford, 1879; Oldham, 1893; Burrard and Hayden, 1908; Wadia, 1919; Heim and Gansser, 1939; Gansser, 1964; Hodges, 2000; Yin, 2006; Dubey, 2014; Dhital, 2015). The modern approach divides Himalayan rocks into four orogen-parallel lithotectonic belts that stretch nearly from syntaxis to syntaxis (Heim and Gansser, 1939). From foreland to hinterland, these lithotectonic units are the: (1) Sub-Himalayan or Siwalik sequence; (2) Lower Himalayan, Lesser Himalayan, or Midlands sequence; (3) Greater Himalayan sequence or Higher Himalayan Crystalline complex; and (4) Tethys Himalayan, Tethyan Himalayan, Tibetan Himalayan, or North Himalayan sequence (Table 1). In this usage, “Tibetan” refers to the part of the Himalaya north of the highest peaks, not strictly a political region. Except for “Tethys Himalaya” and “Tethyan Himalaya” (Auden, 1935), all these appellations originated as geographic and topographic parts of the Himalaya (Cautley, 1840; Medlicott, 1865; Medlicott and Blanford, 1879; Burrard and Hayden, 1908). Geologists appropriated these geographic/topographic terms to refer to rock packages, thus from their first usages as geologic expressions, these labels carried both geologic and geographic/topographic meaning. Though steeped in tradition, this conflation makes it impossible to assign unambiguous meaning to the names (Saxena, 1971; Yin, 2006; Dhital, 2015). For example, description of a rock as “Lesser Himalayan” may mean that the rock crops out at moderate elevations, that it sits structurally between the Main Boundary and Main Central thrusts, that it experienced Cenozoic sub-greenschist to amphibolite facies metamorphism, or that it was deposited as part of a mainly Proterozoic sedimentary succession on the northern margin of India.

I avoid this bewildering conflation by using the nomenclature system shown in Tables 1 and 2. The words “Lower Himalaya,” “Midlands,” and “Higher Himalaya” are reserved for discussions of elevation. I introduce new terms, Himalayan Assemblage A and Himalayan Assemblage B, to classify the rocks based on relationships set at the time of deposition or intrusion. Inclusion in an assemblage means that there was physical contiguity between adjacent members of the assemblage at the time of intrusion or deposition. Stated another way, the original contact between adjacent members of an assemblage was depositional or intrusive, not a high strain zone. As discussed in the following sections, Assemblage A and Assemblage B may not have shared depositional or intrusive relationships prior to the Early Cretaceous Epoch. The Sub-, Lesser, Greater, and Tethyan Himalayan sequences refer exclusively to the structural position of the rocks relative to Cenozoic major high strain zones, plus Cenozoic metamorphic grade for the Greater versus Tethyan distinction. That is, Sub-Himalayan rocks occur between the Main Frontal and Main Boundary thrusts and Lesser Himalayan rocks are present between the Main Boundary and Main Central thrusts. Both Greater and Tethyan Himalayan rocks occur in the hanging wall of the Main Central Thrust. Exposed Greater Himalayan rocks typically reached upper amphibolite to lower eclogite or lower granulite facies whereas Tethyan Himalayan rocks are unmetamorphosed or reached metamorphic grades at or below lower amphibolite facies (e.g., Crouzet et al., 2007; Cottle et al., 2011; Kohn, 2014; Chakraborty et al., 2016). I use a peak Cenozoic temperature of 600 °C as the boundary between Greater and Tethyan Himalayan rocks. 600 °C, like any temperature, is a somewhat arbitrary cutoff. However, near the location of the South Tibet Detachment used by most workers, footwall

Greater Himalayan and hanging wall Tethyan Himalayan rocks reached a Cenozoic peak temperature greater and less than approximately 600 °C, respectively (e.g., Vannay et al., 1999; Kellett et al., 2010; Cottle et al., 2011; He et al., 2016).

The Himalaya is a fold and thrust belt: tens of major thrusts as well as fewer major normal-sense high strain zones pervade all the rocks from the frontal to the rear boundaries of the orogen (Figs. 2, 3; Reddy et al., 1993; Ratschbacher et al., 1994; DeCelles et al., 1998a; 2001; Corfield and Searle, 2000; Grujic et al., 2002; Murphy and Yin, 2003; Kohn et al., 2004; Robinson et al., 2006; Carosi et al., 2010; 2016; Martin et al., 2010; 2015; Murphy et al., 2010; Yin et al., 2010a; Corrie and Kohn, 2011; Long et al., 2011a; Khanal and Robinson, 2013; Montomoli et al., 2013; Rubatto et al., 2013; Webb, 2013; Finch et al., 2014; Larson and Cottle, 2014; McQuarrie et al., 2014; Sorcar et al., 2014; Robinson and Martin, 2014; He et al., 2015; Khanal et al., 2015b; Larson et al., 2015; DeCelles et al., 2016). Six of these high strain zones have been mapped nearly contiguously from the western to the eastern syntaxis and their names convey tectonic and/or organizational importance (Figs. 2, 3). The robustness of the criteria for assigning these orogen-wide names to just a few of the numerous high strain zones present in any particular portion of the orogen is critical to ensure consistent use of the terms within and between regions. I use the following definitions for these six high strain zones (Table 2). The definition of each high strain zone additionally includes displacement during the Cenozoic Era.

1. The Himalayan Sole Thrust (Powell and Conaghan, 1973; Seeber and Armbruster, 1979; 1981) is the structurally lowest through-going thrust in the orogen. The provision that the thrust must be through-going in the dip direction is included in the definition in order to exclude high strain zones that produce earthquakes in the crust and uppermost mantle below the Himalayan Sole Thrust (e.g., Monsalve et al., 2006; Caldwell et al., 2013).

Other names for the Himalayan Sole Thrust include “Main Himalayan Thrust”, “Main Detachment Fault”, and “Grand Decollement.”

2. The Main Frontal Thrust (Nakata, 1972; 1975) is the most frontal foreland-vergent thrust in the orogen. “Himalayan Sole Thrust” and “Main Frontal Thrust” are names for different parts of the same structure: the Main Frontal Thrust is the term for the Himalayan Sole Thrust in the frontal-most part of the orogen where the high strain zone cuts steeply across footwall bedding. The Main Frontal Thrust does not include the high strain zones that bound the Shillong Plateau and Mikir Hills. By this definition, the true Main Frontal Thrust is more forward than the location commonly mapped in some areas of the Himalaya (e.g., Yeats and Thakur, 2008; Thakur, 2013). Alternative names for the Main Frontal Thrust include “Himalayan Front Fault” and “Himalayan Front Thrust.”
3. The Main Boundary Thrust (Middlemiss, 1890) is the most frontal foreland-vergent thrust that carried pre-Cenozoic rocks in its hanging wall, excluding the high strain zones that bound the Shillong Plateau and Mikir Hills. That is, forward of the Main Boundary Thrust, all thrusts carried only Cenozoic supracrustal rocks. The Main Boundary Thrust ends in the down-dip direction where it branches from the Himalayan Sole Thrust. In some locations, particularly in the western Himalaya, the hanging wall pre-Cenozoic strata remain buried by Cenozoic deposits; that is, the hanging wall pre-Cenozoic strata are not visible at Earth’s surface (Figs. 2, 3A). In these sectors, the true Main Boundary Thrust is forward of the commonly identified location, which is based only on mapping exposures of pre-Cenozoic rocks. Middlemiss (1890) named it the “Main Boundary Fault.”

4. The Main Central Thrust (Heim and Gansser, 1939) is the foreland-vergent thrust that juxtaposed Himalayan Assemblage B against Himalayan Assemblage A or other units of the Indian Shield. Although this definition can be difficult to apply in some locations, it fails less commonly than alternative definitions (Martin, 2017). Assemblage A constitutes the footwall between the syntaxes. In the Namche Barwa area of the eastern syntaxis, the footwall consists of Indian Shield rocks related to those exposed in the Shillong Plateau, Eastern Ghats, and Central Indian Tectonic Zone–Chhotanagpur Gneissic Complex–North Singhbhum Mobile Belt (Section 8). In frontal exposures west and south of the western syntaxis, Indian Shield rocks other than Himalayan Assemblage A likewise may form the footwall of the MCT.
5. The South Tibet Detachment (Powell and Conaghan, 1973) is the high strain zone that both accommodated more than 10 km of top-to-the-hinterland displacement and separated rocks with Cenozoic peak temperature greater than approximately 600 °C from rocks with Cenozoic peak temperature less than about 600 °C. In regions such as the Annapurna Range of central Nepal, multiple top-to-the-hinterland high strain zones each accommodated at least several kilometers of displacement (Hodges et al., 1996; Martin et al., 2010; Searle, 2010; Robinson and Martin, 2014; Martin et al., 2015). The peak temperature part of the definition allows identification of just one of these high strain zones as the South Tibet Detachment.
6. The Indus-Yarlung Suture (Gansser, 1964; Dewey and Bird, 1970) is the boundary between continental rocks that were part of either the Indian lithospheric plate or another plate to the north prior to Paleocene collision of these two continental blocks (DeCelles et al., 2014; Hu et al., 2017). In this context, “continental” is a broad term that includes

island arcs and highly extended continental crust. It is irrelevant for this definition of the suture whether the continental rocks of the northern lithospheric plate were the Lhasa terrane/Asia (Najman et al., 2010; 2017; Zhuang et al., 2015) or an island arc or rifted microcontinent (Sinha-Roy, 1976; Fuchs and Willems, 1990; Aitchison et al., 2007; Gibbons et al., 2015; Jagoutz et al., 2015). Other names for the Indus-Yarlung Suture include "Indus-Yalu Suture", "Indus-Tsangpo Suture", and, only near and west of the western syntaxis, "Main Mantle Thrust."

The Himalayan Sole Thrust does not crop out. River cuts and human-dug trenches uncover the Main Frontal Thrust in some locations (Srivastava et al., 2016; Wesnousky et al., 2017; reviewed in Thakur, 2013; Bollinger et al., 2014), but in most areas the Main Frontal Thrust remains covered by Neogene to Quaternary deposits. The Main Boundary Thrust is exposed extensively east of Kumaon, but to the northwest, it too remains buried by Neogene to Quaternary strata in most districts (Figs. 2, 3). The Main Frontal, Main Boundary, and Main Central thrusts crop out extensively in the Salt Range of Pakistan except at the eastern end of the range. Between the syntaxes, the Indus-Yarlung Suture, South Tibet Detachment, and MCT all crop out widely.

DeCelles et al. (1998a; 2001); Robinson et al. (2003), Pearson and DeCelles (2005), He et al. (2015), Khanal et al. (2015b), Larson et al. (2015), and Carosi et al. (2016), among others, emphasized that the MCT is one in a series of foreland-vergent thrusts. A consequence of this recognition is that labeling just one thrust in the series as the MCT suggests unwarranted Cenozoic geometric or kinematic significance for that particular thrust. Likewise, there is nothing geometrically or kinematically special about the Main Boundary or Main Frontal thrusts except that they and neighboring high strain zones currently are active and generate modern earthquakes. Nevertheless, identifying these three thrusts is useful for organizing rocks in the Cenozoic thrust belt as follows. The Main Frontal Thrust demarcates the end of the Himalayan Orogen in the forward direction. The Main Boundary Thrust marks the forward limit of foreland-vergent thrusts that carried pre-Cenozoic rocks in their hanging walls, and thus the forward limit of allocthonous pre-Cenozoic rocks in the Himalayan Orogen. Between the syntaxes, the MCT is the boundary between the Lesser and Greater Himalayan sequences as well as between Assemblage A and B, and differentiating the assemblages is critical for understanding their pre-Cenozoic tectonic development.

3. CORRELATION WITHIN HIMALAYAN ASSEMBLAGE A AND ASSEMBLAGE B

Long et al. (2011b), McKenzie et al. (2011a), Dubey (2014), and others have published single stratigraphic correlation charts that span not only the east-west dimension of the Himalaya but also the north-south dimension: that is, each chart includes both Himalayan Assemblage A and Assemblage B rocks. These correlation charts conflate depositional or intrusive relationships that are observable now with contacts that presently are high strain zones. Such diagrams are confusing because they do not clearly differentiate these very different types of contacts. Figures 7, 8, and 9 avoid this conflation by showing only depositional and intrusive relationships; this depiction is appropriate because depositional or intrusive contacts and not high strain zones define Assemblage A and Assemblage B. In this section I describe observations from these correlation charts. Appendices A and B give details about choices made during construction of the charts as well as references for lithologies and ages. In many locations, the exposed pre-Cenozoic rocks were metamorphosed (Kohn, 2014; Chakraborty et al., 2016).

Metamorphism is irrelevant for assignation to Assemblage A or B, so throughout the article I discuss the rocks in terms of their protoliths.

3.1 Observations from Himalayan Assemblage A correlation chart

The compilation reveals that both rock type and depositional or crystallization age of most Assemblage A rocks were broadly uniform across much of the Himalaya (Fig. 8). Assemblage A mostly consists of three rock packages defined by depositional or crystallization age: Late Paleoproterozoic to Early Mesoproterozoic, Late Carboniferous to Permian, and latest Cretaceous to Pleistocene. The only major exceptions are Lower Cretaceous mafic volcanic and clastic rocks in central Nepal and Cambrian mostly clastic rocks in Bhutan and northeastern India. The depositional substrate for Assemblage A rocks is not exposed anywhere in the Himalaya – the oldest Assemblage A rock unit is metasedimentary along the entire orogen.

3.1.1 Late Paleoproterozoic to Early Mesoproterozoic Assemblage A rocks

Along nearly the entire Himalaya, the oldest exposed rocks in Assemblage A are sandstone-rich formations that were deposited between ca. 1900 and 1850 Ma. In many regions this sandstone-rich unit gradually became more shale-rich stratigraphically upward. Across most of the Himalaya, granite and much less voluminous gabbro intruded this clastic succession between ca. 1880 and 1830 Ma (summarized in Kohn et al., 2010; see also Sakai et al., 2013), but in Arunachal, Assemblage A granite crystallized at ca. 1810, 1770, and 1750 Ma. In eastern Nepal, granite additionally intruded at ca. 1940 Ma (Larson et al., 2016) and 1780 Ma; ca. 1780 Ma granite also intruded central Nepal. Following this widespread bimodal intrusion, accumulation of sandstone recommenced across northwestern India and Nepal. In northwestern

India, interbedded basalt indicates that this sandstone was deposited at ca. 1820 Ma, whereas sandstone deposition occurred after 1770 Ma in Nepal. Between northwestern India and eastern Bhutan, subsequent sedimentation was dominated by shale that gradually became more limestone-rich stratigraphically upward. In all locations west of central Bhutan, deposition of the Upper Paleoproterozoic to Lower Mesoproterozoic succession ended with a several hundred-meter-thick limestone that may have been deposited at ca. 1600 Ma.

3.1.2 Cambrian Assemblage A rocks

Confirmed Cambrian rocks are present in Assemblage A only in central and eastern Bhutan and Arunachal. These rocks are dominantly clastic, although the upper part of the Rupa Group in Arunachal also contains a limestone/dolostone interval up to several hundred meters thick.

3.1.3 Upper Carboniferous to Permian Assemblage A rocks

Upper Carboniferous to Permian rocks are widespread in Assemblage A between central Nepal and Arunachal, but are absent from Assemblage A west of central Nepal. The rocks are dominantly clastic. Basal strata commonly consist in part of diamictite with a mud- or sand-rich matrix surrounding larger clasts that typically reach pebble to cobble size. The diamictite-rich interval gradually passes upward into sandstone and shale that commonly are interbedded with coal. This succession typically is called "Gondwanan" or the "Gondwana Group" because it shares lithologies and depositional ages with Gondwanan rocks in India south of the Himalaya (e.g., Mukhopadhyay et al., 2010; Aggarwal and Jha, 2013).

3.1.4 Uppermost Cretaceous to Pleistocene Assemblage A rocks

An Upper Paleocene/Lower Eocene to Pleistocene succession is present within Assemblage A across the Himalaya. Between northwestern India and central Nepal, depositional age uncertainty extends the possible depositional age of the lowermost part of this succession into the latest Cretaceous Period. In the west, uppermost Cretaceous/Paleocene to Eocene strata are mostly marine limestone, whereas shallow marine sandstone dominated deposition at this time east of northwestern India. In all locations there is an unconformity that spans the late Eocene to earliest Miocene interval. Sandstone, conglomerate, and subordinate mudstone accumulated between the early Miocene Epoch and the present.

The middle Miocene to lower Pleistocene foreland basin deposits have been named the Siwalik Group along nearly all of the orogen between the western and eastern syntaxes (beginning with Cautley, 1840). The Siwalik Group classically, though informally, is divided into lower, middle, and upper members (Middlemiss, 1890). The lower Siwalik member mostly consists of single-story lenticular sandstone bodies surrounded by mudstone (Medlicott, 1865; Middlemiss, 1890; DeCelles et al., 1998a). The middle Siwalik member mainly comprises greater than 20 meter-thick, multi-story sandstone. The upper Siwalik member is dominated by conglomerate.

3.2 Observations from Himalayan Assemblage B correlation chart

Along most of the Himalaya, the oldest Assemblage B rocks are interbedded sandstone and mudstone that were deposited in the Early Neoproterozoic Era. The best documented exception is in northwestern India, where the Neoproterozoic clastic rocks possibly rest depositionally on the ca. 1850 Ma Baragaon granitic gneiss in a small area near the Sutlej river (Webb et al., 2011).

The depositional and magmatic history of Assemblage B is consistent across most of the Himalaya. Notable similarities include the following rock-forming events.

1. The earliest deposition was in the Early or Middle Neoproterozoic Period in most locations.
2. Granitic intrusion at 880-800 Ma was widespread, though granite of this age has not been found in Nepal. This magmatism was not voluminous: in each of the regions listed in Figure 9 that expose the granite, only a few bodies with crystallization ages in this range have been found. Except for a foliated leucogranite lens in northwestern India that crystallized at 804±27 Ma (Horton and Leach, 2013), the range of crystallization ages is small between Pakistan and central Bhutan: ca. 830-820 Ma. In southeastern Tibet and Arunachal, granitic bodies intruded at 878±13, 856±7, 816±3, 809±8, 809±5, and 804±9 Ma (Yin et al., 2010a; Clarke et al., 2016; DeCelles et al., 2016; Y. Wang et al., 2017).
3. In all locations, a several kilometer-thick sedimentary succession was deposited between the Middle or Late Neoproterozoic and Cambrian periods.
4. Granite intrusion at ca. 510-460 Ma was widespread and voluminous. References for locations not listed on Figure 9 are DeCelles et al. (1998a), Gehrels et al. (2006a), and Cottle et al. (2009). Visona et al. (2010) reported ca. 460 Ma mafic dikes in Assemblage B rocks directly east of Mount Everest.
5. Ordovician pebble to boulder conglomerate was deposited between Pakistan and Bhutan.
6. Limestone dominated deposition in many locations during the middle Paleozoic Era.

7. A pebble to cobble-bearing diamictite was deposited in late Carboniferous to early Permian time between Pakistan and Bhutan.
8. Lower Permian basalt was deposited in northern Pakistan and northwestern India as well as central Nepal. In northern Pakistan and northwestern India, these rocks are known as the Panjal Traps. In the western Himalaya, mafic dikes, some in swarms, intruded the pre-Permian Assemblage B strata (Hayden, 1904; Fuchs, 1982; Gaetani et al., 1990). These dikes presumably fed the Panjal Trap volcanoes. Granite intruded during Early and Middle Permian time in northern Pakistan and adjacent parts of northwestern India as well. No Permian igneous rocks have been found in Assemblage B east of central Nepal.
9. Limestone dominated deposition during Triassic to Middle Jurassic time from Pakistan to Sikkim/south-central Tibet.
10. Shale was deposited between Pakistan and Bhutan in the Late Jurassic to earliest Cretaceous periods. The best-known name for these rocks is the Spiti Shale, from northwestern India.
11. Lower Cretaceous sandstone was deposited atop this shale between Pakistan and central Nepal.
12. Upper Cretaceous limestone was deposited between northwestern India and south-central Tibet.
13. At ca. 28-14 Ma, leucogranite intruded all rear and some frontal parts of Assemblage B.

Ediacaran to early Cambrian granite intruded Assemblage B rocks in at least three locations. Granite intruded in Sikkim at 604±28 Ma (Mottram et al., 2014), in northwestern India at 553±2 Ma (Miller et al., 2001), and in the Kampa north Himalayan gneiss dome at

527±6 Ma (Quigley et al., 2008). Scharer et al. (1986) interpreted an igneous crystallization age of 562±4 Ma for granitic gneiss at the core of the Kangmar dome based on a concordant U/Pb isotopic date of a single zircon. However, Lee et al. (2000) obtained zircon U/Pb crystallization ages of ca. 509 Ma for one structurally low and one structurally high sample from ostensibly the same granitic gneiss body, suggesting that at least part of the single crystal dated by Scharer et al. (1986) might have been inherited.

I include the Darla volcanics through Tal succession as part of Assemblage B because this succession's depositional ages and detrital zircon age signatures are similar to other Assemblage B deposits (Fig. 9; Myrow et al., 2003; 2010; 2015; Webb et al., 2011a; Appendix B). The Darla through Tal succession did not reach Cenozoic metamorphic temperatures higher than 600 °C (Webb et al., 2011a; Webb, 2013), so these rocks belong to the Tethyan Himalayan Sequence. I do not include this Neoproterozoic to Cambrian succession in Assemblage A because all but one of the formations are separated from Paleoproterozoic-Lower Mesoproterozoic or terminal Cretaceous-Cenozoic Assemblage A deposits by the Tons or Krol thrust (Auden, 1934; 1937; Webb, 2013). The Tons-Krol Thrust placed Assemblage B on Assemblage A rocks, so it is the MCT in frontal positions (Fig. 3). An exception centers on the Neoproterozoic Mandhali Formation, which is present in both the hanging wall and footwall of the Tons Thrust (McKenzie et al., 2011a; Webb et al., 2011a). In the footwall of the Tons Thrust, it is unknown whether the contact between the Mandhali Formation and Paleoproterozoic Assemblage A rocks is depositional or a high strain zone. If a high strain zone, this high strain zone, not the Tons-Krol thrust, is the MCT.

4. TECTONIC SETTING DURING DEPOSITION OF HIMALAYAN ASSEMBLAGE A

4.1 Late Paleoproterozoic to Early Mesoproterozoic Assemblage A rocks

Exposures of late Paleoproterozoic to Early Mesoproterozoic Himalayan Assemblage A rocks invariably are allocthonous, and these rocks were metamorphosed and internally deformed. Consequently, original relationships with neighboring rocks are obscure, and we are forced to rely on indirect evidence to evaluate the tectonic setting during deposition and intrusion. Geologists have proposed two contrasting tectonic settings for deposition of the ca. 1900-1800 Ma Assemblage A rocks as well as intrusion of the ca. 1880-1830 Ma granite and gabbro: magmatic arc and continental rift. Many analyses concluded that the overlying ca. 1800-1600 Ma sedimentary rocks were deposited in a passive margin setting (Brookfield, 1993; Myrow et al., 2003; Sakai et al., 2013). Alternatively, the wide areal extent of ca. 1800-1600 Ma deposits on Indian continental crust shown on the geologic map in Webb (2013) perhaps suggests deposition in an epi-cratonal basin.

Kohn et al. (2010; see also references therein) supported a magmatic arc origin for the ca. 1900-1800 Ma Assemblage A rocks based on two types of geochemical data. First, zircon-saturation thermometry indicated magmatic temperatures of 800±50 °C for most ca. 1880-1830 Ma granite bodies and broadly coeval, possibly volcanic rocks. Kohn et al. (2010) attributed these temperatures to wet, relatively low-temperature melting in an arc setting. Second, whole-rock trace element concentration discrimination diagrams indicated that many of these granitic and possibly volcanic rocks plotted in the volcanic arc and syn-collisional fields defined by Pearce et al. (1984). Mandal et al. (2016) likewise argued for a magmatic arc or back-arc setting for ca. 1900-1800 Ma felsic igneous and clastic rocks from northwestern India based on whole-rock trace element concentration discrimination diagrams supported by Hf isotopic analyses of spots in zircon.

Rameshwar Rao and Sharma (2011) presented major and trace element concentrations from granitic whole rocks exposed in three klippen in northwestern India near the border with Nepal. The granitic rocks in one of these klippen, the Almora-Dadeldhura Klippe, intruded during late Cambrian to early Ordovician time (Trivedi et al., 1984; DeCelles et al., 1998a; Gehrels et al., 2006a), so these rocks cannot help determine Paleoproterozoic tectonic setting. The crystallization ages of granitic rocks in a second klippe, the Chhiplakot Klippe, are unknown. Granitic rocks in the third klippe, the Askot Klippe, intruded at ca. 1860 Ma (Mandal et al., 2016). Like Kohn et al. (2010) and Mandal et al. (2016), Rameshwar Rao and Sharma (2011) found that some granitic rocks from all three klippen plotted in the volcanic arc field on trace element concentration discrimination diagrams.

The conclusions about tectonic setting inferred from analyzing each of these types of data are ambiguous. First, continental rift-related felsic magma can have an intrusive or pre-eruptive temperature at or below 850 °C (Jiang et al., 2011; Thorarinsson et al., 2011; Pandit et al., 2012; Yang et al., 2012; Wegert et al., 2013; see also Hogan et al., 1997), so the 800±50 °C temperatures for the ca. 1880-1830 Ma Himalayan granite and possible volcanic rocks could indicate either an arc or continental rift setting. Second, Kohn et al. (2010) cautioned that interpretations based on the trace element concentrations should be treated skeptically because the neodymium model ages of at least some of the ca. 1880-1830 Ma Himalayan granite bodies are older than their crystallization ages, possibly indicating contamination of the magmas by their metasedimentary country rocks. Such contamination shifts trace element concentrations away from primary magmatic values. Further, the trace element concentrations for most samples plot near the boundaries between several tectonic fields on the discrimination diagrams, not well into the volcanic arc or syn-collisional fields, and some of the exceptions plot in the within plate field. Thus the trace element concentration data likewise do not yield unequivocal results.

Conversely, Sakai et al. (2013; see also references therein plus Richards et al., 2005) argued for a continental rift setting based on age and stratigraphic similarities between the late Paleoproterozoic Himalayan Assemblage A rocks and lower parts of the late Paleoproterozoic Coronation Supergroup (Melville and Epworth groups) in the Wopmay Orogen of northwestern Canada. The Melville and Epworth groups formed in a continental rift and passive margin setting, respectively (Hildebrand et al., 2010; Hoffman et al., 2011). Although Sakai et al. (2013) correlated the Himalayan ca. 1880-1830 Ma granite with the Hepburn felsic batholith in Wopmay, the tectonically appropriate link would be to the Vaillant basalt in Wopmay. Sakai et al. (2013) postulated that both rift-related rock packages formed as a result of rifting between the Indian, North China, and Slave cratons because these three blocks are shown adjacent to each other in the Late Paleoproterozoic reconstruction of their positions by Hou et al. (2008). Other reconstructions do not show these three cratons adjacent to one another at this time (Rogers and Santosh, 2009; Evans and Mitchell, 2011).

Of these two options, I favor a continental rift setting for the ca. 1900-1800 Ma Himalayan Assemblage A rocks for four reasons. First, the magma temperature and trace element concentration data permit interpretation of either a magmatic arc or continental rift setting. Second, the composition of the magmas appears to be bimodal, felsic and mafic; ca. 1880-1830 Ma magmatic rocks with an intermediate composition are unknown from the Himalaya. Intermediate composition here means 55-65 weight percent SiO_2. Mostly bimodal magmatism is expected for continental rifts because typically only a small fraction of the rift-related magma has an intermediate composition (Hogan and Gilbert, 1997; Li et al., 2002;

Alvaro et al., 2008; Ayalew and Gibson, 2009; Corti, 2009; Zhou et al., 2009; Thorarinsson et al., 2011; Cosca et al., 2014). Dominantly bimodal magmatism is not expected for magmatic arcs, where the crust commonly consists of a mafic to felsic suite, a large percentage of which has intermediate composition (Quinn et al., 1997; Mamani et al., 2010; Cecil et al., 2012; Jagoutz and Schmidt, 2012; Chapman et al., 2014; Kent, 2014; Ducea et al., 2015; Kimbrough et al., 2015; exceptions in Espinoza et al., 2008; Jones et al., 2011; Buhler et al., 2014). The utility of point two for the determination of tectonic setting depends on the accuracy of the interpretation that the granite and gabbro intruded at about the same time; note that the gabbro has not been radiometrically dated anywhere in the Himalaya. Third, as partially pointed out by Sakai et al. (2013), accretionary complexes, subduction melanges, and/or ophiolites commonly are found adjacent to magmatic arcs (Encarnacion, 2004; Hopson et al., 2008; Dumitru et al., 2010; John et al., 2010; Hernaiz Huerta et al., 2012; Thanh et al., 2012; Aoya et al., 2013; Ichiyama et al., 2014), but there are no ca. 1900-1800 Ma rocks that could be interpreted as an accretionary complex, subduction melange, or ophiolite in Assemblage A. Although these tectonic elements could have been removed during or after putative subduction, such removal fortuitously would have had to eliminate all vestiges of the accretionary complex, subduction melange, and ophiolite. Fourth, depositional age correlative rocks in the exposed Indian shield directly south of the Himalaya such as the lower part of the Vindhyan Supergroup may have been deposited in normal fault-bounded basins that resulted from ca. 1900-1800 Ma rifting (Kaila et al., 1989; Verma and Banerjee, 1992; Ram et al., 1996; Das et al., 1999; Ahmad et al., 2005; 2006; Saha and Mazumder, 2012; alternatives in Chakrabarti et al., 2007; Raza et al., 2009). Similarly, depositional age equivalent sedimentary rocks now buried beneath the sedimentary rocks of the Himalayan foreland also may have been deposited in normal fault-bounded basins (Sastri et al., 1971; Rao, 1973; Singh, 1996; Srinivasan and Khar, 1996). These rift basins trend northeast, into the Himalaya (Fig. 5). An alternative interpretation is that the older granite formed in a continent-continent collision zone, followed by intrusion of the gabbro and younger granite in a continental rift.

The geometries of the high strain zones south of the Himalaya allow us to infer depositional strike and dip directions during accumulation of the upper Paleoproterozoic to Lower Mesoproterozoic part of Assemblage A. The map-view pattern of high strain zones is complicated, as expected (Corti, 2009; Philippon et al., 2015). Further, some of the northeast-trending high strain zones such as the Narmada-Sone and Great Boundary faults are long-lived high strain zones that have been active with different senses of motion at different times (Biswas, 1987; Kaila et al., 1989; Roy, 1990; Chamyal et al., 2002; Srivastava and Sahay, 2003). Nevertheless, most of the major late Paleoproterozoic normal-sense high strain zones buried in the Himalayan foreland strike between 20 and 50 degrees east of north, implying a depositional strike of approximately N40E for the sediment that filled the basins produced by these high strain zones. The exposed Kishangarh-Chipri, Great Boundary, and Narmada-Sone faults, as well as most major buried basement structures in the Vindhyan basin, likewise strike northeast (Fig. 5; Mishra et al., 1996). Depositional dip was 90° from N40E, but the deformation and metamorphism of the Himalayan Assemblage A rocks make it difficult to determine whether depositional dip was toward the northwest or southeast. Paleocurrent indicators in broadly age-equivalent rocks in the Vindhyan Supergroup show flow mostly toward the northwest (Bose et al., 1997), so I infer that depositional dip of Himalayan Assemblage A rocks likewise may have been northwest, approximately N50W. Regardless of whether depositional dip was toward the northwest or southeast, in the western Himalaya the strike of major Cenozoic thrusts was nearly at right angles to late Paleoproterozoic to Early Mesoproterozoic depositional strike, in the central Himalaya the strikes were oblique to one another, and in the eastern Himalaya the strikes were broadly parallel.

4.2 Cambrian Assemblage A rocks in the eastern Himalaya

Cambrian Assemblage A rocks are restricted to the eastern Himalaya. Deposition of these strata could be related to the coeval Kuunga Orogeny on the eastern margin of India, as recorded in the Shillong Plateau/Mikir Hills, Namche Barwa region, and Eastern Ghats (Yin et al., 2010b; this paper; reviews in Collins and Pisarevsky, 2005; Cawood and Buchan, 2007). The strike of the orogen was approximately N45E, suggesting that depositional strike of the possible Kuunga foreland basin deposits in eastern Himalayan Assemblage A might have been broadly parallel to this direction. An alternative interpretation is that deposition of the Cambrian Assemblage A strata could be related to the Cambrian orogenic pulse in the Pinjarra Orogen (Collins, 2003; Markwitz et al., 2017). In western Australia, the Pinjarra Orogen trended broadly north.

4.3 Upper Carboniferous to Permian Assemblage A rocks

Upper Carboniferous to Permian sedimentary rocks have been well-studied in India south of the Himalaya, where the strata are called the Gondwana succession (e.g., Mukhopadhyay et al., 2010; Aggarwal and Jha, 2013). This name likewise has been applied to Himalayan continental and shallow marine sedimentary rocks with similar depositional ages. The Himalayan Gondwanan basins are not present west of central Nepal. South of the Himalaya, the Gondwana succession has been little deformed, and it is clear that these rocks were deposited in rift basins, probably related to the breakup of Pangea. In the Himalaya, Cenozoic internal deformation and especially the thrusts that bound the Gondwanan strata obscured the original tectonic setting. However, by analogy with the Gondwanan deposits south of the Himalaya, I infer that the Gondwana succession in the Himalaya likewise was deposited in a series of rift basins. South of the Himalaya, the strike of most Gondwanan rift basins is between 25 and 50 degrees west of north, and this is the most likely range of depositional strikes in the Himalaya as well. Thus in central Nepal, the strike of major Cenozoic thrusts was oblique to late Paleozoic depositional strike, and the obliquity increased toward the east. Minor normal-sense reactivation of high strain zones in central Nepal could have created the accommodation space for the Lower Cretaceous Taltung sandstone and basalt deposited there. The cause of this putative reactivation, as well as the reasons for the apparent absence of deposition at this time throughout the remainder of Assemblage A, are unknown. Sakai (1983) correlated the Taltung basalt with the ca. 118 Ma Rajmahal basalt of northeastern India south of the Himalaya (Kent et al., 2002). Although the available data allow the alternative interpretation that equivalents of the Taltung Formation originally were deposited in other parts of the Himalaya and then eroded, this scenario seems unlikely because we know of no tectonic cause for this erosion between the end of Rajmahal Trap volcanism in northeastern India and deposition of the Amile Formation and its correlatives in terminal Cretaceous to Paleocene time.

The Permian Abor Volcanics are present only in easternmost Assemblage A. This part of northeastern India restores atop the plume generation zone of Torsvik and Cocks (2013) in their reconstruction of Gondwana during the Permian Period (Fig. 6D). This reconstruction implies that the magma that constitutes the Abor Volcanics resulted from partial melting of a mantle plume.

Grujic et al. (2017) showed that detrital muscovite grains in Gondwanan sandstone from Sikkim have a peak in $^{40}Ar/^{39}Ar$ ages at ca. 480 Ma. Based on these ages, the authors concluded that the most likely source of the muscovite detritus was Cambrian-Ordovician granite in Assemblage B. Although Grujic et al. (2017) discounted the Kuunga Orogen on the eastern edge of India as too old to provide ca. 480 Ma muscovite grains, in fact muscovite $^{40}Ar/^{39}Ar$ ages in the Kuunga Orogen extend from 490 to 475 Ma (Crowe et al., 2001). Another possibile sediment source is the Pinjarra Orogen to the east, where metamorphic zircon grew at ca. 525 Ma (Collins, 2003; Markwitz et al., 2017). Muscovite $^{40}Ar/^{39}Ar$ ages resulting from the Cambrian pulse of orogeny in the Pinjarra Orogen would be younger than 525 Ma. Thus both the Kuunga and Pinjarra orogens, in addition to Himalayan Assemblage B, are potential sources of sediment to the Himalayan Gondwanan basins.

4.4 Uppermost Cretaceous to Pleistocene Assemblage A rocks

Following a hiatus, deposition began in the late Paleocene or early Eocene Epoch in Pakistan and in and east of Sikkim. Between northwestern India and central Nepal, sedimentation began in latest Cretaceous or Paleocene time. Globally high sea level undoubtedly contributed to accumulation of the uppermost Cretaceous/Paleocene to Lower Eocene shallow marine sediment on continental crust (Kominz et al., 2008; Muller et al., 2008; Haq, 2014). However, despite global sea level 50-200 meters higher than today's value throughout the preceding Cretaceous and Early Jurassic periods, there was no deposition at this time in Assemblage A except in a small area of central Nepal (Fig. 8). Consequently, it is necessary to find an additional mechanism to generate accommodation space for the terminal Cretaceous/Paleocene to Lower Eocene shallow marine rocks.

The depositional ages of these rocks are not well known, and deposition entirely in the Paleocene and/or early Eocene epochs is possible. Thus considering age uncertainties, deposition of these rocks overlapped in time with the initial collision of Indian continental rocks with more northern terranes at 59 ± 1 Ma (DeCelles et al., 2014; Hu et al., 2015; 2017) or possibly at 64 ± 1 Ma (Ding et al., 2017). The resumption of sedimentation along the entire northern margin of India after hundreds of millions of years of non-deposition (or possibly deposition followed by erosion) at approximately the same time as the initial continental collision suggests the simplest explanation for the new-formed accommodation space involves tying recommencement of sediment accumulation to the collision. That is, these shallow marine rocks may have accumulated in the most distal part of the foreland basin in front of the earliest Himalaya. This tectonic setting for deposition of the Lockhart, Singtali, and Amile formations contrasts with previous conclusions that these rocks do not record Himalayan collision, which was based on the absence of Asian detritus in them (Critelli and Garzanti, 1994; Najman and Garzanti, 2000, DeCelles et al., 2004; 2014; Najman et al., 2005). However, the lack of northerly-derived sediment does not rule out deposition in an earliest Himalayan foreland basin because the most distal parts of underfilled foreland basins may not receive detritus from the upper plate (Heller et al., 1988; Sinclair, 1997; Boulton and Robertson, 2007; Yang and Miall, 2010; Yang, 2011). Reducing the uncertainties on the depositional ages of the Lockhart, Singtali, and Amile formations would allow testing of this interpretation: if they were deposited before ca. 66 Ma, the hypothesis would fail. An alternative interpretation is that the effects of the Deccan Traps hotspot on India caused the subsidence that allowed deposition of these rocks, as proposed by Garzanti and Hu (2015) for Assemblage B rocks. It is surprising that the Amile Formation contains no obvious detritus from the Deccan Traps if the source of Amile Formation sediment were India south of the Indo-Gangetic plain, as suggested by this alternative interpretation as well as DeCelles et al. (2004; 2014).

The oldest rocks in Assemblage A that unequivocally record the Himalayan continental collision were deposited in Late Paleocene or early Eocene time (Critelli and Garzanti, 1994; Najman and Garzanti, 2000; DeCelles et al., 2004; 2014; Najman et al., 2005). This and all subsequent deposition took place in the Himalayan foreland basin. Depositional strike paralleled the frontal Himalayan thrusts, so in the western and west-central Himalaya depositional strike was toward the northwest, in the east-central Himalaya it was broadly east-west, and in Arunachal depositional strike trended northeast.

The coarsening upward succession from the lower through the middle to the upper member of the Siwalik Group reflects increasing proximity to the Himalayan fold-thrust belt (DeCelles et al., 1998b). During deposition of middle Miocene to Pliocene lower and middle Siwalik sandstone and mudstone that we now observe mostly in the footwall of the Main Boundary Thrust, coarser-grained sediment must have been deposited in the hinterland direction. This conclusion opposes that of Medlicott (1865), who argued that the “main boundary” was the original limit of deposition of the Siwalik Group, and that the main boundary was not the location of a major fault. In most locations we no longer can observe the coarser-grained, more hindward equivalents of the lower and middle Siwalik members because those more proximal hinterland deposits have been eroded. In contrast, Main Boundary Thrust footwall pre-Cenozoic strata are covered by Cenozoic deposits everywhere in the thrust belt, and hanging wall pre-Cenozoic rocks remain buried by Cenozoic deposits in some locations, particularly in the western Himalaya (Figs. 2, 3). Consequently, in many locations the Main Boundary Thrust appears not to repeat section at Earth’s surface due to a combination of erosion of hanging wall

Siwalik strata in some sectors, burial of hanging wall pre-Cenozoic rocks in others, and burial of footwall pre-Cenozoic strata along the entire orogen. However, in cross-section we see that the Main Boundary Thrust-Himalayan Sole Thrust actually does repeat section because it places a succession of Upper Paleoproterozoic to Lower Mesoproterozoic Assemblage A strata in the proximal hanging wall above correlative deposits in the footwall (Fig. 3).

5. FAULT REACTIVATION, SALIENTS, AND RECESSES IN THE FRONTAL HIMALAYA

Robust evidence for Cenozoic reactivation of ancient high strain zones is scarce in the Himalaya, in contrast to most other Phanerozoic orogens. The clearest evidence for such reactivation comes from the frontal part of the fold-thrust belt, where the magnitude of slip required to explain the evidence for reactivation is small, less than 1 km in most cases. The reasons the clearest evidence comes from the frontal part are: (1) The small magnitude of deformation and absence of metamorphism of the Sub-Himalayan rocks has not obscured putative structural and stratigraphic evidence for reactivation, in contrast to the hinterland rocks; and (2) geologists can observe structures in the adjacent modern Himalayan foreland that were not deformed in the Cenozoic Era and directly compare them to structures in the frontal part of the Cenozoic thrust belt. In this section I examine reasons that Pliocene to Holocene frontal thrusts mostly were newly-formed as well as causes for the absence of large salients and recesses in the frontal Himalayan thrusts as compared to two other Phanerozoic orogens. These frontal thrusts and their map-view bends are contained in Himalayan Assemblage A rocks.

5.1 Reactivation of high strain zones in the Himalayan Orogen

5.1.1 Review of previous research

Raiverman et al. (1994) presented the most convincing data for reactivation of ancient high strain zones in the Himalaya, seismic reflection profiles with well control from the proximal foreland in northwestern India. This article showed that south of the Main Frontal Thrust, high strain zones that cut pre-Cenozoic rocks end vertically near the base of the Cenozoic strata, whereas farther north, in the Himalaya, high strain zones with similar orientations cut the pre-Cenozoic rocks and continue upward into positive flower structures. The authors suggested Cenozoic strike-slip reactivation of inherited pre-Cenozoic high strain zones at the front of the thrust belt and attributed spatial differences in the thickness of the Eocene and younger sedimentary rocks to renewed motion on these older high strain zones. Although this conclusion is convincing if the interpretations of the seismic data are correct, the published seismic reflection profiles lack sufficient resolution to be confident of the geometric link between structures at depth.

Other Himalayan foreland examples are less certain. The largest magnitude example of possible foreland high strain zone reactivation comes from the 400 km-long Shillong Plateau-Mikir Hills region in the eastern sector, the only location between the syntaxes where pre-Cenozoic rocks crop out in the Himalayan foreland (Fig. 2). Combining fault geometries mostly inferred from geodetic triangulation surveys (Bilham and England, 2001; England and Bilham, 2015) with the locations of steep reaches of rivers that drain the plateau, apatite (U-Th-Sm)/He ages, and stratigraphic and geophysical data, Clark and Bilham (2008) showed that the thrusts that bound these uplands accommodated a modest amount of slip, cumulatively only about 15 km, starting at 14-8 Ma. Although others have argued for different bounding fault geometries, the total magnitude of fault slip must be similar (e.g., Islam et al., 2011; see also Berthet et al., 2014). Clark and Bilham (2008) proposed that the plateau-bounding thrusts rejuvenated normal faults inherited from pre-Cenozoic rifting but did not provide evidence for this recrudescence (see also Talwani et al., 2016). Other instances of foreland features attributed to Cenozoic reactivation of inherited pre-Cenozoic high strain zones include the spatial patterns of deposition of Eocene-Miocene foreland basin strata (Najman et al., 1993; Mugnier and Huyghe, 2006; see also Gansser, 1964), the modern geomorphology of frontal rivers and hills (Khan et al., 1996; Singh, 1996; Valdiya, 2003; Jain and Sinha, 2005; Goswami, 2012; see also Gansser, 1964), and the structural geometries of the Main Boundary and Main Frontal thrusts, nearby faults, and rocks deformed by these faults (Raiverman et al., 1993; Grelaud et al., 2002; Srinivasan, 2003; Roure, 2008; see also Gansser, 1964). Gansser (1964; 1983; 1991), Valdiya (1976; 1981), and Sujit Dasgupta et al. (1987; 2013) all invoked reactivation to explain the structural geometries of transverse faults, folds, and lineaments that the authors mapped stretching from the foreland to the hinterland.

Each of the articles listed in the preceding two paragraphs posited that inherited pre-Cenozoic high strain zones in the north Indian crust slipped during Cenozoic time and fed that slip directly to Paleocene or younger near-surface faults and/or folds. Except for Raiverman et al. (1994), this postulated kinematic link was based on either correlation between the locations and trends of the Cenozoic and older structures or an expectation that inherited high strain zones should reactivate (Mukhopadhyay, 1984), or both; none of the articles showed data that require Cenozoic slip on the inherited high strain zones. Instead, the Paleocene or younger faults and folds could be localized and have their geometries shaped by the presence of strength contrasts in the upper Indian crust set up by juxtaposition of structural highs composed of metamorphic and intrusive rocks with thinner pre-Cenozoic sedimentary cover on the one hand and structural lows with thicker pre-Cenozoic sedimentary successions on the other hand (Nakata, 1975). This type of indentation tectonics does not require Cenozoic slip on the high strain zones that bound the structural highs and lows (Dominguez et al., 2000; Zeumann and Hampel, 2015). Although Paleocene or younger reactivation of inherited pre-Cenozoic high strain zones cannot be ruled out, in all of the listed cases except the Shillong Plateau, Cenozoic slip of only 10 to 1000 meters is sufficient to explain the available data. Bollinger et al. (2004) and Martin et al. (2015) proposed such a purely geometric, non-kinematic role for one foreland structural high in central Nepal. These articles explained east-west differences in the presence of Greater Himalayan klippen (Bollinger) and Greater and Lesser Himalayan muscovite ^{40}Ar/^{39}Ar ages (Martin) by suggesting that the Faizabad ridge, a Paleoproterozoic horst in the downgoing Indian crust, may have passively impacted the tectonic architecture of overlying hanging wall rocks solely as a geometric template (Fig. 5). The explanations do not require, nor is there evidence for, Cenozoic motion on the Paleoproterozoic normal-sense high strain zones. Godin and Harris (2014) and Gibson et al. (2016) instead preferred to call on reactivation of the ancient normal-sense high strain zones to explain Cenozoic tectonic features in the Himalaya. Godin and Harris (2014) postulated that buried Paleoproterozoic foreland ridges controlled the locations of late Cenozoic north-trending grabens in the northern Himalaya and Gibson et al. (2016) suggested that reactivation of the high strain zones that bound the Faizabad ridge caused east-west differences in muscovite ^{40}Ar/^{39}Ar and monazite ^{208}Pb/^{232}Th ages in west-central Nepal. Again, however, neither model demands Cenozoic motion on the Paleoproterozoic high strain zones.

In contrast to the examples in the previous paragraphs, the following cases imply large magnitude Cenozoic reactivation. Their validity remains uncertain, however, because the Paleocene or younger structural overprint of any pre-Cenozoic tectonic fabrics was intense and nearly ubiquitous. Therefore, as in the foreland, geologists have not found robust indicators of renewed motion and workers rely on inferences mostly derived from stratigraphic correlations, interpretations of sediment provenance, and regional tectonic analysis.

Gehrels et al. (2003) found metamorphic, magmatic, structural, and stratigraphic evidence that Himalayan Assemblage B rocks participated in orogeny during late Cambrian-early Ordovician time and suggested that the South Tibet Detachment began as a thrust at this time. In their model, this ancient thrust was revived as a normal-sense high strain zone in Oligocene-Miocene time.

Several scientists, recognizing major pre-Cenozoic stratigraphic discontinuities across the MCT, proposed that Oligo-Miocene thrusting on the MCT reactivated a pre-Cenozoic high strain zone. However, despite agreement that these stratigraphic incompatibilities are present, no consensus exists about the possible pre-Cenozoic sense of motion on this high strain zone: strike-slip-, normal-, and thrust-sense motion all have been inferred. Brookfield (1993) explained pre-Cenozoic juxtaposition of sedimentary rocks deposited in contrasting water depths and/or at different times by proposing up to 1000 km of Late Jurassic-Early Cretaceous sinistral transcurrent motion of Assemblage B rocks relative to Assemblage A rocks and cratonal India, which suggests Late Jurassic-Early Cretaceous strike-slip on the proto-MCT. Vannay and Spring (1993) and Vannay and Steck (1995) instead postulated that Cenozoic contraction inverted Carboniferous transtensional normal faults observed entirely within Assemblage B rocks in northwestern India (see also Draganits et al., 2005). Yin (2006) expanded this idea by incorporating the widespread evidence for late Carboniferous to Permian rifting of northern India (Sinha-Roy, 1976; Brookfield, 1993; Garzanti, 1999). Yin (2006) proposed that the MCT began as a Carboniferous hinterland-dipping normal fault and that motion on the normal fault uplifted the footwall, allowing erosional removal of Ordovician to (lower) Carboniferous strata from footwall Assemblage A but not from hanging wall Assemblage B. Mottram et al. (2014) similarly suggested the MCT might reactivate a rift-related normal fault, but in their model this rifting occurred in Neoproterozoic time. A high strain zone with initial normal-sense motion is one of several ways to explain the younger-on-older relationship across the MCT found in hinterland exposures in the western Himalaya. Dubey et al. (2004), Dubey and Bhakuni (2007), Devrani and Dubey (2009), Dubey (2010), and Dubey (2014) also suggested that the Cenozoic Indus-Yarlung Suture, MCT, and Main Boundary Thrust are reactivated pre-Cenozoic normal-sense high strain zones largely because of the younger-on-older relationship across hinterland exposures of the MCT in the western Himalaya and perceived similarities between the MCT and these other Cenozoic thrusts. In contrast, DeCelles et al. (2000) proposed that the MCT began as a hinterland-dipping thrust that placed Assemblage B rocks onto Assemblage A rocks in Late Cambrian to Early Ordovician time. The authors inferred thrusting at this time largely because of evidence for Late Cambrian to Early Ordovician orogeny involving Assemblage B rocks (later summarized in Gehrels et al., 2003; 2006a; 2006b; Cawood et al., 2007).

5.1.2 Controls on reactivation of high strain zones that cut Himalayan Assemblage A

Many factors influence thrust-sense reactivation of ancient high strain zones during convergent orogeny. Hand and Sandiford (1999), Buiter et al. (2009), Stephenson et al. (2009), and Pinto et al. (2010) showed the effect of variable thicknesses of sedimentary rocks surrounding the high strain zones, and Del Ventisette et al. (2006), Panien et al. (2006), and Soto et al. (2007) discussed the importance of strong coupling between the sedimentary cover and metamorphic and igneous basement. Rocks weaker than their surroundings due to higher temperature (Hand and Sandiford, 1999; Buiter et al., 2009; Stephenson et al., 2009; Cunningham, 2013), the mineralogy and mechanical properties of the high strain zones and enclosing rocks (Panien et al., 2005; 2006; Buiter et al., 2009; Di Domenica et al., 2014; Munteanu et al., 2014), or fluid overpressure (Turner and Williams, 2004) are critical for reactivation. Dubois et al. (2002), Turner and Williams (2004), Panien et al. (2005), Del Ventisette et al. (2006), Cunningham (2013), Di Domenica et al. (2014), and Munteanu et al. (2014) emphasized the importance of favorable high strain zone orientations. In some cases, convergence slightly oblique to the dip direction of ancient normal faults promoted thrust-sense reactivation more than exactly parallel convergence and dip directions, however convergence highly oblique to the dip direction did not result in thrust-sense reactivation.

It is difficult to assess the importance of many of these factors in the Himalaya. The mineralogy and strength of the ancient high strain zones are poorly known because the Paleoproterozoic normal-sense high strain zones present in the subsurface in front of the Himalaya have not been penetrated by wells and the normal-sense high strain zones have not been recognized in outcrop. The fluid pressure in the high strain zones likewise is unknown. The thicknesses of the strata cut by and overlying the Paleoproterozoic normal-sense high strain zones are known: a maximum of 24 km from Arunachal to central Bhutan (Long et al., 2011b) and a maximum of 14 km west of central Bhutan (Robinson et al., 2006; Bhattacharyya and Mitra, 2009; Webb et al., 2011a; Khanal and Robinson, 2013; Robinson and Martin, 2014). Low temperature might not be a good explanation for the absence of reactivation because, at least in Sikkim, the exposed metasedimentary rocks generate more heat than mean upper continental crust (Faccenda et al., 2008). Further, parts of the northern Indian margin were located near flood basalt provinces, and thus inferred mantle hotspots, in the Early Cretaceous Epoch (Kent et al., 2002; Zhu et al., 2008) and also at ca. 66 Ma (Renne et al., 2015; Schoene et al., 2015).

Although all these ingredients undoubtedly played a role in controlling ancient high strain zone reactivation in the frontal part of the Himalaya, I suggest that the direction of convergence compared to ancient high strain zone dip direction may have been one of the most important components across much of the orogen. This factor seems relevant in the Himalaya because across the western and central sectors of the fold-thrust belt, the strikes of the Pliocene to Holocene thrusts are highly oblique to the strikes of the Paleoproterozoic normal-sense high strain zones in the foreland (Fig. 5). The existence of a northeast trending, linear, highly electrically conductive body in the middle and lower crust of Garhwal and Kumaon, interpreted to be related to the northeast trending rift structures in the foreland (Arora and Mahashabde, 1987), suggests the northeast trending high strain zones continue beneath the Himalaya in northwestern India. Stated another way, the Pliocene-Holocene thrusts may have broken new paths rather than reactivated ancient normal-sense high strain zones because the convergence direction was highly oblique to the dip direction of the normal-sense high strain zones.

This explanation can be partially tested because the strikes of the Pliocene to Holocene frontal thrusts bend along the fold-thrust belt such that in the eastern Himalaya, the thrusts are approximately parallel to the strikes of the foreland normal-sense high strain zones (Fig. 5). My interpretation predicts that some ancient normal-sense high strain zones in the eastern sector of the thrust belt were more likely to reactivate as thrusts than in the western and central portions. The Neogene-Quaternary Dauki Thrust on the southern edge of the Shillong Plateau could be an example. The Dauki Thrust is broadly parallel or slightly oblique to both buried Paleoproterozoic normal-sense high strain zones and the Narmada-Sone Fault. This geometry would be favorable for reactivation of one or more similarly-oriented normal-sense high strain zones as the Dauki Thrust starting in middle or late Miocene time (Clark and Bilham, 2008).

5.2 Large salients and recesses in Himalayan frontal deformation

Unlike the Himalaya between the western and eastern syntaxes, many other Phanerozoic orogens have salients and recesses with map-view amplitudes up to 200-500 km and half-wavelengths up to 600-1200 km (Fig. 4). To understand their absence in the Himalaya between the syntaxes, it is instructive to examine the origins of these large map-view bends in the frontal thrusts of other orogens. In this subsection I examine the proposed causes of large salients for two tectonic settings and compare them to Himalayan geologic history.

Hyndman et al. (2005), Currie and Hyndman (2006), and Currie et al. (2008), showed that continental backarcs are characteristically hotter, and thus weaker, than more inboard continental lithosphere. In these models, a hot, weak continental backarc permits stress transfer from the lithospheric plate boundary to foreland fold-thrust belts many hundreds of kilometers inboard of the plate boundary. In the northern Canadian Cordillera, Mazzotti and Hyndman (2002) argued that transpressive collision of the Yakutat terrane with the northwestern North American plate boundary drove the inboard shortening that resulted in the Mackenzie Mountains salient (Fig. 4A). A necessary component of this model is a preexisting hot and weak backarc region produced prior to terrane accretion.

The late Paleozoic Alleghanian pulse of the Appalachian orogeny resulted from collision of the continents Gondwana and Laurentia (Hatcher et al., 1989). Salients and recesses with amplitudes and half-wavelengths up to 200 and 900 km, respectively, formed in the frontal thrusts that resulted from this collision (Fig. 4D). Thomas (2006) showed that preexisting high strain zone architecture inherited from Neoproterozoic rifting determined the locations and sizes of these late Paleozoic salients and recesses. In the Thomas (2006) interpretation, the rifting controlled subsequent thrust belt architecture in two ways. First, former rift embayments accumulated thicker foreland basin strata than adjacent promontories, with large thickness changes across ancient transform faults. The greater and lesser sediment thicknesses promoted development of salients and recesses, respectively. Second, rift-related high strain zones reactivated during convergent orogeny. Vertical, lithosphere-scale rift-related transform faults reactivated as strike-slip faults, compartmentalizing salients and recesses, whereas upper crustal rift-related normal faults, which were listric and did not penetrate across the entire crust, reactivated as thrusts. Critically, the directions of Neoproterozoic divergence and late Paleozoic convergence were nearly parallel.

Comparison of the geologic history of these two orogens to that of the Himalaya leads to explanations about why the Himalaya does not have large salients and recesses between the syntaxes, at least in regards to these two mechanisms of salient and recess formation. First, Cenozoic arc and backarc processes are not relevant to the Himalayan foreland because the pre-collisional magmatic arc developed on a plate north of India, not the Indian plate where the Himalaya exists. Second, along the western and central Himalaya, Pliocene to Holocene thrusts strike at high-angles to Paleoproterozoic normal-sense high strain zones and broadly parallel to associated Paleoproterozoic transform faults. Accordingly, putative large stratigraphic thickness changes across the transform faults are oriented perpendicular to the Pliocene-Holocene thrusts, not parallel as in the Appalachians. Further, in part due to their orientation, the Paleoproterozoic normal-sense high strain zones experienced little or no reactivation as thrusts in the western and central Himalaya. Although Paleoproterozoic transform faults strike broadly parallel to the

Pliocene-Holocene thrusts in the western and central Himalaya, the vertical dips expected for the transform faults do not favor reactivation as thrusts. In summary, along the western and central Himalayan front, the ancient high strain zones and related sedimentary basins were not favorably oriented relative to the Pliocene-Holocene convergence direction to produce large salients and recesses in the Pliocene-Holocene thrusts. The results of analog simulation support the interpretation that the angle between the convergence direction and the strike of reactivated high strain zones is a control on the formation of map-view bends in orogens (Calignano et al., 2017).

One question remains: Why did the small salients and recesses in the Himalayan frontal thrusts form? The causes may have length scales similar to the sizes of the bends. For example, Bollinger et al. (2004) argued that the largest recess in the Main Frontal Thrust (Fig. 4C) resulted from indentation of the Faizabad ridge, a Paleoproterozoic horst (Fig. 5). Prasad et al. (2011) suggested that the Kangra Recess in the Main Central Thrust and other thrusts in northwestern India (Fig. 4C) at least partially resulted from thinner sedimentary cover over igneous and metamorphic rocks as compared to regions directly along strike. Goswami (2012) showed that a 5 km-amplitude reentrant in the frontal topography that sits astride the India-western Nepal border is controlled by two Cenozoic foreland faults that in turn likely are localized by a pre-Cenozoic basement high. In all these cases, there is no evidence that the pre-Cenozoic high strain zones reactivated during Cenozoic time.

6. HIMALAYAN ASSEMBLAGE B IS A SUSPECT TERRANE

Coney et al. (1980) defined a suspect terrane as possessing three qualities. (1) The suspect terrane rocks have an internally consistent geologic history. (2) The suspect terrane rocks have a very different geologic history than neighboring rocks. (3) The boundaries between the suspect terrane and neighboring rocks are fundamental discontinuities that cannot be explained by conventional unconformities or lithological changes. In practice, suspect terrane boundaries are always major high strain zones. In this section, I explain how Himalayan Assemblage B meets all parts of the definition of a suspect terrane for its pre-Cretaceous geologic history.

6.1 Suspect terrane definition part one: Internally consistent geologic history

The along- and across-strike consistencies of the times and compositions of Assemblage B deposition and intrusion are shown in Figure 9 and discussed in Section 3.2. An additional internal consistency is widespread ca. 500-470 Ma metamorphism and deformation (summarized in Gehrels et al., 2003; Cawood et al., 2007; see also Martin et al., 2007). Assemblage B thus meets part one of the definition of a suspect terrane.

6.2 Suspect terrane definition part two: Different geologic history than neighboring rocks

6.2.1 North of Assemblage B

The Indus-Yarlung Suture and Main Mantle Thrust separate Assemblage B from terranes to the north (Fig. 5). The Indus-Yarlung Suture consists of ophiolite, serpentinite melange, sedimentary melange, trench deposits, and forearc strata (Gansser, 1964; Cai et al., 2012; Guilmette et al., 2012; Hebert et al., 2012; Huang et al., 2015b; Orme et al., 2015; Orme and Laskowski, 2016). These rocks initially crystallized or were deposited mostly during Late Jurassic to Paleocene time and were structurally emplaced during Late Cretaceous to Paleocene time. At least some of the ophiolitic and sedimentary rocks appear to have been part of a coherent Cretaceous arc-trench system along the southern margin of the Lhasa terrane (Huang et al., 2015b; Orme and Laskowski, 2016). The suture zone rocks thus do not constitute pre-Late Jurassic terranes. Therefore, to determine whether the pre-Late Jurassic history of Himalayan Assemblage B renders it a suspect terrane, the appropriate comparison is to the terranes north of the Indus-Yarlung Suture and Main Mantle Thrust.

Figure 10 shows that the geologic history of Himalayan Assemblage B is quite different from that of the adjacent Lhasa terrane to the north; references for lithologies and ages are provided in Appendix C. Major differences include:

1. Ca. 1350-1250 Ma granite and tonalite are exposed in the southeastern Lhasa terrane, but granitic rocks of this age are unknown from Himalayan Assemblage B.
2. Ca. 880-800 Ma granite is widespread (but not voluminous) in Assemblage B but granite of this age has not been found in the southern and central Lhasa terrane.
3. Ca. 750 Ma gabbro and granite are exposed in the Nam Lake area of the central Lhasa terrane but magmatism of this age is unknown from Assemblage B.
4. Ca. 371-355 Ma gabbro and granite are exposed in the southeastern Lhasa terrane, but magmatism of this age is unknown from Assemblage B.
5. Mesozoic and Cenozoic arc intrusive and volcanic rocks are widespread in the southern and central Lhasa terrane but arc magmatism of this age is unknown from Assemblage B. The only Mesozoic magmatic rocks in Assemblage B are Early Cretaceous mafic rocks in southeastern Tibet. Zhu et al. (2008) inferred that heat from a mantle plume drove the melting to produce these mafic rocks. Cenozoic Assemblage B magmatism was limited to granitic rocks produced by the India-Asia collision and related processes.

In the western Himalaya, the uppermost Cretaceous to Eocene Ladakh batholith (Singh et al., 2007; White et al., 2011) and Cretaceous to Eocene Kohistan magmatic arc (Heuberger et al., 2007; Jagoutz et al., 2009) lie directly north of the Indus-Yarlung Suture and Main Mantle Thrust, respectively (Fig. 5). These magmatic rocks represent intra-oceanic magmatic arcs. The geologic history of these regions thus is different from adjacent Assemblage B, which does not contain a Cretaceous to Eocene magmatic arc.

6.2.2 South of Assemblage B

Figure 10 shows that the pre-Cretaceous geologic histories of assemblages A and B are very different from each other. Major differences include:

1. Ca. 1880-1830 Ma intrusion of granite and gabbro was ubiquitous in Assemblage A. In contrast, granite of this age possibly is present in Assemblage B only in northwestern India. There, it did not intrude Assemblage B sedimentary rocks but rather may have formed their depositional basement. Ca. 1880-1830 Ma gabbro has not been found in Assemblage B.
2. Paleoproterozoic to Lower Mesoproterozoic strata are omnipresent in Assemblage A but are unknown from Assemblage B.
3. Ca. 880-800 Ma granite is widespread (but not voluminous) in Assemblage B but is unknown from Assemblage A.
4. Ca. 510-460 Ma granite is widespread and voluminous in Assemblage B but is unknown from Assemblage A.
5. Ca. 500-470 Ma metamorphism and deformation were widespread in Assemblage B but Assemblage A contains no evidence for metamorphism or deformation at this time.

6. Assemblage B Neoproterozoic to Lower Carboniferous sedimentary rocks were deposited widely. In contrast, Assemblage A deposits in this age range were limited to Arunachal and Bhutan.
7. Upper Carboniferous and Permian sedimentary rocks were deposited extensively in Assemblage B, but Assemblage A deposits of this age are present only east of western Nepal.
8. Permian granite intruded Assemblage B in Pakistan and northwestern India but granitic rocks of this age are not present anywhere in Assemblage A.
9. Likewise, the Permian basalt that constitutes the Panjal Traps is widespread in Assemblage B in Pakistan and northwestern India, but Permian basalt is unknown from Assemblage A or northern cratonal India. Its absence in Assemblage A strata cannot be due to erosion because in central Nepal, Permian basalt makes up part of Assemblage B, but basalt is not present in Permian Assemblage A strata 120 km to the south (present distance).
10. In the western Himalaya, presumably Permian mafic dikes, some in swarms, intruded pre-Permian Assemblage B strata. However, Permian mafic intrusions are unknown from Assemblage A except for a poorly-dated, possibly Permian lamprophyre that intruded Assemblage A rocks in Sikkim.
11. Mesozoic deposits are widespread in Assemblage B. In contrast, Mesozoic strata older than uppermost Cretaceous are absent from Assemblage A, except for a small region of central Nepal (Taltung Formation; Fig. 8).

6.2.3 East and west of Assemblage B

The geology of the ends of the Himalayan Orogen is known less well than that of the portion between the syntaxes. However, Figure 2 shows that Himalayan Assemblage B likely does not continue westward past the Chaman Fault (DiPietro and Pogue, 2004) nor eastward past the Sagaing Fault. Thus, while acknowledging the geologic uncertainties at the western and eastern extremities of the orogen, Assemblage B meets part two of the definition of a suspect terrane because its geologic history differs significantly from terranes to the north, south, east, and west.

6.3 Suspect terrane definition part three: Bounded by high strain zones

Figures 2 and 5 show that the Indus-Yarlung Suture and Main Mantle Thrust separate the entire length of Himalayan Assemblage B from the Lhasa terrane, Ladakh batholith, and Kohistan magmatic arc. At the western and eastern extremities of the orogen, Assemblage B apparently ends at the Chaman and Sagaing faults, respectively. In the foreland direction, Figure 2 shows that the MCT currently juxtaposes Assemblage B against Assemblage A or other rocks of the Indian Shield between Pakistan and Arunachal. However, there is uncertainty about the presence of a high strain zone between Assemblage A and Assemblage B at the western and eastern ends of the orogen.

In frontal parts of the orogen in Pakistan, the Salt Range Thrust and related thrusts along strike placed hanging wall Neoproterozoic to Cenozoic shallow marine and continental strata over presumed Indian Shield rocks in the footwall. In this article (Appendix B), I argue that the hanging wall strata are part of Assemblage B, not Assemblage A, and thus label the Salt Range Thrust the MCT on Figure 2. If this stratigraphic correlation is correct, then Assemblage B satisfies part three of the definition of a suspect terrane in frontal parts of the orogen in Pakistan.

In hinterland regions of Pakistan, DiPietro and Pogue (2004) proposed that the contact between Assemblage A and Assemblage B currently is depositional. In this paper (Appendix A), I question this interpretation, arguing that in at least some areas mapped by these authors, the contact is likely a high strain zone.

The MCT currently separates Assemblage A and B rocks in Arunachal and Bhutan, making it a candidate high strain zone to satisfy criterion three of the suspect terrane definition in the eastern Himalaya. However, Yin et al. (2010a), Long et al. (2011b), McQuarrie et al. (2013), Webb et al. (2013), and DeCelles et al. (2016) correlated lower Paleozoic Assemblage A deposits in Arunachal and Bhutan (the Rupa Group and the Manas and Phuentsholing formations) with similar age strata in Assemblage B based on similarities in depositional ages and detrital zircon U/Pb age spectra. If correct, this depositional contiguity between assemblages A and B would rule out Assemblage B as a suspect terrane after the time of deposition of the correlative rocks. However, the depositional contiguity inferred by these authors is not required by the available data for the following two reasons. First, depositional age alone does not indicate nor even suggest depositional contiguity. Second, during early Paleozoic time, sediment was derived from all main parts of East Gondwana (DeCelles et al., 2000; Yoshida and Upreti, 2006; Cawood et al., 2007; Myrow et al., 2010; Gehrels et al., 2011; McKenzie et al., 2011a; McQuarrie et al., 2013) and homogenized during transport with the effect that detrital zircon age spectra from lower Paleozoic strata are similar no matter where on the northern margin of East Gondwana the sediment was deposited (Myrow et al., 2010; Gehrels et al., 2011). Thus the similar detrial zircon U/Pb ages indicate that the lower Paleozoic Assemblage B sediment was deposited somewhere on the northern margin of East Gondwana, not that it was deposited directly outboard of Assemblage A and thus correlates with Assemblage A deposits.

In summary, Himalayan Assemblage B satisfies part three of the definition of a suspect terrane on the hindward, western, and eastern edges of the assemblage. On the frontal side, Assemblage B indisputably meets part three of the definition along the central three-fourths of the orogen. In this article I argue that it likely fulfills this part of the definition in the eastern and western Himalaya as well.

7. PRE-CENOZOIC LOCATION OF HIMALAYAN ASSEMBLAGE B

Section 6 describes how Himalayan Assemblage B meets the three parts of the definition of a suspect terrane. A suspect terrane is not necessarily exotic with respect to its neighboring rocks; recognition of a suspect terrane indicates nothing about the magnitude of transport of the terrane relative to its neighbors. In Section 7, I examine four ideas for where the Himalayan Assemblage B terrane might have been located during the Neoproterozoic through Mesozoic eras and how it came to be juxtaposed against Himalayan Assemblage A. References for lithologies and depositional or intrusive ages are given in appendices A, B, and C.

7.1 Geosyncline Model

With reservation, Wadia (1919) applied geosyncline theory to the Himalaya. Wadia (1939) inferred that Greater Himalayan rocks consist of metasedimentary strata deposited in the Archean and Proterozoic eons plus metamorphosed mafic bodies and granite, and that the granite intruded at several different times, including the Cenozoic Era. Wadia (1939) posited that Greater Himalayan rocks are basement of the Indian shield that formed a geanticline, or ridge, that shed sediment into Paleozoic to Eocene Tethyan and Lesser Himalayan geosynclinal basins to the north and south, respectively (Fig. 6A; see also Saxena, 1971). Note that the depositional ages of lower Tethyan Himalayan rocks are now recognized to be Neoproterozoic. Several lines of evidence indict the geosyncline interpretation. First, both lower Tethyan Himalayan and at least the upper Greater Himalayan parts of Assemblage B were deposited at the same time, in contrast to the requirements of the Geosyncline Model. Second, Greater Himalayan strata were deposited in the Neoproterozoic to early Paleozoic eras, not during Archean and Paleoproterozoic time. In contrast, metamorphic and igneous basement rocks exposed in interior parts of the Indian peninsula mostly did crystallize in Archean and Paleoproterozoic time (Meert et al., 2010). Third, Greater Himalayan rocks were metamorphosed during Cambrian-Ordovician and Cenozoic time (Gehrels et al., 2003; Cawood et al., 2007; Martin et al., 2007; Kohn, 2014; Chakraborty et al., 2016), not in the Archean and Proterozoic eons as for interior parts of the Indian shield (Meert et al., 2010). Points two and three demonstrate the Greater Himalayan rocks are not basement of the Indian shield, contradicting the Geosyncline Model. Although Myrow et al. (2003) referred to the Geosyncline Model as the “Crystalline Axis Model”, this term can be confusing because Wadia (1919; 1939), Saxena (1971), Bhargava et al. (2011), and others used “crystalline axis” to refer to the belt of modern exposures of igneous and high-grade metamorphic rocks, whereas the model described in this subsection references a hypothetical ridge that existed in Neoproterozoic through Eocene time. The name “Geosyncline Model” both avoids this confusion and includes the depositional basins on either side of the supposed ridge.

7.2 Contiguous Deposition Outboard of India Model

The contact between Himalayan Assemblage B and Himalayan Assemblage A or other rocks of the Indian Shield is a major thrust-sense high strain zone everywhere between Pakistan and Arunachal (Fig. 2). Despite the undisputed presence of the high strain zone, many workers regard the original contact as depositional (e.g., Burrard and Hayden, 1908; Frank et al., 1973; Colchen et al., 1982; Searle, 1986; Myrow et al., 2003; DiPietro and Pogue, 2004; Yin, 2006; Cawood et al., 2007; Gehrels et al., 2011; McKenzie et al., 2011a; McQuarrie et al., 2013). This interpretation is allowed but not required by the data. The data also allow but do not require the alternative interpretation that the contact between Assemblage B and Assemblage A or the Indian Shield was never depositional and originated as a high strain zone. The Contiguous Deposition Outboard of India Model champions the former interpretation.

The Contiguous Deposition Outboard of India Model descended from the Geosyncline Model by placing Assemblage B deposition directly outboard of Assemblage A; a key difference is the absence of the geanticline (Fig. 6). There are several variants of the Contiguous Deposition Outboard of India Model (Fig. 6B). I include all these variations as modifications of the model because each proposes deposition of all Assemblage B strata and crystallization of all Assemblage B intrusions on the northern margin of India adjacent to Assemblage A. The simplest version calls for deposition on a contiguous, northward deepening passive margin on the northern edge of India starting in the Paleoproterozoic Era and continuing (with unconformities) through Early Paleocene time until India-Asia collision (Burrard and Hayden, 1908; Frank et al., 1973; Colchen et al., 1982; Searle, 1986; Myrow et al., 2003). Several scientists added one or more normal-sense high strain zones to this basic setup: throughout Proterozoic and Phanerozoic time (Dubey et al., 2004; Dubey and Bhakuni, 2007; Devrani and Dubey, 2009; Dubey, 2010; Dubey, 2014), during Middle to Late Ordovician time (Wang et al., 2012), in the Carboniferous Period (Sinha-Roy, 1976; Yin, 2006), or during the Cretaceous Period (Fuchs and Willems, 1990; van Hinsbergen et al., 2012; Huang et al., 2015a). Adding normal-sense high strain zones to the model does not change the interpretation of an original depositional contact between Assemblage A and Assemblage B strata deposited before and after motion on the normal-sense high strain zones. DeCelles et al. (2000), Gehrels et al. (2003; 2011), Cawood et al. (2007), Spencer et al. (2011), and Wang et al. (2012) argued that Cambrian-Ordovician convergence interrupted the Proterozoic to Paleocene north Indian passive margin setting; the latter three articles additionally postulated collision of a small continental block in latest Cambrian to Middle Ordovician time. This convergence and possible collision led to construction of a magmatic arc at ca. 530-490 Ma and concomitant deformation, metamorphism, and magmatism. In these models, the subduction zone and magmatic arc were located north of the part of Assemblage B that became the Tethyan Himalayan Sequence, and Cambrian and Ordovician Assemblage B sediment was deposited in a retro-arc setting. DeCelles et al. (2000), Gehrels et al. (2003; 2011), and Cawood et al. (2007) showed the magmatic arc as distinct and spatially separate from the ca. 510-460 Ma granitic intrusions in Assemblage B. I concur that the ca. 510-460 Ma intrusions in Assemblage B are unlikely to represent the magmatic arc because this Assemblage B magmatism was almost entirely felsic (Fig. 9), whereas magmatic arcs typically show a range of compositions from mafic to felsic (Quinn et al., 1997; Mamani et al., 2010; Cecil et al., 2012; Jagoutz and Schmidt, 2012; Chapman et al., 2014; Kent, 2014; Ducea et al., 2015; Kimbrough et al., 2015). In the models, following Cambrian-Ordovician orogeny, the northern edge of India returned to a passive margin state until Paleocene collision with Asia.

The Greater Himalayan Sequence contains abundant and widespread evidence for orogeny at a convergent margin during the Cambrian and Ordovician periods (summarized in Gehrels et al., 2003; Cawood et al., 2007; Wang et al., 2012). The data that support this conclusion include 510-460 Ma granite in all regions where Greater Himalayan rocks are exposed, metamorphic minerals that crystallized during the Cambrian-Ordovician periods, and Cambrian-Ordovician deformation. Further, Spencer et al. (2011) used whole rock major and trace element concentrations as well as fluid inclusion compositions to show that Greater Himalayan sediment in northwestern India was derived from an active continental margin, at least partially from magmatic sources. In Tethyan Himalayan rocks, an unconformity that spans Late Cambrian to Early Ordovician time is present across the orogen (Fig. 9; summarized in Wang et al., 2012; Myrow et al., 2016); this is an angular unconformity in western Nepal (Gehrels et al., 2006a) and part of northwestern India (Fuchs, 1982). Together, this evidence indicates that a Cambrian-Ordovician convergent margin is a necessary element of any model for the origin of Himalayan Assemblage B.

The main strength of the Contiguous Deposition Outboard of India Model is its simplicity. However, the following flaws raise doubts about its correctness. Individually, none of these challenges is a fatal blow to the Contiguous Deposition Outboard of India Model. Together, however, they sum to make it highly unlikely that Assemblage B was located directly outboard of Assemblage A before the Cretaceous Period.

(1) Ca. 1000-800 Ma shallow marine deposits are widespread in the Vindhyan and Ganga supergroups in peninsular India as well as in Himalayan Assemblage B, but putatively intervening Himalayan Assemblage A contains no strata that were deposited at this time (Figs. 2, 10; the Mandhali Formation may be an exception). If the sea flooded the Indian continent from the north as called for by the Contiguous Deposition Outboard of India Model (McKenzie et al., 2011a), allowing deposition of shallow marine sediment in Assemblage B and in peninsular India, there also should have been deposition in Assemblage A. Assemblage A does not record deformation, metamorphism, or magmatism at this time nor in the previous 800-1000 M.y., so it

is difficult to envision a tectonic explanation for any imaginary Early Neoproterozoic Assemblage A highland separating depositional basins to the north and south. In the western and central Himalaya, erosion of several kilometers of Lower to Middle Neoproterozoic strata from Assemblage A could explain the modern absence of deposits of this age there. Yin (2006) hypothesized that a north-dipping Carboniferous normal-sense high strain zone at the present-day location of the MCT uplifted Assemblage A rocks in its footwall, causing erosion of conjectural Ordovician to Carboniferous Assemblage A strata. This concept could be extended to include erosion of suppositious ca. 1000-800 Ma Assemblage A strata. However, there is no direct evidence for this high strain zone. Yin (2006) suggested its existence to explain the absence of Ordovician to Carboniferous deposits in Assemblage A and the fact that in the hinterland west of central Nepal, the MCT places younger rocks in its hanging wall on older rocks in its footwall. Yin (2006) set the age of normal-sense motion in the Carboniferous Period because Upper Carboniferous and Permian sediment was deposited in the eastern half of Assemblage A and because Assemblage B experienced Carboniferous-Early Permian rifting (Garzanti, 1999). Erosion in the normal fault scenario fortuitously would need to remove all ca. 1000-800 Ma Assemblage A deposits everywhere in the Himalaya without eliminating Paleoproterozoic Assemblage A strata anywhere. In the eastern Himalaya, the presence of Cambrian deposits rules out Carboniferous erosion of Lower Neoproterozoic strata. Likewise, Neogene erosion (e.g., Myrow et al., 2015) cannot explain the absence of Lower Neoproterozoic strata anywhere in Himalayan Assemblage A because Paleogene strata depositionally overlie Paleoproterozoic Assemblage A rocks west of central Nepal, and Upper Paleozoic plus Paleogene strata depositionally overlie Paleoproterozoic Assemblage A rocks in central Nepal and to the east. Neogene erosion would have removed these Phanerozoic deposits prior to removal of hypothetical underlying Neoproterozoic rocks.

(2) It is difficult to explain intrusion of granite at ca. 880-800 Ma in Himalayan Assemblage B but not in Himalayan Assemblage A if the two assemblages were adjacent to each other at this time. Further, granitic rocks also intruded the Aravalli Range area at ca. 870-800 Ma (Deb et al., 2001; van Lente et al., 2009; Just et al., 2011). If this Aravalli Range magmatism were related to the granite in Assemblage B as part of a contiguous craton to margin transect, it likewise is difficult to explain the absence of magmatism at this time in putatively intervening Assemblage A. The presence of the granite in Assemblage B but not Assemblage A cannot result simply from differences in hinterland-foreland position. In northwestern India, western Nepal, eastern Nepal, and Sikkim, Paleoproterozoic Assemblage A rocks exposed 80-100 km hindward of the frontalmost exposure of the MCT do not contain ca. 880-800 Ma granite (Fig. 2). In northern Pakistan, the ca. 823 Ma Black Mountain Complex crops out in Assemblage B as much as 50 km forward of exposures of Paleoproterozoic Assemblage A rocks, but ca. 880-800 Ma granite did not intrude these Assemblage A rocks (DiPietro and Isachsen, 2001). The claim that no major high strain zone separates Assemblage A from Assemblage B in northern Pakistan is a major pillar of support for the Contiguous Deposition Outboard of India Model (Appendix A). Thus in the no-major-high strain zone interpretation, the ca. 823 Ma Black Mountain Complex remains now at approximately the same position relative to Paleoproterozoic Assemblage A rocks as during the Neoproterozoic Era. That is, in this interpretation, the ca. 823 Ma Black Mountain Complex intruded 50 km forward of the most hindward Paleoproterozoic Assemblage A rocks that currently crop out, yet granite of this age did not intrude these Assemblage A rocks. Further, granitic magmatism in the Aravalli Range area occurred even

more forward, farther into the craton from the north, than the location of Assemblage A. In summary, intrusion of ca. 880-800 Ma granite in Assemblage B but not Assemblage A cannot be easily explained if Assemblage B were adjacent to Assemblage A at this time.

(3) The model requires conversion of a Proterozoic-early Cambrian passive margin to a subduction zone by middle Cambrian time. At least in the simple version shown by Cawood et al. (2007), sinking of oceanic lithosphere at its boundary with passive margin continental lithosphere led to spontaneous nucleation of the subduction zone. However, this mechanism of subduction initiation may be impossible in the Phanerozoic Eon (Stern, 2004). To be complete, future editions of the model must describe the process of subduction initiation.

(4) If a magmatic arc existed north of the Assemblage B depositional basin at ca. 510-490 Ma, we might expect (I) widespread arc volcanic rocks of this age in the Tethyan Sequence portion of Assemblage B and/or (II) magmatic arc clasts in coeval or slightly younger deposits. However, (I) middle or Upper Cambrian volcanic rocks may be absent from Assemblage B. One possible exception is in the Zanskar region of northwestern India, where Garzanti et al. (1986) reported arc-derived tuffaceous layers up to 60 cm thick in middle Cambrian strata. In contrast, Myrow et al. (2006a) did not find tuffaceous deposits in the same section. A second possible exception exists in Bhutan, where Tangri and Pande (1995) found andesite and basaltic andesite in the lower part of the Pele La Group. The depositional age of these volcanic rocks has not been directly determined, however. (II) With few exceptions, there was no input from an eroded magmatic arc into Assemblage B Lower and Middle Ordovician clastic strata; along most of the orogen, Lower and Middle Ordovician conglomerate clasts and sandstone lithic clasts are sedimentary and metasedimentary lithic fragments (Hayden, 1904; Garzanti et al., 1986; Pogue et al., 1992; Liu and Einsele, 1994; McQuarrie et al., 2013; Myrow et al., 2016). The exceptions

occur in western and central Nepal. In western Nepal, gravel-sized fragments in the basal conglomerate of the Ordovician Damgad Formation are quartzite and schist, but Damgad Formation sandstone is arkosic (Gehrels et al., 2006a). In central Nepal, granite clasts constitute the gravel-sized grains in the Ordovician Jurikhet Conglomerate, and most of the related sandstone is arkosic (Gehrels et al., 2006b). The Ordovician North Face Quartzite, located in a more northern part of central Nepal, likewise is arkosic (Bodenhausen et al., 1964). The abundance of ca. 1185-995 Ma detrital zircon coupled with the absence of ca. 500 Ma detrital zircon in pebbly quartz arenite from near the top of the Jurikhet Conglomerate led Gehrels et al. (2006b) to conclude that middle Proterozoic, not Cambrian-Ordovician, granite was the source for the granite gravel in the Jurikhet Conglomerate. Detrital zircon from the Ordovician arkosic sandstone yielded a peak in crystallization ages at ca. 520-480 Ma (Gehrels et al., 2006a; 2006b; 2011). The arkose could have been derived from equivalents of locally exposed Cambrian-Ordovician granite (Gehrels et al., 2006a; 2006b); there is no need to call on a hypothetical northern arc source for the arkose. The compositional immaturity of the arkose likewise argues against long-distance transport from a putative arc to the north of Assemblage B. Most paleocurrent determinations for exposed Assemblage B rocks indicate sediment transport broadly from south to north during Cambrian and Ordovician time (Garzanti et al., 1986; Bagati et al., 1991; Myrow et al., 2006a; 2006b). Northward sediment transport could explain the scarcity or absence of middle Cambrian to Ordovician volcanic flows and volcaniclastic rocks in Assemblage B, but not the scarcity or absence of ash fall tuff that was transported by air. The Late Cambrian-Early Ordovician unconformity that occurs in Assemblage B rocks along nearly all of the Himalaya cannot explain the absence of magmatic arc clasts in overlying Middle Ordovician conglomerate and sandstone because after the erosion represented by the unconformity, at least the intrusive part of the hypothetical arc should have been exposed at Earth's surface. Suppositious rifting after the end of the orogeny in the Middle Ordovician Epoch (Cawood et al., 2007; Wang et al., 2012) cannot explain the scarcity or absence of older arc volcanic and volcaniclastic rocks in Assemblage B. Further, such rifting fortuitously would have had to remove all traces of the magmatic arc, leaving no vestige to contribute sediment to the Middle and Upper Ordovician clastic strata. The rifting also would have had to remove all traces of southward sediment transport off the highstanding arc.

(5) If Assemblage B were thrust over Assemblage A during middle Cambrian-Middle Ordovician time as shown by DeCelles et al. (2000), we would expect contemporaneous deformation and metamorphism of footwall Assemblage A rocks (e.g., Figs. 9b1 and 9b2 in Wang et al., 2012). However, middle Cambrian-Middle Ordovician deformation and metamorphism have not been demonstrated in Assemblage A rocks, even where they are exposed far into the Himalayan hinterland.

(6) In the model, the Cambrian-Ordovician deformation and metamorphism of Assemblage B rocks occurred in a thick and regionally extensive retro-arc fold-thrust belt. Accompanying the fold-thrust belt, we would expect a widespread middle Cambrian to Ordovician foreland basin extending hundreds of kilometers south of the pre-Cenozoic position of the deformed and metamorphosed Assemblage B rocks. However, middle Cambrian to Ordovician foreland basin deposits are not present south of the deformed and metamorphosed Assemblage B rocks along most of the orogen. Although Assemblage A strata of this age in Bhutan and northeastern India (Manas and Phuentsholing formations, Rupa Group, possibly Miri Quartzite depending on its depositional age) could be interpreted as these foreland basin deposits, linking both these eastern Himalayan deposits as well as age-equivalent Shillong

Plateau strata to the Kuunga Orogeny in eastern India more easily explains the presence of the strata in eastern India but not in the remainder of the Himalaya (Section 4.2). Pre-Cenozoic erosion of suppositious middle Cambrian to Ordovician foreland basin deposits could explain their absence; this erosion could have occurred during Permian rifting, for example. However, there are no Permian deposits in Assemblage A west of central Nepal, which means that in the western half of the orogen, Permain rifting fortuitously would have had to remove all hypothetical middle Cambrian to Ordovician strata without leaving any Permian deposits in accompanying rift basins.

(7) Following the termination of subduction, ribbon continent collision, and orogeny, the model calls for Middle to Late Ordovician rifting of the arc, forearc, and collided continent away from northern India. However, Himalayan Assemblage B contains neither Middle to Late Ordovician normal-sense high strain zones nor stratigraphic evidence for normal faulting at this time.

(8) It is difficult to explain intrusion of granite at ca. 290-260 Ma in western Himalayan Assemblage B but not in Himalayan Assemblage A if the two assemblages were adjacent to each other at this time. Like for the ca. 880-800 Ma granite discussed in point 2, differences in hinterland-foreland position cannot simply explain the absence of the ca. 290-260 Ma granite in Assemblage A because in northern Pakistan, the ca. 265 Ma Swat granitic gneiss crops out 50 km forward of the most hindward exposures of Paleoproterozoic Assemblage A rocks (DiPietro and Isachsen, 2001). In the context of the model, translation of Assemblage B relative to Assemblage A after the Permian Period cannot explain the lack of ca. 290-260 Ma granite intrusion into these Paleoproterozoic Assemblage A rocks because support for the Contiguous

Deposition Outboard of India Model relies on the interpretation that no high strain zone exists between the assemblages in northern Pakistan (Appendix A).

(9) Similarly, it is difficult to explain the presence of abundant, presumably Permian mafic dikes, some in swarms, in western Assemblage B but not western Assemblage A if the two assemblages were adjacent during intrusion of the dikes.

(10) It is difficult to explain deposition of Permian basalt in Assemblage B in central Nepal but neither basalt nor volcaniclastic sediment in coeval Assemblage A rocks to the south in central Nepal if the two assemblages were near each other at this time.

(11) Similarly, it is difficult to explain deposition of the Abor Volcanics in easternmost Assemblage A but not in eastern Assemblage B if the two assemblages were adjacent to each other during deposition of the Abor Volcanics.

(12) To help locate continental blocks within Gondwana, Torsvik and Cocks (2013) placed most large igneous provinces above a “plume generation zone” located at the edge of a large low shear-wave velocity province in the lowermost mantle. The basis for such placement is the observation that most Cenozoic deep mantle plumes are found on the edges of the two modern large low shear-wave velocity provinces directly above the core-mantle boundary (see also French and Romanowicz, 2015; Doubrovine et al., 2016). If Assemblage B were located adjacent to northern India during the Permian Period, the Panjal Traps Large Igneous Province (Shellnutt et al., 2015) would violate this terrane placement rule: a large igneous province would be located not at the margin of the African large low shear-wave velocity province, but within it (Fig. 11). Further, contrary to the terrane placement rule used by Torsvik and Cocks (2013), there would be no magmatism above the plume generation zone, in eastern Assemblage B.

(13) During the Triassic Period, India was rotated clockwise in map view relative to its current orientation such that the present west-east trend of the northern margin of India was oriented northwest-southeast (Fig. 12). This paleo-orientation means that the paleolatitude of Himalayan Assemblage B rocks should have been monotonically more southerly from the western to the eastern Himalaya if Assemblage B were located directly outboard of the Indian craton during Triassic time. Figure 13 and Table 3 show paleolatitude determinations from Triassic Assemblage B rocks. Although the geographic distribution of the sample localities does not encompass the entire longitudinal span of the Himalaya, the existing data show no hint of an eastward increase in southerly paleolatitude.

(14) If Triassic, Jurassic, and Lower Cretaceous Assemblage B marine strata were deposited outboard of Assemblage A as part of a contiguous passive margin, we might expect deposition at this time in Assemblage A as well. Imaginary Assemblage A depositional environments could be shallow marine, rivers draining toward the sea where Assemblage B strata were deposited, or other continental deposits. However, Assemblage A contains no Triassic or Jurassic strata anywhere, and the only Lower Cretaceous Assemblage A deposits are ca. 118 Ma sandstone and basalt restricted to central Nepal (Taltung Formation; Fig. 8).

(15) In northwestern India, Webb et al. (2011a) correlated the ca. 1850 Ma Baragaon granitic gneiss, which probably formed the depositional substrate for Himalayan Assemblage B, to the ca. 1866 Ma Wangtu granitic gneiss, which intruded Himalayan Assemblage A (Richards et al., 2005). Webb et al. (2011a) argued that the similarities in lithologies and crystallization ages of the two granites require connection of assemblages A and B at ca. 1850 Ma. However, many continents experienced ca. 1880-1780 Ma felsic magmatism, including Arabia (Whitehouse et al., 2001; Stern and Johnson, 2010), Australia (Griffin et al., 2000; Sheppard et

al., 2001; Bagas, 2004; Rubatto et al., 2006; Crispe et al., 2007; Bierlein et al., 2008; Reid et al., 2008), and East Antarctica (Will et al., 2009; Goodge et al., 2013). Thus the ca. 1850 Ma Baragaon granite perhaps ties Himalayan Assemblage B to Gondwana, but certainly not to northern India specifically.

(16) Likewise, ca. 600-480 Ma detrital zircon is common in Ediacaran and younger strata from East Gondwana (Veevers, 2000; 2012; Goodge et al., 2004; Kolodner et al., 2006; Cawood et al., 2013; Xu et al., 2013). Detrital zircon of this age in Himalayan Assemblage B Ediacaran-Ordovician deposits thus ties the assemblage to East Gondwana in general, not the northern margin of India specifically.

Exposed frontal Assemblage B strata in most parts of the western Himalaya experienced greenschist facies or lower-grade metamorphism and were not intruded by ca. 510-460 Ma granite. Examples include the deposits in the Salt Range of Pakistan and those near Shimla in northwestern India (Fig. 9). In contrast, many exposed frontal Assemblage B strata in the central and eastern Himalaya were metamorphosed to amphibolite facies and intruded by ca. 510-460 Ma granite. Examples include some of the rocks in the Almora-Dadeldhura Klippe, the Kathmandu Nappe, and the frontal Assemblage B rocks in eastern Nepal, Sikkim, and western Bhutan (Fig. 9; Johnson, 2005). Along the entire Himalaya, Assemblage B rocks exposed to the rear similarly experienced amphibolite facies or higher-grade metamorphism and intrusion of ca. 510-460 Ma granite (Fig. 9). Contrasts in foreland versus hinterland position cannot simply explain these disparities because the western, central, and eastern frontal rocks all are at approximately the same structural position, yet have dissimilar properties. Instead, the differences must be due to different exposure depths of the Cambrian-Ordovician and Cenozoic crust. Western frontal Assemblage B rocks are the shallow parts of the crust that never were metamorphosed above greenschist facies nor intruded by granite. Central and eastern frontal Assemblage B rocks, as well as all hinterland Assemblage B rocks, are deeper parts of the Cambrian-Ordovician and Cenozoic crust.

Many workers accept the interpretation that in hinterland exposures, the MCT placed younger hanging wall rocks on older footwall rocks. This relationship was one line of evidence that led Dubey et al. (2004), Yin (2006), and Dubey (2014) to suggest that the MCT began as an older normal-sense high strain zone that was reactivated as a thrust in Cenozoic time. However, both in Bhutan and in central Nepal, the proximal hanging wall consists of Neoproterozoic rocks (lower part of Assemblage B) and the proximal footwall is composed of Paleozoic strata (Gondwana Group or Jaishidanda Formation), an older-on-younger relationship. An older-on-younger relationship may be a common arrangement in central Nepal and to the east, where Paleozoic successions are present in Assemblage A. This setup is not present west of central Nepal because Paleozoic Assemblage A strata are absent, so Paleoproterozoic Assemblage A rocks form the proximal footwall of the MCT in hinterland exposures. However, in some frontal locations west of central Nepal, the MCT placed Neoproterozoic strata in the hanging wall on terminal Cretaceous or Cenozoic deposits in the footwall (Figs. 2, 3A).

7.3 Noncontiguous Deposition Outboard of India Model

Jain and Kanwar (1970) proposed that Neoproterozoic to Cretaceous Assemblage B strata were deposited at least 5000 km outboard of India's northern margin and that Assemblage B accreted to the northern margin during Cenozoic northward drift of India (Fig. 6C). Similar to the Contiguous Deposition Outboard of India Model, the following flaws combine to make it highly unlikely that the Noncontiguous Deposition Outboard of India Model is correct.

1. All major sectors of East Gondwana, including Australia, East Antarctica, India, and East Africa or Arabia, contributed sediment to the Neoproterozoic to Jurassic Assemblage B basin (DeCelles et al., 2000; Yoshida and Upreti, 2006; Cawood et al., 2007; Myrow et al., 2010; Gehrels et al., 2011; McKenzie et al., 2011a; McQuarrie et al., 2013). It is unlikely that sand and mud from East Gondwana could be transported across at least 5000 km of ocean and then up into shallow-water depositional environments, as required by the model.
2. The model provides no explanation for the ca. 880-800, 510-460, or 290-260 Ma granite in Assemblage B.
3. 5000 km equates to 45° outboard of the northern margin of cratonal India. At the beginning of the Triassic Period, the northern edge of cratonal India was located between 31° and 50° south (Torsvik and Cocks, 2013; their figure 18) and by the end, the northern edge was located between 9° and 27° south (Fig. 12). Thus the Noncontiguous Deposition Outboard of India Model implies that Assemblage B was located near or north of the equator during Triassic time. However, all paleolatitude determinations place Assemblage B at moderate southerly latitudes during the Triassic Period (Table 3; Fig. 13).
4. Assemblage B was at the latitude of cratonal India in the southern hemisphere at ca. 118 Ma (van Hinsbergen et al., 2012). This location likewise contradicts the model.
5. In the model, accretion of Assemblage B occurred in a Cenozoic subduction zone between Assemblage A and Assemblage B. Therefore, near the boundary between these assemblages, we would expect to find subduction zone rocks such as ophiolites, accretionary complexes, or subduction melange (Encarnacion, 2004; Hopson et al.,

2008; Dumitru et al., 2010; John et al., 2010; Hernaiz Huerta et al., 2012; Thanh et al., 2012; Aoya et al., 2013; Ichiyama et al., 2014). However, none of these rock types is present in Assemblage A or Assemblage B near their contact.

6. Similarly, we would expect to find Cenozoic low dT/dP metamorphism of the rocks near the putative paleo-subduction zone (Brown, 2010). However, low dT/dP metamorphism near the contact between Assemblage A and Assemblage B has not been found, although it is possible that younger, higher dT/dP metamorphism obscured any older, low dT/dP metamorphism.
7. A Cenozoic subduction zone between Assemblage A and Assemblage B implies the existence of a Cenozoic magmatic arc within either Assemblage A or Assemblage B, depending on the dip of the subduction zone. Cenozoic magmatic arc rocks are not present in Assemblage A or Assemblage B, however.

7.4 Assemblage B Deposition and Intrusion East of India Model

Brookfield (1993) argued that approximately 1000 km of sinistral transcurrent motion juxtaposed Assemblage B against Assemblage A during Jurassic to Early Cretaceous time. The flaws with the Geosyncline, Contiguous Deposition Outboard of India, and Noncontiguous Deposition Outboard of India models described in the preceding subsections make the transcurrent emplacement option attractive. Accordingly, in this subsection I argue for Neoproterozoic to Middle Jurassic deposition and intrusion of Assemblage B north of western Australia followed by approximately 3000 km of left-handed motion of Assemblage B relative to Assemblage A and cratonal India during the Late Jurassic to Early Cretaceous epochs (Fig. 6D).

This motion juxtaposed Assemblage B against Assemblage A across a system of transcurrent faults.

The Assemblage B Deposition and Intrusion East of India Model satisfies all data in Section 3 and does not suffer from the flaws described in Sections 7.1, 7.2, and 7.3. The following points also support the Assemblage B Deposition and Intrusion East of India Model. Some of the following points also can be explained by the alternative models listed in Sections 7.1, 7.2, and 7.3.

1. Detrital zircon age spectra from Neoproterozoic and Paleozoic Assemblage B deposits are similar to those from Lhasa terrane and Qiangtang terrane strata (Gehrels et al., 2011) because Himalayan Assemblage B was laterally contiguous along strike with parts of these Tibetan terranes during some of this interval (Fig. 6D).
2. Ca. 880-800, 510-460, and 290-260 Ma granite intruded Neoproterozoic Assemblage B strata but not Paleoproterozoic-Lower Mesoproterozoic Assemblage A rocks because the assemblages were not adjacent to each other during Neoproterozoic to Paleozoic time.
3. Middle Cambrian to Middle Ordovician orogeny affected Assemblage B but not Assemblage A because these rock packages were not adjacent to each other during that time interval. There are no middle Cambrian to Middle Ordovician foreland basin deposits presently in front of Assemblage B (that is, in Assemblage A) because the orogeny occurred when Assemblage B was located north of Australia. According to the Assemblage B Deposition and Intrusion East of India Model, these foreland basin deposits would be located in northwestern Australia or the northern sector of Himalayan Assemblage B, depending on the polarity of subduction during the orogeny (see below for further discussion of subduction polarity).

4. The depositional ages of lower Paleozoic strata in the Carnarvon and northern Perth basins of northwestern and western Australia are not well known. However, Mory et al. (2003) inferred an unconformity between an unnamed deposit of possible Cambrian or earliest Ordovician age and the terminal Ordovician to Lower Silurian Tumblagooda Sandstone (Kettanah et al., 2015). The unconformity in Himalayan Assemblage B caused by the middle Cambrian to Middle Ordovician orogeny represents Late Cambrian through Early Ordovician time. The Himalayan unconformity thus spans part of the interval represented by the northwestern Australian unconformity. There are many possible tectonic explanations for the northwestern Australian unconformity. However, the synchroneity in the two regions is easily explained if Assemblage B were located outboard of northern Australia during Cambrian-Ordovician time so that the same tectonic event caused the unconformity in both Assemblage B and northwestern Australia. This tectonic event may have involved collision among Himalayan Assemblage B, Australia, and the Tarim and North China cratons (Han et al., 2016).
5. If Himalayan Assemblage B were located north of Australia, the western part of Assemblage B would lie above the plume generation zone of Torsvik and Cocks (2013) in the Permian Period but the eastern sector of Assemblage B would not (Fig. 6D), explaining the presence of the Lower Permian Panjal Traps (Shellnutt et al., 2015) and possibly related mafic dikes only in the western part of Assemblage B.
6. In the model, the Permian basalt in the eastern part of the Southern and Central Lhasa terrane is contiguous with the Panjal Traps basalt of western Himalayan Assemblage B (Fig. 6D). The basalt from both terranes restores atop the plume generation zone of Torsvik and Cocks (2013).

7. Cai et al. (2016) showed that the eastern part of Assemblage B received sediment from northwestern Australia and/or Australian fringing terranes during the Late Triassic Epoch. Location of Assemblage B outboard of northwestern Australia at this time easily explains this provenance.
8. The MCT did not repeat pre-Cretaceous stratigraphy because footwall rocks (Assemblage A) and hanging wall rocks (Assemblage B) did not share depositional contiguity until the middle Early Cretaceous Epoch. In central Nepal, correlative middle Lower Cretaceous deposits are present in Assemblage A and Assemblage B, and these strata could be viewed as repeated across the MCT plus the other high strain zones that intervene between the exposures of these rocks. Similarly, Cenozoic deposits in both assemblages along most of the orogen could be treated as repeated, although in many locations these deposits are not in the proximal footwall or hanging wall of the MCT.

When did the left-handed transcurrent movement occur? Brookfield (1993) argued for Jurassic-Early Cretaceous time, and the geologic histories of Assemblage A and Assemblage B support this interpretation. As discussed in Sections 6.2 and 7.2, the geologic histories of the two Himalayan assemblages are inconsistent with their juxtaposition during the Proterozoic to Jurassic interval. Although the eastern half of Assemblage A and nearly all of Assemblage B contain Upper Carboniferous to Lower Permian glacial deposits such as diamictite, glaciation affected much of Gondwana during this interval (Gehrels et al., 2011; Torsvik and Cocks, 2013), so the shared glacial deposits tie Assemblage A and Assemblage B to Gondwana, not to each other. The oldest potential geologic tie between Assemblage A and Assemblage B consists of lithologically compatible middle Lower Cretaceous deposits in central Nepal: Taltung Formation basalt and conglomerate with mafic clasts in Assemblage A (Upreti, 1996) and Chukh Group mafic volcaniclastic conglomerate and sandstone in Assemblage B (Garzanti, 1999). Sakai (1983) correlated the Taltung basalt with the ca. 118 Ma Rajmahal basalt of northeastern India south of the Himalaya (Kent et al., 2002), providing a date for Taltung basalt deposition. If the similar lithologies in the Taltung Formation and Chukh Group do not in fact demonstrate a depositional link between Assemblage A and Assemblage B, then the oldest shared depositional history between the assemblages may consist of the uppermost Cretaceous to Paleocene strata that are widespread in both assemblages. Plate reconstructions provide another means to assess favorable intervals for left-handed transcurrent movement. The initiation of southeastward motion of India away from Africa at ca. 160 Ma and/or the northward motion of West Burma relative to Australia at ca. 156 Ma (Seton et al., 2012) are plate-scale events that may have instigated the westward translation of Himalayan Assemblage B relative to India and Australia. The separation of India from East Antarctica and Australia starting at ca. 132 Ma (Seton et al., 2012) could have ended the left-handed offset of Assemblage B. In conclusion, based on the geologic histories of Assemblage A and Assemblage B and considerations from plate reconstructions, the left-handed transcurrent motion that juxtaposed the two assemblages most likely occurred during the Late Jurassic to middle Early Cretaceous interval.

The heart of the Assemblage B Deposition and Intrusion East of India Model is deposition of Assemblage B east of northern India during Neoproterozoic to Middle Jurassic time followed by Late Jurassic to Early Cretaceous juxtaposition of Assemblage B against Assemblage A along a left-handed transcurrent fault system. The speculation in the remainder of this paragraph is peripheral to the core model. The Late Jurassic-Early Cretaceous transcurrent fault north of India could have been reactivated as part of the late Early to Late Cretaceous extensional fault system proposed by Fuchs and Willems (1990). I further speculate that the transcurrent fault north of western Australia (Fig. 6D) similarly could have converted to extensional motion based on the similar orientations of the two transcurrent faults. Seton et al. (2012) showed rifting north of northwestern Australia during Late Jurassic to earliest Cretaceous time.

McKenzie et al. (2011b) argued that the North China Craton was located near the eastern part of Himalayan Assemblage B during the Cambrian Period based on similarities in detrital zircon U/Pb age spectra and shared trilobite species. The Assemblage B Deposition and Intrusion East of India Model allows the North China Craton to be positioned near the eastern sector of Assemblage B at this time if both were located north of western Australia.

Ali and Aitchison (2014) proposed that a right-handed transform fault affected the central and eastern parts of the northern Indian margin between ca. 132 and 110 Ma. This interpretation does not conflict with the Assemblage B Deposition and Intrusion East of India Model because the proposed dextral motion occurred after the end of the left-handed offset required by the Assemblage B Deposition and Intrusion East of India Model.

The following data and observations either challenge the Assemblage B Deposition and Intrusion East of India Model or they are more easily explained by the Contiguous Deposition Outboard of India Model.

1. It is unknown whether the contact between the Neoproterozoic Mandhali/Basantpur Formation in the footwall of the Tons Thrust and Paleoproterozoic-Lower Mesoproterozoic Assemblage A strata is depositional or a high strain zone. The presence of Neoproterozoic strata deposited atop Paleoproterozoic-Lower Mesoproterozoic Assemblage A rocks in northwestern India would not rule out the Assemblage B

Deposition and Intrusion East of India Model because the model makes no prediction about Neoproterozoic deposition in Assemblage A. However, the presence of similar Neoproterozoic deposits in both assemblages in northwestern India may be more easily explained if Assemblage B were deposited directly outboard of Assemblage A.

2. Torsvik et al. (2009) measured paleolatitude recorded by hematite in hand samples of folded meta-red beds collected from six sites around a plunging anticline in the Lower Ordovician Tethyan Himalayan Shian Formation in the Parahio Valley of Spiti, northwestern India. Although the mean of the paleolatitude measurements places this part of Assemblage B in a position that appears to be too far south and thus tectonically unlikely, the uncertainty on the results permits deposition adjacent to the Indian craton but apparently not adjacent to western Australia. Similarly, Zou et al. (2013) determined the paleolatitude of Ordovician carbonate and clastic strata north of Mount Everest to be farther south than appears tectonically reasonable given Ordovician reconstructions of Gondwana. Taken at face value, the results of Zou et al. (2013) indicate that during the Ordovician Period, Assemblage B was too far south to be located not only adjacent to western Australia, but also to most of cratonal India, outside the reported uncertainty. Assessing the significance of these two extreme southern apparent paleolatitude measurements for the Assemblage B Deposition and Intrusion East of India Model will require more data from these and other localities.

3. There are no structural observations that directly indicate the existence of a Late Jurassic-Early Cretaceous strike-slip fault at the location of the Cenozoic MCT. An explanation for this absence could be the strong ductile overprint of older structural fabrics in rocks near the MCT during Cenozoic thrusting.

Because the northern margin of India was oriented northwest-southeast during the Triassic and Jurassic periods, in principle, paleolatitude determinations for this interval from the longitudinal span of Himalaya Assemblage B permit discrimination between the Contiguous Deposition Outboard of India and Assemblage B Deposition and Intrusion East of India models (Fig. 12). The Contiguous Deposition Outboard of India Model predicts increasing southerly paleolatitudes from western to eastern Himalayan Assemblage B rocks, whereas the Assemblage B Deposition and Intrusion East of India Model predicts approximately constant paleolatitude. However, existing paleomagnetic paleolatitude determinations do not rule out either model (Fig. 13, Table 3).

Detrital zircon U/Pb ages from Assemblage A and Assemblage B strata cannot rule out the Contiguous Deposition Outboard of India Model or the Assemblage B Deposition and Intrusion East of India Model. During Neoproterozoic to Jurassic time, the sources of sediment into Assemblage A and Assemblage B basins included all major sectors of East Gondwana, including Australia, East Antarctica, India, and East Africa or Arabia (DeCelles et al., 2000; Yoshida and Upreti, 2006; Cawood et al., 2007; Myrow et al., 2010; Gehrels et al., 2011; McKenzie et al., 2011a; McQuarrie et al., 2013). Further, this detritus was homogenized so that the detrital zircon age spectra are nearly identical along the length and breadth of the Himalaya as well as across the Lhasa and Qiangtang terranes (Myrow et al., 2010; Gehrels et al., 2011). Deposition outboard of India or northwestern Australia can explain equally well the cosmopolitan provenance of Neoproterozoic to Jurassic Assemblage A and Assemblage B detrital zircon (Fig. 6D, 11). For the same reasons, no method of sediment provenance determination can distinguish between the two models.

The location of Himalayan Assemblage B during Neoproterozoic to Middle Jurassic time has implications for mineral exploration in the Himalaya and beyond. For example, gold-antimony deposits in Assemblage B in southern Tibet are related to syn-sedimentary Sedex sulfide layers interbedded with the Assemblage B Jurassic strata (Zhai et al., 2014). If these strata were deposited north of western Australia, one would explore in northern Australia, Timor, or New Guinea for correlative Sedex layers along depositional strike (Fig. 6D). In contrast, if the Jurassic Assemblage B strata were deposited on the northern margin of India, along-strike correlative strata would be expected in southern Australia or the conjugate part of East Antarctica (Fig. 11).

8. COMPARISONS TO EASTERN INDIA AND THE NAMCHE BARWA REGION

The Namche Barwa and Shillong Plateau/Mikir Hills regions share similar Late Paleoproterozoic to Cambrian depositional and intrusive histories (Fig. 10; references in Appendix C). Parallels include intrusion of granite at ca. 1600 and 500 Ma and deposition of a mostly clastic sedimentary succession during Neoproterozoic to Cambrian time. In the Namche Barwa region, sandstone additionally was deposited after ca. 480 Ma and granite intrusion and migmatization occurred at ca. 30-24 and 5 Ma. In the Shillong Plateau/Mikir Hills, granite additionally intruded at ca. 1110-1080 Ma. In the Shillong region, deposition of Upper Carboniferous to Lower Permian diamictite and overlying sandstone was followed by intrusion of alkaline, mafic, and ultramafic rocks and deposition of basalt at ca. 115-105 Ma. A mostly clastic succession was deposited in the Shillong Plateau/Mikir Hills in Late Cretaceous and Cenozoic time.

The pre-Late Cretaceous depositional and intrusive histories of the Namche Barwa and Shillong Plateau/Mikir Hills regions contrast with those of Himalayan Assemblage A and Himalayan Assemblage B. The following rock-forming events distinguish the Namche Barwa and Shillong Plateau/Mikir Hills regions from Himalayan Assemblage A. (1) Deposition of a several kilometer-thick Paleoproterozoic sedimentary succession was widespread in Assemblage A but sedimentary rocks of this age may be absent from the Namche Barwa and Shillong Plateau/Mikir Hills regions. (2) Ca. 1880-1830 Ma granite is widespread in Assemblage A but may be absent from the Namche Barwa and Shillong Plateau/Mikir Hills regions. (3) Ca. 1600 Ma granite is present in the Namche Barwa and Shillong Plateau/Mikir Hills regions but absent from Assemblage A. (4) Ca. 1100 Ma granite is present in the Shillong Plateau/Mikir Hills region but absent from Assemblage A. (5) Ca. 500 Ma granite is present in both the Namche Barwa and Shillong Plateau/Mikir Hills regions but absent from Assemblage A.

The following rock-forming events differentiate the Namche Barwa and Shillong Plateau/Mikir Hills regions from Himalayan Assemblage B. (1) Ca. 1600 Ma granite is present in the Namche Barwa and Shillong Plateau/Mikir Hills regions but absent from Assemblage B. (2) Ca. 1100 Ma granite is present in the Shillong Plateau/Mikir Hills region but absent from Assemblage B. (3) Ca. 880-800 Ma granite is widespread in Assemblage B but may be absent from both the Namche Barwa and Shillong Plateau/Mikir Hills regions. (4) In the eastern Himalaya, Assemblage B contains clastic rocks deposited between Triassic and Early Cretaceous time, but supracrustal rocks of this age may be absent from the Namche Barwa and Shillong Plateau/Mikir Hills regions.

The Central Indian Tectonic Zone–Chhotanagpur Gneissic Complex–North Singhbhum Mobile Belt trends northeast across central India between the Narmada-Sone Fault and the

Dharwar, Chhattisgarh-Bastar, and Singbhum cratons (Fig. 5). It resulted from ca. 1600 and ca. 1000 Ma suturing of the South and North Indian blocks (Bhowmik et al., 2012). These authors concluded that the Shillong Plateau/Mikir Hills region is the eastern end of the Central Indian Tectonic Zone–Chhotanagpur Gneissic Complex–North Singhbhum Mobile Belt based on two lines of evidence. First, the Shillong Plateau and Mikir Hills lie along trend of the Central Indian Tectonic Zone–Chhotanagpur Gneissic Complex–North Singhbhum Mobile Belt. Second, this suture zone experienced ca. 1600 and 1100-950 Ma metamorphism and magmatism (see also Bhowmik et al., 2014), similar to the crystallization ages of granite bodies in the Shillong Plateau/Mikir Hills. Working at the same time, Zhang et al. (2012) argued that the Paleoproterozoic-Mesoproterozoic rocks of the Namche Barwa region also are part of this suture zone. I concur that both the ca. 1600 Ma magmatism in the Namche Barwa and Shillong Plateau/Mikir Hills regions and the ca. 1100 Ma magmatism in Shillong/Mikir correlate well with the metamorphic and intrusive history of the Central Indian Tectonic Zone–Chhotanagpur Gneissic Complex–North Singhbhum Mobile Belt. However, these links do not explain the ca. 500 Ma granite in both the Shillong Plateau/Mikir Hills and Namche Barwa regions because ca. 500 Ma metamorphism and magmatism is unknown from the Central Indian Tectonic Zone–Chhotanagpur Gneissic Complex–North Singhbhum Mobile Belt. The ca. 500 Ma magmatism likely resulted from the late Ediacaran to Cambrian Kuunga Orogeny on the eastern margin of India, as recorded in the Eastern Ghats (Mezger and Cosca, 1999; Crowe et al., 2001; Collins and Pisarevsky, 2005; Cawood and Buchan, 2007; Simmat and Raith, 2008; Upadhyay et al., 2009; Somnath Dasgupta et al., 2013). The Cambrian pulse of orogeny in the Pinjarra Orogen is another potential cause of ca. 500 Ma granite in the Shillong Plateau/Mikir Hills and Namche Barwa regions (Collins, 2003; Markwitz et al., 2017).

The conclusion that the rocks of the Namche Barwa region share Late Paleoproterozoic-Mesoproterozoic tectonic affinity with rocks of the Shillong Plateau/Mikir Hills region and the Central Indian Tectonic Zone–Chhotanagpur Gneissic Complex–North Singhbhum Mobile Belt matches the interpretation of Guo et al. (2017), who wrote that the ca. 1600 Ma granitic gneiss in the Namche Barwa region represents the crystalline basement of the Indian craton. In contrast to my conclusions, however, Guo et al. (2017) postulated that the Neoproterozoic to Cambrian Namche Barwa strata were deposited on the northern margin of India and thus originally shared depositional relationships with Assemblage A and Assemblage B. Guo et al. (2017) based this interpretation on similar detrital zircon U/Pb ages in Neoproterozoic to Cambrian Namche Barwa, Assemblage A, and Assemblage B strata. Similarly, Webb et al. (2013) tied two Shillong Plateau sandstone samples to two Himalayan Assemblage A sandstone samples from Arunachal based on similar detrital zircon U/Pb age distributions. All four of the Webb et al. (2013) samples were deposited in latest Neoproterozoic to Cambrian time. There are two reasons that the apparent matches between these detrital zircon U/Pb age signatures do not require depositional contiguity of the Shillong Plateau, Assemblage A, Assemblage B, and Namche Barwa strata. First, matching detrital zircon age populations cannot be used for such statistics-based correlation without taking great care to reduce bias in the assembly of ages used for the comparison, and without numerous analyses (Slama and Kosler, 2012; Gehrels, 2014; Pullen et al., 2014). The authors acquired fewer than 100 U/Pb ages from all of the apparently matching samples, which is not enough for statistics-based comparison (Gehrels, 2014). Second, in both the Contiguous Deposition Outboard of India and the Assemblage B Deposition and Intrusion East of India models, both Assemblage B and eastern India (including the Namche Barwa region, Himalayan Assemblage A, and the Shillong Plateau/Mikir Hills region) received sediment from the same sources during Neoproterozoic to Middle Jurassic time (Figs. 6D, 11). Thus detrital zircon isotopic data cannot distinguish between these two models, nor whether the Namche Barwa sedimentary rocks were deposited contiguously with Assemblage A or Assemblage B strata.

In conclusion, the Late Paleoproterozoic to Cambrian rocks of the Namche Barwa and Shillong Plateau/Mikir Hills regions are not parts of and are not directly related to either Himalayan assemblage. The only exception is Cambrian Assemblage A rocks in the eastern Himalaya, which correlate with similar rocks in the Shillong Plateau/Mikir Hills area (Section 4.2) and possibly the Namche Barwa region (Figure 10). Instead, the Namche Barwa and Shillong Plateau/Mikir Hills regions share Late Paleoproterozoic to Cambrian affinities with eastern Indian rocks such as those that crop out in the Eastern Ghats and the Central Indian Tectonic Zone–Chhotanagpur Gneissic Complex–North Singhbhum Mobile Belt. The Cenozoic metamorphic, intrusive, and deformational histories of the Namche Barwa region are broadly similar to those of many Greater Himalayan rocks throughout the orogen (Zhang et al., 2010; 2012; Xu et al., 2010; Guilmette et al., 2011; Liu et al., 2011).

9. CONCLUSIONS

1. To avoid confusion with names based on topographic, Cenozoic structural, and Cenozoic metamorphic characteristics, in this paper I introduce the terms Himalayan Assemblage A and Himalayan Assemblage B. These new names denote physical contiguity between members of an assemblage at the time of deposition or intrusion.
2. Assemblage A and Assemblage B may not have shared depositional or intrusive relationships prior to the Early Cretaceous Epoch.

3. The depositional substrate for Assemblage A rocks is not exposed anywhere in the Himalaya. The depositional substrate for Assemblage B rocks possibly crops out only in a small area of northwestern India. Thus for both assemblages, the oldest exposed unit is metasedimentary everywhere except possibly in this exposure of Assemblage B.
4. Assemblage A consists of three rock packages defined by depositional or crystallization age: Paleoproterozoic to Early Mesoproterozoic, Late Carboniferous to Permian, and terminal Cretaceous to Pleistocene. The only exceptions are Lower Cretaceous mafic volcanic and clastic rocks in central Nepal and Cambrian mostly clastic rocks in Bhutan and northeastern India.
5. Ca. 1900-1800 Ma Assemblage A strata as well as the ca. 1880-1830 Ma granite and gabbro that intruded them may have formed in a continental rift setting.
6. Depositional strike during deposition of Upper Paleoproterozoic to Lower Mesoproterozoic Assemblage A strata was toward the northeast.
7. Cambrian Assemblage A strata are restricted to the eastern Himalaya. Like similar-aged deposits in the Shillong Plateau/Mikir Hills region, these could be foreland basin strata deposited in front of the Kuunga Orogen of eastern India.
8. Along nearly the entire orogen, the lowest strata in the youngest Assemblage A package may have been deposited in Paleocene time, not in the latest Cretaceous Period. These rocks may be the oldest Himalayan foreland basin deposits.
9. Deposition of middle Miocene to Pliocene (Siwalik) foreland basin strata extended hinterland-ward of the branch line between the Main Boundary and Himalayan Sole thrusts, in contrast to the conclusion of Medlicott (1865).

10. In many locations, the late Cenozoic Main Boundary Thrust seems not to repeat stratigraphic section in map view. The apparent absence of repetition results from a combination of erosion of the hanging wall Siwalik equivalents in some sectors of the orogen, burial of hanging wall pre-Cenozoic strata in others, and ubiquitous burial of footwall pre-Cenozoic strata. However, the Main Boundary Thrust-Himalayan Sole Thrust actually does repeat stratigraphy because it places a section of Upper Paleoproterozoic to Lower Mesoproterozoic Assemblage A strata in the hanging wall above correlative formations in the footwall.
11. Assemblage B consists of a succession of mostly sedimentary rocks deposited between the Early Neoproterozoic and Quaternary periods, plus granitic intrusions at ca. 880-800, 510-460, and 28-14 Ma. Lower Permian basalt and Early to Middle Permian granite are present in the western part of Assemblage B.
12. Identification of the Main Frontal, Main Boundary, and Main Central thrusts is useful for organizing rocks in the Cenozoic thrust belt. There is nothing special about the Cenozoic geometry, kinematics, or mechanics of these high strain zones relative to other nearby high strain zones.
13. West of central Nepal, in hinterland exposures the MCT typically places Neoproterozoic Assemblage B deposits in the hanging wall on Paleoproterozoic Assemblage A strata in the footwall, a younger-on-older relationship. In contrast, in at least some locations in and east of central Nepal, proximal footwall strata were deposited in the Phanerozoic Eon, resulting in an older-on-younger relationship across the high strain zone.
14. One important factor that explains why Pliocene to Holocene frontal thrusts mostly did not reactivate ancient high strain zones (except possibly in the eastern Himalaya) is that

across the western and central sectors of the Himalaya, the ancient high strain zones are not oriented favorably relative to the late Cenozoic convergence direction and the resulting thrusts.

15. The Shillong Plateau is the only location along the entire orogen where deformation jumped far forward of the main thrust belt. The late Cenozoic Dauki Thrust, which bounds the Shillong Plateau on its southern margin, is interpreted to have reactivated Cretaceous rift-related normal faults. The Dauki Thrust is broadly parallel or slightly oblique to buried Paleoproterozoic normal-sense high strain zones as well as the Narmada-Sone Fault. It is possible that Paleoproterozoic normal-sense high strain zones with similar orientations were reactivated in the Shillong Plateau region during both Cretaceous rifting and Cenozoic thrusting.
16. Compared to other Phanerozoic fold-thrust belts, Himalayan salients and recesses have small amplitudes and wavelengths. Three factors that contributed to the small amplitudes and wavelengths of map-view bends in the Himalayan frontal thrusts are: (A) The absence of a hot, and thus weak, back-arc region in the Indian foreland prior to continental collision, in contrast to the northern Canadian Cordillera. (B) In the western and central Himalaya, large changes in foreland stratigraphic thickness may be oriented perpendicular to Himalayan Pliocene to Holocene thrusts, in contrast to the Appalachian Orogen. (C) There was no large-magnitude reactivation of ancient high strain zones (except possibly in the eastern Himalaya), in contrast to the Appalachians.
17. The Namche Barwa and Shillong Plateau/Mikir Hills regions have pre-Late Cretaceous geologic histories distinct from Assemblage A and Assemblage B and the rocks of these two regions do not belong to either Himalayan assemblage. The Namche Barwa and

Shillong Plateau/Mikir Hills rocks were deformed, metamorphosed, and intruded in Late Paleoproterozoic to Mesoproterozoic time along with rocks of the Central Indian Tectonic Zone–Chhotanagpur Gneissic Complex–North Singhbhum Mobile Belt. The Namche Barwa and Shillong Plateau/Mikir Hills rocks additionally were affected by the late Ediacaran to Cambrian Kuunga Orogeny, as also recorded in the Eastern Ghats. Cambrian strata of eastern Assemblage A may have been deposited in a foreland basin in front of the Kuunga Orogeny, like similar-age deposits in the Shillong Plateau/Mikir Hills and Namche Barwa areas.

18. Assemblage B is a suspect terrane: it has an internally consistent geologic history, a pre-Cretaceous geologic history different from neighboring rocks, and it is bounded by major high strain zones.
19. Assemblage B may have been located north of western Australia during Neoproterozoic to Middle Jurassic time.
20. 3000 km of left-handed motion may have juxtaposed Assemblage B against Assemblage A across a transcurrent fault system during Late Jurassic to Early Cretaceous time.
21. The Main Central Thrust is unusual because it does not repeat stratigraphy. It did not repeat pre-Cretaceous stratigraphic section because the assemblages on either side of the high strain zone did not share depositional contiguity until the middle Early Cretaceous Epoch.
22. If it were simply an extensional high strain zone, the South Tibet Detachment would be globally unique because it repeats stratigraphy in many locations.

ACKNOWLEDGEMENTS

I thank the editors for inviting this contribution. I am grateful to Albert Bally for sharing, during my visit in 2000, the insight that Cenozoic structural strike is highly oblique to Paleoproterozoic depositional and structural strike along most of the orogen. Discussions with Peter DeCelles, Joseph DiPietro, Ryan McKenzie, Nadine McQuarrie, Delores Robinson, Douwe van Hinsbergen, and Alexander Webb were invaluable for clarifying the ideas presented here. I thank the following geologists for generously providing vector format files: Dian He (Fig. 3C), Subodha Khanal (Fig. 3B), Nadine McQuarrie (Fig. 3D), and Alexander Webb (Figs. 2 and 3A). The rotation file for the paleomagnetic reference frame used in Figures 6 and 13 was downloaded from http://www.geologist.nl/. Formal reviews by Eduardo Garzanti, Ryan McKenzie, Delores Robinson, Alexander Webb, and two anonymous reviewers greatly improved the article; Associate Editor Zeming Zhang provided judicious editorial handling.

Appendix A: Notes on making Assemblage A correlation chart

Appendix B: Notes on making Assemblage B correlation chart

Appendix C: Notes on making wider correlation chart

Appendix D: Supplemental references

REFERENCES CITED

Acharyya, S.K., 2015, Indo-Burma Range: a belt of accreted microcontinents, ophiolites and Mesozoic–Paleogene flyschoid sediments: International Journal of Earth Sciences, v. 104, p. 1235–1251, doi: 10.1007/s00531-015-1154-6.

Aggarwal, N., and Jha, N., 2013, Permian palynostratigraphy and palaeoclimate of Lingala–Koyagudem coalbelt, Godavari Graben, Andhra Pradesh, India: Journal of Asian Earth Sciences, v. 64, p. 38-57, doi:10.1016/j.jseaes.2012.11.041.

Agyei-Dwarko, N. Y., Augland, L. E., and Andresen, A., 2012, The Heggmovatn supracrustals, North Norway—A late Mesoproterozoic to early Neoproterozoic (1050–930 Ma) terrane of Laurentian origin in the Scandinavian Caledonides: Precambrian Research, v. 212-213, p. 245-262, doi:10.1016/j.precamres.2012.06.008.

Ahmad, A. H. M., Rais, S., Khan, A. F., and Zafar, H., 2005, Petrofacies, provenance and diagenesis of Patherwa Formation sandstones, Semri Group, Son Valley, India: Gondwana Geological Magazine, v. 20, p. 61-72.

Aitchison, J. C., Ali, J. R., and Davis, A. M., 2007, When and where did India and Asia collide?: Journal of Geophysical Research, v. 112, B05423, doi:10.1029/2006JB004706.

Ali, J. R., and Aitchison, J. C., 2014, Greater India's northern margin prior to its collision with Asia: Basin Research, v. 26, p. 73-84, doi:10.1111/bre.12040.

Alvaro, J. J., Macouin, M., Ezzouhairi, H., Charif, A., Ayad, N. A., Ribeiro, M. L., and Ader, M., 2008, Late Neoproterozoic carbonate productivity in a rifting context: the Adoudou Formation and its associated bimodal volcanism onlapping the western Saghro inlier, Morocco, *in* Ennih, N., and Liegeois, J.-P., eds., The boundaries of the West African Craton, Geological Society, London, Special Publications, 297, p. 285-302, doi:10.1144/SP297.14.

Aoya, M., Endo, S., Mizukami, T., and Wallis, S. R., 2013, Paleo-mantle wedge preserved in the Sambagawa high-pressure metamorphic belt and the thickness of forearc continental crust: Geology, v. 41, p. 451-454, doi:10.1130/G33834.1.

Appel, E., Muller, R., and Widder, R. W., 1991, Palaeomagnetic results from the Tibetan sedimentary series of the Manang area (north central Nepal): Geophysical Journal International, v. 104, p. 255-266, doi:10.1111/j.1365-246X.1991.tb02510.x.

Arora, B.R., and Mahashabde, M.V., 1987, A transverse conductive structure in the northwest Himalaya: Physics of the Earth and Planetary Interiors, v. 45, p. 119–127, doi:10.1016/0031-9201(87)90046-X.

Auden, J.B., 1934, The geology of the Krol belt: Records of the Geological Survey of India, v. 67, p. 357–454.

Auden, J. B., 1935, Traverses in the Himalaya: Records of the Geological Survey of India, v. 69, p. 123-167.

Auden, J.B., 1937, The structure of the Himalaya in Garhwal: Records of the Geological Survey of India, v. 71, p. 407–433.

Augland, L. E., Andresen, A., Corfu, F., Agyei-Dwarko, N. Y., and Larionov, A. N., 2014, The Bratten–Landegode gneiss complex: a fragment of Laurentian continental crust in the Uppermost Allochthon of the Scandinavian Caledonides *in* Corfu, F., Gasser, D., and Chew, D. M., eds., New perspectives on the Caledonides of Scandinavia and related areas, Geological Society, London, Special Publications, 390, p. 633-654, doi:10.1144/SP390.1.

Ayalew, D., and Gibson, S. A., 2009, Head-to-tail transition of the Afar mantle plume: geochemical evidence from a Miocene bimodal basalt–rhyolite succession in the Ethiopian Large Igneous Province: Lithos, v. 112, p. 461-476, doi:10.1016/j.lithos.2009.04.005.

Bagas, L., 2004, Proterozoic evolution and tectonic setting of the northwest Paterson Orogen, Western Australia: Precambrian Research, v. 128, p. 475-496, doi:10.1016/j.precamres.2003.09.011.

Bagati, T.N., Kumar, R., and Ghosh, S.K., 1991, Regressive-transgressive sedimentation in the Ordovician sequence of the Spiti (Tethys) basin, Himachal Pradesh, India: Sedimentary Geology, v. 73, p. 171–184, doi: 10.1016/0037-0738(91)90029-D.

Balakrishnan, T. S., Unnikrishnan, P., and Murty, A. V. S., 2009, The tectonic map of India and contiguous areas: Journal of the Geological Society of India, v. 74, p. 158-168, doi:10.1007/s12594-009-0119-4.

Balkwill, H. R., 1972, Structural geology, lower Kicking Horse River region, Rocky Mountains, British Columbia: Bulletin of Canadian Petroleum Geology, v. 20, p. 608-633.

Beaumont, C., Jamieson, R. A., Nguyen, M. H., and Lee, B., 2001, Himalayan tectonics explained by extrusion of a low-viscosity crustal channel coupled to focused surface denudation: Nature, v. 414, p. 738-742, doi:10.1038/414738a.

Berthet, T., Ritz, J.-F., Ferry, M., Pelgay, P., Cattin, R., Drukpa, D., Braucher, R., and Hetenyi, G., 2014, Active tectonics of the eastern Himalaya: New constraints from the first tectonic geomorphology study in southern Bhutan: Geology, v. 42, p. 427-430, doi:10.1130/G35162.1.

Bhargava, O.N., Frank, W., and Bertle, R., 2011, Late Cambrian deformation in the Lesser Himalaya: Journal of Asian Earth Sciences, v. 40, p. 201–212, doi:10.1016/j.jseaes.2010.07.015.

Bhattacharyya, K., and Mitra, G., 2009, A new kinematic evolutionary model for the growth of a duplex — an example from the Rangit duplex, Sikkim Himalaya, India: Gondwana Research, v. 16, p. 697-715, doi:10.1016/j.gr.2009.07.006.

Bhowmik, S. K., Wilde, S. A., Bhandari, A., Pal, T., and Pant, N. C., 2012, Growth of the Greater Indian landmass and its assembly in Rodinia: geochronological evidence from the Central Indian Tectonic Zone: Gondwana Research, v. 22, p. 54-72, doi:10.1016/j.gr.2011.09.008.

Bhowmik, S. K., Wilde, S. A., Bhandari, A., and Sarbadhikari, A. B., 2014, Zoned monazite and zircon as monitors for the thermal history of granulite terranes: an example from the Central Indian Tectonic Zone: Journal of Petrology, v. 55, p. 585-621, doi:10.1093/petrology/egt078.

Bierlein, F. P., Black, L. P., Hergt, J., and Mark, G., 2008, Evolution of Pre-1.8 Ga basement rocks in the western Mt Isa Inlier, northeastern Australia—insights from SHRIMP U–Pb dating and in-situ Lu–Hf analysis of zircons: Precambrian Research, v. 163, p. 159-173, doi:10.1016/j.precamres.2007.08.017.

Bilham, R., and England, P., 2001, Plateau 'pop-up' in the great 1897 Assam earthquake: Nature, v. 410, p. 806-809, doi:10.1038/35071057.

Biswas, S. K., 1987, Regional tectonic framework, structure and evolution of the western marginal basins of India: Tectonophysics, v. 135, p. 307-327, doi:10.1016/0040-1951(87)90115-6.

Bodenhausen, J. W. A., De Booy, T., Egeler, C. G., and Nijhuis, H. J., 1964, On the geology of central west Nepal – A preliminary note: Reports of the 22nd International Geological Congress, Delhi, XI, p. 101-122.

Bollinger, L., Avouac, J.-P., Beyssac, O., Catlos, E. J., Harrison, T. M., Grove, M., Goffe, B., and Sapkota, S., 2004, Thermal structure and exhumation history of the Lesser Himalaya in central Nepal: Tectonics, v. 23, TC5015, doi:10.1029/2003TC001564.

Bollinger, L., Sapkota, S. N., Tapponnier, P., Klinger, Y., Rizza, M., Van der Woerd, J., Tiwari, D. R., Pandey, R., Bitri, A., and Bes de Berc, S., 2014, Estimating the return times of great Himalayan earthquakes in eastern Nepal: evidence from the Patu and Bardibas strands of the Main Frontal Thrust: Journal of Geophysical Research Solid Earth, v. 119, p. 7123–7163, doi:10.1002/2014JB010970.

Bose, P. K., Banerjee, S., and Sarkar, S., 1997, Slope-controlled seismic deformation and tectonic framework of deposition: Koldaha Shale, India: Tectonophysics, v. 269, p. 151-169, doi:10.1016/S0040-1951(96)00110-2.

Boulton, S. J., and Robertson, A. H. F., 2007, The Miocene of the Hatay area, S Turkey: transition from the Arabian passive margin to an underfilled foreland basin related to closure of the Southern Neotethys Ocean: Sedimentary Geology, v. 198, p. 93-124, doi:10.1016/j.sedgeo.2006.12.001.

Bracciali, L., Parrish, R.R., Najman, Y., Smye, A., Carter, A., and Wijbrans, J.R., 2016, Plio-Pleistocene exhumation of the eastern Himalayan syntaxis and its domal “pop-up”: Earth-Science Reviews, v. 160, p. 350–385, doi: 10.1016/j.earscirev.2016.07.010.

Brookfield, M. E., 1993, The Himalayan passive margin from Precambrian to Cretaceous times: Sedimentary Geology, v. 84, p. 1-35, doi:10.1016/0037-0738(93)90042-4.

Brown, M., 2010, Paired metamorphic belts revisited: Gondwana Research, v. 18, p. 46-59, doi:10.1016/j.gr.2009.11.004.

Buhler, B., Breitkreuz, C., Pfander, J., Hofmann, M., Becker, S., Linnemann, U., and Eliwa, H. A., 2014, New insights into the accretion of the Arabian-Nubian Shield: depositional setting, composition and geochronology of a Mid-Cryogenian arc succession (North Eastern Desert, Egypt): Precambrian Research, v. 243, p. 149-167, doi:10.1016/j.precamres.2013.12.012.

Buiter, S. J. H., Pfiffner, O. A., and Beaumont, C., 2009, Inversion of extensional sedimentary basins: a numerical evaluation of the localisation of shortening: Earth and Planetary Science Letters, v. 288, p. 492-504, doi:10.1016/j.epsl.2009.10.011.

Burchfiel, B. C., Chen, Z., Hodges, K. V., Liu, Y., Royden, L. H., Deng, C., and Xu, J., 1992, The South Tibetan detachment system, Himalayan orogen: Extension contemporaneous with and parallel to shortening in a collisional mountain belt, Geological Society of America Special Paper 269, 41 p., doi:10.1130/SPE269.

Burchfiel, B. C., and Royden, L. H., 1985, North-south extension within the convergent Himalayan region: Geology, v. 13, p. 679-682, doi:10.1130/0091-7613(1985)13<679:NEWTCH>2.0.CO;2.

Burg, J. P., Brunel, M., Gapais, D., Chen, G. M., and Liu, G. H., 1984, Deformation of leucogranites of the crystalline Main Central Sheet in southern Tibet (China): Journal of Structural Geology, v. 6, p. 535-542, doi:10.1016/0191-8141(84)90063-4.

Burrard, S. G., and Hayden, H. H., 1908, A sketch of the geography and geology of the Himalaya Mountains and Tibet: Calcutta, Geological Survey of India, 308 p.

Caby, R., Pecher, A., and Le Fort, P., 1983, Le grand chevauchement central himalayen: nouvelles donnees sur le metamorphisme inverse a la base de la Dalle du Tibet: Revue de geologie dynamique et de geographie physique, v. 24, p. 89-100.

Cai, F., Ding, L., Leary, R.J., Wang, H., Xu, Q., Zhang, L., and Yue, Y., 2012, Tectonostratigraphy and provenance of an accretionary complex within the Yarlung-Zangpo suture zone, southern Tibet: Insights into subduction-accretion processes in the Neo-Tethys: Tectonophysics, v. 574, p. 181–192, doi: 10.1016/j.tecto.2012.08.016.

Cai, F., Ding, L., Laskowski, A.K., Kapp, P., Wang, H., Xu, Q., and Zhang, L., 2016, Late Triassic paleogeographic reconstruction along the Neo–Tethyan Ocean margins, southern Tibet: Earth and Planetary Science Letters, v. 435, p. 105–114, doi:10.1016/j.epsl.2015.12.027.

Calder, J., 1833, General observations on the geology of India: Asiatic Researches, v. 18, p. 1-22.

Caldwell, W. B., Klemperer, S. L., Lawrence, J. F., Rai, S. S., and Ashish, 2013, Characterizing the Main Himalayan Thrust in the Garhwal Himalaya, India with receiver function CCP stacking: Earth and Planetary Science Letters, v. 367, p. 15-27, doi:10.1016/j.epsl.2013.02.009.

Calignano, E., Sokoutis, D., Willingshofer, E., Brun, J.-P., Gueydan, F., and Cloetingh, S., 2017, Oblique contractional reactivation of inherited heterogeneities: Cause for arcuate orogens: Tectonics, doi: 10.1002/2016TC004424.

Carosi, R., Montomoli, C., Rubatto, D., and Visona, D., 2010, Late Oligocene high-temperature shear zones in the core of the Higher Himalayan Crystallines (Lower Dolpo, western Nepal): Tectonics, v. 29, TC4029, doi:10.1029/2008TC002400.

Carosi, R., Montomoli, C., Iaccarino, S., Massonne, H.-J., Rubatto, D., Langone, A., Gemignani, L., and Visona, D., 2016, Middle to late Eocene exhumation of the Greater Himalayan Sequence in the central Himalayas: Progressive accretion from the Indian plate: Geological Society of America Bulletin, v. 128, p. 1571–1592, doi: 10.1130/B31471.1.

Cautley, P. T., 1840, XXII.—On the structure of the Sevalik Hills, and the organic remains found in them: Transactions of the Geological Society of London, v. s2-5, p. 267-278, doi:10.1144/transgslb.5.2.267.

Cawood, P. A., and Buchan, C., 2007, Linking accretionary orogenesis with supercontinent assembly: Earth-Science Reviews, v. 82, p. 217-256, doi:10.1016/j.earscirev.2007.03.003.

Cawood, P. A., Johnson, M. R. W., and Nemchin, A. A., 2007, Early Palaeozoic orogenesis along the Indian margin of Gondwana: Tectonic response to Gondwana assembly: Earth and Planetary Science Letters, v. 225, p. 70-84, doi:10.1016/j.epsl.2006.12.006.

Cawood, P. A., Wang, Y., Xu, Y., and Zhao, G., 2013, Locating South China in Rodinia and Gondwana: a fragment of greater India lithosphere?: Geology, v. 41, p. 903-906, doi:10.1130/G34395.1.

Cecil, M. R., Rotberg, G. L., Ducea, M. N., Saleeby, J. B., and Gehrels, G. E., 2012, Magmatic growth and batholithic root development in the northern Sierra Nevada, California: Geosphere, v. 8, p. 592-606, doi:10.1130/GES00729.1.

Celerier, J., Harrison, T. M., Webb, A. A. G., and Yin, A., 2009, The Kumaun and Garwhal Lesser Himalaya, India: Part 1. Structure and stratigraphy: Geological Society of America Bulletin, v. 121, p. 1262-1280, doi:10.1130/B26344.1.

Chakrabarti, R., Basu, A. R., and Chakrabarti, A., 2007, Trace element and Nd-isotopic evidence for sediment sources in the mid-Proterozoic Vindhyan Basin, central India: Precambrian Research, v. 159, p. 260-274, doi:10.1016/j.precamres.2007.07.003.

Chakraborty, S., Anczkiewicz, R., Gaidies, F., Rubatto, D., Sorcar, N., Faak, K., Mukhopadhyay, D.K., and Dasgupta, S., 2016, A review of thermal history and timescales of tectonometamorphic processes in Sikkim Himalaya (NE India) and implications for rates of metamorphic processes: Journal of Metamorphic Geology, v. 34, p. 785–803, doi: 10.1111/jmg.12200.

Chakraborty, S., Mukhopadhyay, D.K., Chowdhury, P., Rubatto, D., Anczkiewicz, R., Trepmann, C., Gaidies, F., Sorcar, N., and Dasgupta, S., 2017, Channel flow and localized fault bounded slice tectonics (LFBST): Insights from petrological, structural, geochronological and geospeedometric studies in the Sikkim Himalaya, NE India: Lithos, doi: 10.1016/j.lithos.2017.01.024.

Chamyal, L. S., Maurya, D. M., Bhandari, S., and Raj, R., 2002, Late Quaternary geomorphic evolution of the lower Narmada valley, western India: implications for neotectonic activity along the Narmada–Son Fault: Geomorphology, v. 46, p. 177-202, doi:10.1016/S0169-555X(02)00073-9.

Chapman, A. D., Ducea, M. N., Kidder, S., and Petrescu, L., 2014, Geochemical constraints on the petrogenesis of the Salinian arc, central California: implications for the origin of intermediate magmas: Lithos, v. 200-201, p. 126-141, doi:10.1016/j.lithos.2014.04.011.

Childs, C., Manzocchi, T., Walsh, J. J., Bonson, C. G., Nicol, A., and Schopfer, M. P. J., 2009, A geometric model of fault zone and fault rock thickness variations: Journal of Structural Geology, v. 31, p. 117-127, doi:10.1016/j.jsg.2008.08.009.

Clark, M. K., and Bilham, R., 2008, Miocene rise of the Shillong Plateau and the beginning of the end for the Eastern Himalaya: Earth and Planetary Science Letters, v. 269, p. 336-350, doi:10.1016/j.epsl.2008.01.045.

Clarke, G.L., Bhowmik, S.K., Ireland, T.R., Aitchison, J.C., Chapman, S.L., and Kent, L., 2016, Inverted Oligo-Miocene metamorphism in the Lesser Himalaya Sequence, Arunachal Pradesh, India; age and grade relationships: Journal of Metamorphic Geology, v. 34, p. 805–820, doi: 10.1111/jmg.12202.

Colchen, M., Bassoullet, J. P., and Mascle, G., 1982, La paleogeographie des orogenes, l'example de l'Himalaya: Memoires geologiques de l'Universite de Dijon, v. 7, p. 453-471.

Colebrook, H. T., 1822, X.—On the valley of the Sutluj River in the Himalaya Mountains: Transactions of the Geological Society of London, v. s2-1, p. 124-131, doi:10.1144/transgslb.1.1.124.

Collins, A.S., 2003, Structure and age of the northern Leeuwin Complex, Western Australia: constraints from field mapping and U–Pb isotopic analysis: Australian Journal of Earth Sciences, v. 50, p. 585–599, doi: 10.1046/j.1440-0952.2003.01014.x.

Collins, A. S., and Pisarevsky, S. A., 2005, Amalgamating eastern Gondwana: the evolution of the circum-Indian orogens: Earth-Science Reviews, v. 71, p. 229-270, doi:10.1016/j.earscirev.2005.02.004.

Coney, P. J., Jones, D. L., and Monger, J. W. H., 1980, Cordilleran suspect terranes: Nature, v. 288, p. 329-333, doi:10.1038/288329a0.

Corfield, R. I., and Searle, M. P., 2000, Crustal shortening estimates across the north Indian continental margin, Ladakh, NW India, *in* Treloar, P. J., Searle, M. P., Khan, M. A., and Jan, M. Q., eds., Tectonics of the Nanga Parbat syntaxis and the western Himalaya: London, Geological Society of London Special Publication 170, p. 395-410, doi:10.1144/GSL.SP.2000.170.01.21.

Corrie, S. L., and Kohn, M. J., 2011, Metamorphic history of the central Himalaya, Annapurna region, Nepal, and implications for tectonic models: Geological Society of America Bulletin, v. 123, p. 1863-1879, doi:10.1130/B30376.1.

Corrie, S. L., Kohn, M. J., McQuarrie, N., and Long, S. P., 2012, Flattening the Bhutan Himalaya: Earth and Planetary Science Letters, v. 349-350, p. 67-74, doi:10.1016/j.epsl.2012.07.001.

Corti, G., 2009, Continental rift evolution: from rift initiation to incipient break-up in the Main Ethiopian Rift, East Africa: Earth-Science Reviews, v. 96, p. 1-53, doi:10.1016/j.earscirev.2009.06.005.

Cosca, M. A., Thompson, R. A., Lee, J. P., Turner, K. J., Neymark, L. A., and Premo, R. A., 2014, ^{40}Ar/^{39}Ar geochronology, isotope geochemistry (Sr, Nd, Pb), and petrology of alkaline lavas near Yampa, Colorado: migration of alkaline volcanism and evolution of the northern Rio Grande rift: Geosphere, v. 10, p. 374-400, doi:10.1130/GES00921.1.

Cottle, J. M., Jessup, M. J., Newell, D. L., Searle, M. P., Law, R. D., and Horstwood, M. S. A., 2007, Structural insights into the early stages of exhumation along an orogen-scale detachment: the South Tibetan Detachment system, Dzakaa Chu section, eastern Himalaya: Journal of Structural Geology, v. 29, p. 1781-1797, doi:10.1016/j.jsg.2007.08.007.

Cottle, J. M., Jessup, M. J., Newell, D. L., Horstwood, M. S. A., Noble, S. R., Parrish, R. R., Waters, D. J., and Searle, M. P., 2009, Geochronology of granulitized eclogite from the Ama Drime Massif: implications for the tectonic evolution of the south Tibetan Himalaya: Tectonics, v. 28, TC1002, doi:10.1029/2008TC002256.

Cottle, J.M., Waters, D.J., Riley, D., Beyssac, O., and Jessup, M.J., 2011, Metamorphic history of the South Tibetan Detachment System, Mt. Everest region, revealed by RSCM thermometry and phase equilibria modelling: Journal of Metamorphic Geology, v. 29, p. 561–582, doi:10.1111/j.1525-1314.2011.00930.x.

Cottle, J. M., Larson, K. P., and Kellett, D. A., 2015, How does the mid-crust accommodate deformation in large, hot collisional orogens? A review of recent research in the Himalayan orogen: Journal of Structural Geology, v. 78, p. 119-133, doi:10.1016/j.jsg.2015.06.008.

Crispe, A. J., Vandenberg, L. C., and Scrimgeour, I. R., 2007, Geological framework of the Archean and Paleoproterozoic Tanami region, Northern Territory: Mineralium Deposita, v. 42, p. 3-26, doi:10.1007/s00126-006-0107-1.

Critelli, S., and Garzanti, E., 1994, Provenance of the Lower Tertiary Murree redbeds (Hazara-Kashmir Syntaxis, Pakistan) and initial rising of the Himalayas: Sedimentary Geology, v. 89, p. 265-284, doi:10.1016/0037-0738(94)90097-3.

Crouzet, C., Dunkl, I., Paudel, L., Arkai, P., Rainer, T.M., Balogh, K., and Appel, E., 2007, Temperature and age constraints on the metamorphism of the Tethyan Himalaya in Central Nepal: A multidisciplinary approach: Journal of Asian Earth Sciences, v. 30, p. 113–130, doi: 10.1016/j.jseaes.2006.07.014.

Crowe, W. A., Cosca, M. A., and Harris, L. B., 2001, ^{40}Ar/^{39}Ar geochronolgy and Neoproterozoic tectonics along the northern margin of the Eastern Ghats Belt in north Orissa, India: Precambrian Research, v. 108, p. 237-266, doi:10.1016/S0301-9268(01)00132-2.

Cunningham, D., 2013, Mountain building processes in intracontinental oblique deformation belts: lessons from the Gobi Corridor, Central Asia: Journal of Structural Geology, v. 46,

p. 255-282, doi:10.1016/j.jsg.2012.08.010.

Currie, C. A., Huismans, R. S., and Beaumont, C., 2008, Thinning of continental backarc lithosphere by flow-induced gravitational instability: Earth and Planetary Science Letters, v. 269, p. 435-446, doi:10.1016/j.epsl.2008.02.037.

Currie, C. A., and Hyndman, R. D., 2006, The thermal structure of subduction zone back arcs: Journal of Geophysical Research, v. 111, B08404, doi:10.1029/2005JB004024.

Das, A. K., Baruah, R. M., Bisht, S. S., and Agrawal, B., 1999, An integrated analysis of Late Proterozoic lower Vindhyan sediments for hydrocarbon exploration in western part of Son Valley, central India: Journal of the Geological Society of India, v. 53, p. 239-253.

Dasgupta, Somnath, Bose, S., and Das, K., 2013, Tectonic evolution of the Eastern Ghats Belt, India: Precambrian Research, v. 227, p. 247-258, doi:10.1016/j.precamres.2012.04.005.

Dasgupta, Sujit, Mukhopadhyay, B., Mukhopadhyay, M., and Nandy, D. R., 2013, Role of transverse tectonics in the Himalayan collision: further evidences from two contemporary earthquakes: Journal of the Geological Society of India, v. 81, p. 241-247, doi:10.1007/s12594-013-0027-5.

Dasgupta, S., Mukhopadhyay, M., and Nandy, D. R., 1987, Active transverse features in the central portion of the Himalaya: Tectonophysics, v. 136, p. 255-264, doi:10.1016/0040-1951(87)90028-X.

Dasgupta, S., Pande, P., Ganguly, D., Iqbal, Z., Sanyal, K., Venkatraman, N. V., Dasgupta, S., Sural, B., Harendranath, L., Mazumdar, K., Sanyal, S., Roy, A., Das, L. K., Misra, P. S., and Gupta, H., 2000, Seismotectonic atlas of India and its environs: Calcutta, Geological Survey of India.

Deb, M., Thorpe, R.I., Krstic, D., Corfu, F., and Davis, D.W., 2001, Zircon U–Pb and galena Pb isotope evidence for an approximate 1.0 Ga terrane constituting the western margin of the Aravalli–Delhi orogenic belt, northwestern India: Precambrian Research, v. 108, p. 195–213, doi:10.1016/S0301-9268(01)00134-6.

DeCelles, P. G., Gehrels, G. E., Quade, J., Ojha, T. P., Kapp, P. A., and Upreti, B. N., 1998a, Neogene foreland basin deposits, erosional unroofing, and the kinematic history of the Himalayan fold-thrust belt, western Nepal: Geological Society of America Bulletin, v. 110, p. 2-21, doi:10.1130/0016-7606(1998)110<0002:NFBDEU>2.3.CO;2.

DeCelles, P. G., Gehrels, G. E., Quade, J., and Ojha, T. P., 1998b, Eocene-early Miocene foreland basin development and the history of Himalayan thrusting, western and central Nepal: Tectonics, v. 17, p. 741-765, doi:10.1029/98TC02598.

DeCelles, P. G., Gehrels, G. E., Quade, J., La Reau, B., and Spurlin, M., 2000, Tectonic implications of U-Pb zircon ages of the Himalayan orogenic belt in Nepal: Science, v. 288, p. 497-499, doi:10.1016/j.jseaes.2010.04.027.

DeCelles, P.G., Robinson, D.M., Quade, J., Ojha, T.P., Garzione, C.N., Copeland, P., and Upreti, B.N., 2001, Stratigraphy, structure, and tectonic evolution of the Himalayan fold-thrust belt in western Nepal: Tectonics, v. 20, p. 487–509, doi: 10.1029/2000TC001226.

DeCelles, P. G., Gehrels, G. E., Najman, Y., Martin, A. J., Carter, A., and Garzanti, E., 2004, Detrital geochronology and geochemistry of Cretaceous-Early Miocene strata of Nepal: Implications for timing and diachroneity of initial Himalayan orogenesis: Earth and Planetary Science Letters, v. 227, p. 313-330, doi:10.1016/j.epsl.2004.08.019.

DeCelles, P. G., Kapp, P., Gehrels, G. E., and Ding, L., 2014, Paleocene-Eocene foreland basin evolution in the Himalaya of southern Tibet and Nepal: implications for the age of initial India-Asia collision: Tectonics, v. 33, p. 824-849, doi:10.1002/2014TC003522.

DeCelles, P.G., Carrapa, B., Gehrels, G.E., Chakraborty, T., and Ghosh, P., 2016, Along-strike continuity of structure, stratigraphy, and kinematic history in the Himalayan thrust belt: The view from Northeastern India: Tectonics, v. 35, p. 2995–3027, doi: 10.1002/2016TC004298.

Del Ventisette, C., Montanari, D., Sani, F., and Bonini, M., 2006, Basin inversion and fault reactivation in laboratory experiments: Journal of Structural Geology, v. 28, p. 2067–2083, doi:10.1016/j.jsg.2006.07.012.

Devrani, U., and Dubey, A. K., 2009, Anisotropy of magnetic susceptibility and petrofabric studies in the Garhwal synform, Outer Lesser Himalaya: evidence of pop-up klippen: Island Arc, v. 18, p. 428-443, doi:10.1111/j.1440-1738.2008.00628.x.

Dewey, J. F., and Bird, J. M., 1970, Mountain belts and the new global tectonics: Journal of Geophysical Research, v. 75, p. 2625-2647, doi:10.1029/JB075i014p02625.

Dezes, P. J., Vannay, J.-C., Steck, A., Bussy, F., and Cosca, M., 1999, Synorogenic extension: quantitative constraints on the age and displacement of the Zanskar shear zone (northwest Himalaya): Geological Society of America Bulletin, v. 111, p. 364-374, doi:10.1130/0016-7606(1999)111<0364:SEQCOT>2.3.CO;2.

Dhital, M. R., 2015, Geology of the Nepal Himalaya: Regional Perspective of the Classic Collided Orogen, Springer International Publishing, 498 p., doi:10.1007/978-3-319-02496-7.

Di Domenica, A., Bonini, L., Calamita, F., Toscani, G., Galuppo, C., and Seno, S., 2014, Analogue modeling of positive inversion tectonics along differently oriented pre-thrusting normal faults: an application to the Central-Northern Apennines of Italy Geological Society of America Bulletin, v. 126, p. 943-955, doi:10.1130/B31001.1.

Ding, L., Maksatbek, S., Cai, F., Wang, H., Song, P., Ji, W., Xu, Q., Zhang, L., Muhammad, Q., and Upendra, B., 2017, Processes of initial collision and suturing between India and Asia: Science China Earth Sciences, v. 60, p. 635–651, doi: 10.1007/s11430-016-5244-x.

DiPietro, J. A., and Isachsen, C. E., 2001, U-Pb zircon ages from the Indian plate in northwest Pakistan and their significance to Himalayan and pre-Himalayan geologic history: Tectonics, v. 20, p. 510-525, doi:10.1029/2000TC001193.

DiPietro, J. A., and Pogue, K. R., 2004, Tectonostratigraphic subdivisions of the Himalaya: A view from the west: Tectonics, v. 23, TC5001, doi:10.1029/2003TC001554.

Dominguez, S., Malavieille, J., and Lallemand, S. E., 2000, Deformation of accretionary wedges in response to seamount subduction: insights from sandbox experiments: Tectonics, v. 19, p. 182-196, doi:10.1029/1999TC900055.

Doubrovine, P.V., Steinberger, B., and Torsvik, T.H., 2016, A failure to reject: Testing the correlation between large igneous provinces and deep mantle structures with EDF statistics: Geochemistry, Geophysics, Geosystems, v. 17, p. 1130–1163, doi:10.1002/2015GC006044.

Draganits, E., Grasemann, B., and Hager, C., 2005, Conjugate, cataclastic deformation bands in the Lower Devonian Muth Formation (Tethyan Zone, NW India): Evidence for pre-Himalayan deformation structures: Geological Magazine, v. 142, p. 765–781, doi:10.1017/S0016756805001056.

Druschke, P., Hanson, A. D., and Well, M. L., 2009, Structural, stratigraphic, and geochronologic evidence for extension predating Palaeogene volcanism in the Sevier hinterland, east-central Nevada: International Geology Review, v. 51, p. 743-775, doi:10.1080/00206810902917941.

Dubey, A. K., 2010, Role of inversion tectonics in structural development of the Himalaya: Journal of Asian Earth Sciences, v. 39, p. 627-634, doi:10.1016/j.jseaes.2010.04.027.

-, 2014, Understanding an Orogenic Belt: Structural Evolution of the Himalaya, Springer International Publishing, 401 p., doi:10.1007/978-3-319-05588-6.

Dubey, A. K., and Bhakuni, S. S., 2007, Younger hanging wall rocks along the Vaikrita thrust of the high Himalaya: a model based on inversion tectonics: Journal of Asian Earth Sciences, v. 29, p. 424-429, doi:10.1016/j.jseaes.2005.10.005.

Dubey, A. K., Bhakuni, S. S., and Selokar, A. D., 2004, Structural evolution of the Kangra recess, Himachal Himalaya: a model based on magnetic and petrofabric strains: Journal of Asian Earth Sciences, v. 24, p. 245-258, doi:10.1016/j.jseaes.2003.11.002.

Dubois, A., Odonne, F., Massonnat, G., Lebourg, T., and Fabre, R., 2002, Analogue modelling of fault reactivation: tectonic inversion and oblique remobilisation of grabens: Journal of Structural Geology, v. 24, p. 1741-1752, doi:10.1016/S0191-8141(01)00129-8.

Ducea, M. N., Saleeby, J. B., and Bergantz, G., 2015, The architecture, chemistry, and evolution of continental magmatic arcs: Annual Review of Earth and Planetary Sciences, v. 43, p. 299-331, doi:10.1146/annurev-earth-060614-105049.

Dumitru, T. A., Wakabayashi, J., Wright, J. E., and Wooden, J. L., 2010, Early Cretaceous transition from nonaccretionary behavior to strongly accretionary behavior within the Franciscan subduction complex: Tectonics, v. 29, TC5001, doi:10.1029/2009TC002542.

Encarnacion, J., 2004, Multiple ophiolite generation preserved in the northern Philippines and the growth of an island arc complex: Tectonophysics, v. 392, p. 103-130, doi:10.1016/j.tecto.2004.04.010.

England, P., and Bilham, R., 2015, The Shillong Plateau and the great 1897 Assam earthquake: Tectonics, v. 34, p. 1792–1812, doi:10.1002/2015TC003902.

Espinoza, F., Morata, D., Polve, M., Lagabrielle, Y., Maury, R. C., Guivel, C., Cotten, J., Bellon, H., and Suarez, M., 2008, Bimodal back-arc alkaline magmatism after ridge subduction: Pliocene felsic rocks from Central Patagonia (47°S): Lithos, v. 101, p. 191-217, doi:10.1016/j.lithos.2007.07.002.

Evans, D. D. A., and Mitchell, R. N., 2011, Assembly and breakup of the core of Paleoproterozoic–Mesoproterozoic supercontinent Nuna: Geology, v. 39, p. 443-446, doi:10.1130/G31654.1.

Faccenda, M., Gerya, T. V., and Chakraborty, S., 2008, Styles of post-subduction collisional orogeny: influence of convergence velocity, crustal rheology and radiogenic heat production: Lithos, v. 103, p. 257-287, doi:10.1016/j.lithos.2007.09.009.

Finch, M., Hasalova, P., Weinberg, R. F., and Fanning, C. M., 2014, Switch from thrusting to normal shearing in the Zanskar shear zone, NW Himalaya: implications for channel flow: Geological Society of America Bulletin, v. 126, p. 892-924, doi:10.1130/B30817.1.

Frank, W., Hoinkes, G., Miller, C., Purtscheller, F., Richter, W., and Thoni, M., 1973, Relations between metamorphism and orogeny in a typical section of the Indian Himalayas: Tschermaks mineralogische und petrographische Mitteilungen, v. 20, p. 303-332, doi:10.1007/BF01081339.

Fraser, J., 1821, VI. Notes, accompanying a set of specimens from the Himalay Mountains: Transactions of the Geological Society of London, v. s1-5, p. 60-72, doi:10.1144/transgsla.5.60.

French, S.W., and Romanowicz, B., 2015, Broad plumes rooted at the base of the Earth's mantle beneath major hotspots: Nature, v. 525, p. 95–99, doi:10.1038/nature14876.

Fuchs, G., 1982, The geology of the Pin valley in Spiti, H.P., India: Jahrbuch der Geologischen Bundesanstalt Wien, v. 124, p. 325-359.

Fuchs, G., and Willems, H., 1990, The final stages of sedimentation in the Tethyan zone of Zanskar and their geodynamic significance (Ladakh-Himalaya): Jahrbuch der Geologischen Bundesanstalt Wien, v. 133, p. 259-273.

Gaetani, M., Garzanti, E., and Tintori, A., 1990, Permo-Carboniferous stratigraphy in SE Zanskar and NW Lahul (NW Himalaya, India): Eclogae Geologicae Helvetiae, v. 83, p. 143–161.

Gansser, A., 1964, Geology of the Himalayas: London, Interscience, 289 p.

-, 1983, Geology of the Bhutan Himalaya. Denskschriten der Schweizerischen Naturforschenden Gesellschaft, v. 96: Basel, Birkhauser-Verlag, 181 p.

-, 1991, Facts and theories on the Himalayas: Eclogae Geologicae Helvetiae, v. 84, p. 33-59, doi:10.5169/seals-166762.

Gapais, D., Pecher, A., Gilbert, E., and Ballevre, M., 1992, Synconvergence spreading of the higher Himalaya crystalline in Ladakh: Tectonics, v. 11, p. 1045-1056, doi:10.1029/92TC00819.

Garzanti, E., 1999, Stratigraphy and sedimentary history of the Nepal Tethys Himalaya passive margin: Journal of Asian Earth Sciences, v. 17, p. 805-827, doi:10.1016/S1367-9120(99)00017-6.

Garzanti, E., Casnedi, R., and Jadoul, F., 1986, Sedimentary evidence of a Cambro-Ordovician orogenic event in the northwestern Himalaya: Sedimentary Geology, v. 48, p. 237-265, doi:10.1016/0037-0738(86)90032-1.

Garzanti, E., and Hu, X., 2015, Latest Cretaceous Himalayan tectonics: obduction, collision or Deccan-related uplift?: Gondwana Research, v. 28, p. 165-178, doi:10.1016/j.gr.2014.03.010.

Gehrels, G., 2014, Detrital zircon U-Pb geochronology applied to tectonics: Annual Review of Earth and Planetary Sciences, v. 42, p. 127-149, doi:10.1146/annurev-earth-050212-124012.

Gehrels, G., Kapp, P., DeCelles, P., Pullen, A., Blakey, R., Weislogel, A., Ding, L., Guynn, J., Martin, A., McQuarrie, N., and Yin, A., 2011, Detrital zircon geochronology of pre-Tertiary strata in the Tibetan-Himalayan orogen: Tectonics, v. 30, TC5016, doi:10.1029/2011TC002868.

Gehrels, G. E., DeCelles, P. G., Martin, A., Ojha, T. P., Pinhassi, G., and Upreti, B. N., 2003, Initiation of the Himalayan Orogen as an early Paleozoic thin-skinned thrust belt: GSA Today, v. 13, p. 4-9, doi:10.1130/1052-5173(2003)13<4:IOTHOA>2.0.CO;2.

Gehrels, G. E., DeCelles, P. G., Ojha, T. P., and Upreti, B. N., 2006a, Geologic and U–Pb geochronologic evidence for early Paleozoic tectonism in the Dadeldhura thrust sheet, far-west Nepal Himalaya: Journal of Asian Earth Sciences, v. 28, p. 385-408, doi:10.1016/j.jseaes.2005.09.012.

-, 2006b, Geologic and U-Th-Pb geochronologic evidence for early Paleozoic tectonism in the Kathmandu thrust sheet, central Nepal Himalaya: Geological Society of America Bulletin, v. 118, p. 185-198, doi:10.1130/B25753.1.

Gibbons, A.D., Zahirovic, S., Muller, R.D., Whittaker, J.M., and Yatheesh, V., 2015, A tectonic model reconciling evidence for the collisions between India, Eurasia and intra-oceanic arcs of the central-eastern Tethys: Gondwana Research, v. 28, p. 451–492, doi:10.1016/j.gr.2015.01.001.

Gibson, R., Godin, L., Kellett, D.A., Cottle, J.M., and Archibald, D., 2016, Diachronous deformation along the base of the Himalayan metamorphic core, west-central Nepal: Geological Society of America Bulletin, v. 128, p. 860–878, doi:10.1130/B31328.1.

Godin, L., and Harris, L. B., 2014, Tracking basement cross-strike discontinuities in the Indian crust beneath the Himalayan orogen using gravity data – relationship to upper crustal faults Geophysical Journal International, v. 198, p. 198-215, doi:10.1093/gji/ggu131.

Goodge, J. W., Fanning, C. M., Vervoort, J. D., and Fisher, C., 2013, Mesoproterozoic and Paleoproterozoic igneous crust of central East Antarctica: age and origins revealed from glacial clasts: Mineralogical Magazine, v. 77, p. 1196, doi:10.1180/minmag.2013.077.5.7.

Goodge, J. W., Williams, I. S., and Myrow, P., 2004, Provenance of Neoproterozoic and lower Paleozoic siliciclastic rocks of the central Ross orogen, Antarctica: detrital record of rift-, passive-, and active-margin sedimentation: Geological Society of America Bulletin, v. 116, p. 1253-1279, doi:10.1130/B25347.1.

Goswami, P. K., 2012, Geomorphic evidences of active faulting in the northwestern Ganga Plain, India: implications for the impact of basement structures: Geosciences Journal, v. 16, p. 289-299, doi:10.1007/s12303-012-0030-7.

Greco, A., Martinotti, G., Papritz, K., Ramsay, J.G., and Rey, R., 1989, The crystalline rocks of the Kaghan Valley (NE-Pakistan): Eclogae Geologicae Helvetiae, v. 82, p. 629–653, doi: 10.5169/seals-166393.

Grelaud, S., Sassi, W., Frizon de Lamotte, D., Jaswal, T., and Roure, F., 2002, Kinematics of eastern Salt Range and south Potwar Basin (Pakistan): a new scenario: Marine and Petroleum Geology, v. 19, p. 1127-1139, doi:10.1016/S0264-8172(02)00121-6.

Griffin, T. J., Page, R. W., Sheppard, S., and Tyler, I. M., 2000, Tectonic implications of Palaeoproterozoic post-collisional, high-K felsic igneous rocks from the Kimberley region of northwestern Australia: Precambrian Research, v. 101, p. 1-23, doi:10.1016/S0301-9268(99)00084-4.

Grujic, D., Hollister, L. S., and Parrish, R. R., 2002, Himalayan metamorphic sequence as an orogenic channel: insight from Bhutan: Earth and Planetary Science Letters, v. 198, p. 177-191, doi:10.1016/S0012-821X(02)00482-X.

Grujic, D., Coutand, I., Doon, M., and Kellett, D.A., 2017, Northern provenance of the Gondwana Formation in the Lesser Himalayan Sequence: constraints rom 40Ar/39Ar dating of detrital muscovite in Darjeeling-Sikkim Himalaya: Italian Journal of Geosciences, v. 136, p. 15–27, doi: 10.3301/IJG.2015.28.

Guilmette, C., Indares, A., and Hébert, R., 2011, High-pressure anatectic paragneisses from the Namche Barwa, Eastern Himalayan Syntaxis: Textural evidence for partial melting, phase equilibria modeling and tectonic implications: Lithos, v. 124, p. 66–81, doi: 10.1016/j.lithos.2010.09.003.

Guilmette, C., Hebert, R., Dostal, J., Indares, A., Ullrich, T., Bedard, E., and Wang, C., 2012, Discovery of a dismembered metamorphic sole in the Saga ophiolitic melange, South Tibet: Assessing an Early Cretaceous disruption of the Neo-Tethyan supra-subduction zone and consequences on basin closing: Gondwana Research, v. 22, p. 398–414, doi: 10.1016/j.gr.2011.10.012.

Guo, L., Zhang, H.-F., Harris, N., Xu, W.-C., and Pan, F.-B., 2017, Detrital zircon U–Pb geochronology, trace-element and Hf isotope geochemistry of the metasedimentary rocks in the Eastern Himalayan syntaxis: Tectonic and paleogeographic implications: Gondwana Research, v. 41, p. 207–221, doi: 10.1016/j.gr.2015.07.013.

Guo, Z., and Wilson, M., 2012, The Himalayan leucogranites: Constraints on the nature of their crustal source region and geodynamic setting: Gondwana Research, v. 22, p. 360–376, doi: 10.1016/j.gr.2011.07.027.

Han, Y., Zhao, G., Cawood, P.A., Sun, M., Eizenhofer, P.R., Hou, W., Zhang, X., and Liu, Q., 2016, Tarim and North China cratons linked to northern Gondwana through switching accretionary tectonics and collisional orogenesis: Geology, v. 44, p. 95–98, doi:10.1130/G37399.1.

Hand, M., and Sandiford, M., 1999, Intraplate deformation in central Australia, the link between subsidence and fault reactivation: Tectonophysics, v. 305, p. 121-140, doi:10.1016/S0040-1951(99)00009-8.

Haq, B. U., 2014, Cretaceous eustasy revisited: Global and planetary change, v. 113, p. 44-58, doi:10.1016/j.gloplacha.2013.12.007.

Harris, N., 2007, Channel flow and the Himalayan-Tibetan orogen: A critical review: Journal of the Geological Society, v. 164, p. 511–523, doi: 10.1144/0016-76492006-133.

Hatcher, R. D., Jr., Thomas, W. A., Geiser, P. A., Snoke, A. W., Mosher, S., and Wiltschko, D. V., 1989, Alleghanian orogen, *in* Hatcher, R. D., Jr., Thomas, W. A., and Viele, G. W., eds., The Appalachian-Ouachita orogen in the United States, Geological Society of America, The Geology of North America, v. F-2, p. 233-318.

Hayden, H. H., 1904, The geology of Spiti, with part of Bashahr and Rupshu: Memoirs of the Geological Survey of India, v. 36, p. 1-129.

He, D., Webb, A. A. G., Larson, K. P., Martin, A. J., and Schmitt, A. K., 2015, Extrusion vs. duplexing models of Himalayan mountain building 3: duplexing dominates from the Oligocene to Present: International Geology Review, v. 57, p. 1-27, doi:10.1080/00206814.2014.986669.

He, D., Webb, A.A.G., Larson, K.P., and Schmitt, A.K., 2016, Extrusion vs. duplexing models of Himalayan mountain building 2: The South Tibet detachment at the Dadeldhura klippe: Tectonophysics, v. 667, p. 87–107, doi:10.1016/j.tecto.2015.11.014.

Hebert, R., Bezard, R., Guilmette, C., Dostal, J., Wang, C.S., and Liu, Z.F., 2012, The Indus–Yarlung Zangbo ophiolites from Nanga Parbat to Namche Barwa syntaxes, southern Tibet: First synthesis of petrology, geochemistry, and geochronology with incidences on geodynamic reconstructions of Neo-Tethys: Gondwana Research, v. 22, p. 377–397, doi: 10.1016/j.gr.2011.10.013.

Heim, A., and Gansser, A., 1939, Central Himalaya: geological observations of the Swiss expedition 1936: Zurich, Memoirs of the Swiss Society of Natural Sciences, v. 73, 245 p.

Heller, P. L., Angevine, C. L., Winslow, N. S., and Paola, C., 1988, Two-phase stratigraphic model of foreland-basin sequences: Geology, v. 16, p. 501-504, doi:10.1130/0091-7613(1988)016<0501:TPSMOF>2.3.CO;2.

Herbert, J. D., 1844, Geological map of Captain Herbert's Himalaya survey: Journal of the Asiatic Society of Bengal, v. 13, p. 171.

Hernaiz Huerta, P. P., Perez-Valera, F., Abad, M., Monthel, J., and Diaz de Neira, A., 2012, Melanges and olistostromes in the Puerto Plata area (northern Dominican Republic) as a record of subduction and collisional processes between the Caribbean and North-American plates: Tectonophysics, v. 568-569, p. 266-281, doi:10.1016/j.tecto.2011.10.020.

Herren, E., 1987, Zanskar shear zone: Northeast-southwest extension within the Higher Himalayas (Ladakh, India): Geology, v. 15, p. 409-413, doi:10.1130/0091-7613(1987)15<409:ZSZNEW>2.0.CO;2.

Heuberger, S., Schaltegger, U., Burg, J.-P., Villa, I. M., Frank, M., Dawood, H., Hussain, S., and Zanchi, A., 2007, Age and isotopic constraints on magmatism along the Karakoram-Kohistan Suture Zone, NW Pakistan: evidence for subduction and continued convergence after India-Asia collision: Swiss Journal of Geosciences, v. 100, p. 85-107, doi:10.1007/s00015-007-1203-7.

Hildebrand, R. S., Hoffman, P. F., and Bowring, S. A., 2010, The Calderian orogeny in Wopmay orogen (1.9 Ga), northwestern Canadian Shield: Geological Society of America Bulletin, v. 122, p. 794-814, doi:10.1130/B26521.1.

Hodges, K. V., 2000, Tectonics of the Himalaya and southern Tibet from two perspectives: Geological Society of America Bulletin, v. 112, p. 324-350, doi:10.1130/0016-7606(2000)112<324:TOTHAS>2.0.CO;2.

Hodges, K. V., Parrish, R. R., and Searle, M. P., 1996, Tectonic evolution of the central Annapurna Range, Nepalese Himalayas: Tectonics, v. 15, p. 1264-1291, doi:10.1029/96TC01791.

Hoffman, P. F., Bowring, S. A., Buchwaldt, R., and Hildebrand, R. S., 2011, Birthdate for the Coronation paleocean: age of initial rifting in Wopmay orogen, Canada: Canadian Journal of Earth Sciences, v. 48, p. 281-293, doi:10.1139/E10-038.

Hogan, J. P., and Gilbert, M. C., 1997, Intrusive style of A-type sheet granites in a rift environment: the Southern Oklahoma Aulacogen, *in* Ojakangas, R. W., Dickas, A. B., and Green, J. C., eds., Middle Proterozoic to Cambrian rifting, central North America: Boulder, Geological Society of America Special Paper 312, p. 299-311, doi:10.1130/0-8137-2312-4.299.

Honegger, K., Dietrich, V., Frank, W., Gansser, A., Thoni, M., and Trommsdorff, V., 1982, Magmatism and metamorphism in the Ladakh Himalayas (the Indus-Tsangpo suture zone): Earth and Planetary Science Letters, v. 60, p. 253–292, doi:10.1016/0012-821X(82)90007-3.

Hopson, C. A., Mattinson, J. M., Pessagno Jr., E. A., and Luyendyk, B. P., 2008, California Coast Range ophiolite: composite Middle and Late Jurassic oceanic lithosphere, *in* Wright, J. E., and Shervais, J. W., eds., Ophiolites, arcs, and batholiths: a tribute to Cliff Hopson: Boulder, Geological Society of America Special Paper 438, p. 1-101, doi:10.1130/2008.2438(01).

Horton, F., Lee, J., Hacker, B., Bowman-Kamaha'o, M., and Cosca, M., 2015, Himalayan gneiss dome formation in the middle crust and exhumation by normal faulting: new geochronology of Gianbul dome, northwestern India Geological Society of America Bulletin, v. 127, p. 162-180, doi:10.1130/B31005.1.

Hou, G., Santosh, M., Qian, X., Lister, G. S., and Li, J., 2008, Configuration of the Late Paleoproterozoic supercontinent Columbia: insights from radiating mafic dyke swarms: Gondwana Research, v. 14, p. 395-409, doi:10.1016/j.gr.2008.01.010.

Hu, X., Garzanti, E., Moore, T., and Raffi, I., 2015, Direct stratigraphic dating of India-Asia collision onset at the Selandian (middle Paleocene, 59 ± 1 Ma): Geology, v. 43, p. 859-862, doi:10.1130/G36872.1.

Hu, X., Wang, J., An, W., Garzanti, E., and Li, J., 2017, Constraining the timing of the India-Asia continental collision by the sedimentary record: Science China Earth Sciences, v. 60, p. 603–625, doi: 10.1007/s11430-016-9003-6.

Huang, W., van Hinsbergen, D. J. J., Lippert, P. C., Guo, Z., and Dupont-Nivet, G., 2015a, Paleomagnetic tests of tectonic reconstructions of the India-Asia collision zone: Geophysical Research Letters, v. 42, p. 2642-2649, doi:10.1002/2015GL063749.

Huang, W., van Hinsbergen, D.J.J., Maffione, M., Orme, D.A., Dupont-Nivet, G., Guilmette, C., Ding, L., Guo, Z., and Kapp, P., 2015b, Lower Cretaceous Xigaze ophiolites formed in the Gangdese forearc: Evidence from paleomagnetism, sediment provenance, and stratigraphy: Earth and Planetary Science Letters, v. 415, p. 142–153, doi: 10.1016/j.epsl.2015.01.032.

Hyndman, R. D., Currie, C. A., and Mazzotti, S. P., 2005, Subduction zone backarcs, mobile belts, and orogenic heat: GSA Today, v. 15, p. 4-10.

Ichiyama, Y., Ishiwatari, A., Kimura, J.-I., Senda, R., and Miyamoto, T., 2014, Jurassic plume-origin ophiolites in Japan: accreted fragments of oceanic plateaus: Contributions to Mineralogy and Petrology, v. 168:1019, doi:10.1007/s00410-014-1019-1.

Islam, M. S., Shinjo, R., and Kayal, J. R., 2011, Pop-up tectonics of the Shillong Plateau in northeastern India: Insight from numerical simulations: Gondwana Research, v. 20, p. 395-404, doi:10.1016/j.gr.2010.11.007.

Jagoutz, O., Royden, L., Holt, A. F., and Becker, T. W., 2015, Anomalously fast convergence of India and Eurasia caused by double subduction: Nature Geoscience, v. 8, p. 475-478, doi:10.1038/ngeo2418.

Jagoutz, O., and Schmidt, M. W., 2012, The formation and bulk composition of modern juvenile continental crust: the Kohistan arc: Chemical Geology, v. 298-299, p. 79-96, doi:10.1016/j.chemgeo.2011.10.022.

Jagoutz, O. E., Burg, J.-P., Hussain, S., Dawood, H., Pettke, T., Iizuka, T., and Maruyama, S., 2009, Construction of the granitoid crust of an island arc part I: geochronological and geochemical constraints from the plutonic Kohistan (NW Pakistan): Contributions to Mineralogy and Petrology, v. 158, p. 739-755, doi:10.1007/s00410-009-0408-3.

Jain, A. K., and Manickavasagam, R. M., 1993, Inverted metamorphism in the intracontinental ductile shear zone during Himalayan collision tectonics: Geology, v. 21, no. 5, p. 407-410, doi:10.1130/0091-7613(1993)021<0407:IMITID>2.3.CO;2.

Jain, S. P., and Kanwar, R. C., 1970, Himalayan ridge in the light of the theory of continental drift: Nature, v. 227, p. 829, doi:10.1038/227829a0.

Jain, V., and Sinha, R., 2005, Response of active tectonics on the alluvial Baghmati River, Himalayan foreland basin, eastern India: Geomorphology, v. 70, p. 339-356, doi:10.1016/j.geomorph.2005.02.012.

Jiang, Y.-H., Zhao, P., Zhou, Q., Liao, S.-Y., and Jin, G.-D., 2011, Petrogenesis and tectonic implications of Early Cretaceous S- and A-type granites in the northwest of the Gan-Hang rift, SE China: Lithos, v. 121, p. 55-73, doi:10.1016/j.lithos.2010.10.001.

John, T., Scherer, E. E., Schenk, V., Herms, P., Halama, R., and Garbe-Schonberg, D., 2010, Subducted seamounts in an eclogite-facies ophiolite sequence: the Andean Raspas Complex, SW Ecuador: Contributions to Mineralogy and Petrology, v. 159, p. 265-284, doi:10.1007/s00410-009-0427-0.

Johnson, M.R.W., 2005, Structural settings for the contrary metamorphic zonal sequences in the internal and external zones of the Himalaya: Journal of Asian Earth Sciences, v. 25, p.

695–706, doi:10.1016/j.jseaes.2004.04.010.

Jones, D. S., Barnes, C. G., Premo, W. R., and Snoke, A. W., 2011, The geochemistry and petrogenesis of the Paleoproterozoic Green Mountain arc: a composite(?), bimodal, oceanic, fringing arc: Precambrian Research, v. 185, p. 231-249, doi:10.1016/j.precamres.2011.01.011.

Just, J., Schulz, B., de Wall, H., Jourdan, F., and Pandit, M.K., 2011, Monazite CHIME/EPMA dating of Erinpura granitoid deformation: Implications for Neoproterozoic tectono-thermal evolution of NW India: Gondwana Research, v. 19, p. 402–412, doi:10.1016/j.gr.2010.08.002.

Kaila, K. L., Murty, P. R. K., and Mall, D. M., 1989, The evolution of the Vindhyan basin vis-à-vis the Narmada-Son lineament, central India, from deep seismic soundings: Tectonophysics, v. 162, p. 277-289, doi:10.1016/0040-1951(89)90249-7.

Kaur, P., Zeh, A., Chaudhri, N., Gerdes, A., and Okrusch, M., 2013, Nature of magmatism and sedimentation at a Columbia active margin: Insights from combined U-Pb and Lu-Hf isotope data of detrital zircons from NW India: Gondwana Research, v. 23, p. 1040–1052, doi:10.1016/j.gr.2012.07.008.

Kayal, J.R., Arefiev, S.S., Barua, S., Hazarika, D., Gogoi, N., Kumar, A., Chowdhury, S.., and Kalita, S., 2006, Shillong plateau earthquakes in northeast India region: complex tectonic model: Current Science, v. 91, p. 109–114.

Kellett, D. A., and Grujic, D., 2012, New insight into the South Tibetan detachment system: not a single progressive deformation: Tectonics, v. 31, TC2007, doi:10.1029/2011TC002957.

Kellett, D.A., Grujic, D., Warren, C., Cottle, J., Jamieson, R., and Tenzin, T., 2010, Metamorphic history of a syn-convergent orogen-parallel detachment: The South Tibetan detachment system, Bhutan Himalaya: Journal of Metamorphic Geology, v. 28, p. 785–808, doi:10.1111/j.1525-1314.2010.00893.x.

Kent, A. J. R., 2014, Preferential eruption of andesitic magmas: implications for volcanic magma fluxes at convergent margins, *in* Gomez-Tuena, A., Straub, S. M., and Zellmer, G. F., eds., Orogenic andesites and crustal growth, Geological Society, London, Special Publications, 385, p. 257-280, doi:10.1144/SP385.10.

Kent, R. W., Pringle, M. S., Muller, R. D., Saunders, A. D., and Ghose, N. C., 2002, ^{40}Ar/^{39}Ar geochronology of the Rajmahal Basalts, India, and their relationship to the Kerguelen Plateau: Journal of Petrology, v. 43, p. 1141-1153, doi:10.1093/petrology/43.7.1141.

Keppie, J. D., Dostal, J., Murphy, J. B., Galaz-Escanilla, G., Ramos-Arias, M. A., and Nance, R. D., 2012, High pressure rocks of the Acatlan Complex, southern Mexico: Large-scale subducted Ordovician rifted passive margin extruded into the upper plate during the Devonian–Carboniferous: Tectonophysics, v. 560-561, p. 1-21, doi:10.1016/j.tecto.2012.06.015.

Kettanah, Y.A., Mory, A.J., Wach, G.D., and Wingate, M.T.D., 2015, Provenance of the Ordovician–lower Silurian Tumblagooda Sandstone, Western Australia: Australian Journal of Earth Sciences, v. 62, p. 817–830, doi:10.1080/08120099.2015.1117020.

Khan, A. U., Bhartiya, S. P., and Kumar, G., 1996, Cross faults in Ganga Basin and their surface manifestations, Geological Survey of India Special Publication 21: Calcutta, p. 215-220.

Khanal, S., and Robinson, D. M., 2013, Upper crustal shortening and forward modeling of the Himalayan thrust belt along the Budhi-Gandaki River, central Nepal: International Journal of Earth Sciences, v. 102, p. 1871-1891, doi:10.1007/s00531-013-0889-1.

Khanal, S., Robinson, D. M., Kohn, M. J., and Mandal, S., 2015a, Evidence for a far-traveled thrust sheet in the Greater Himalayan thrust system, and an alternative model to building the Himalaya: Tectonics, v. 34, p. 31–52, doi:10.1002/2014TC003616.

Khanal, S., Robinson, D. M., Mandal, S., and Simkhada, P., 2015b, Structural, geochronological and geochemical evidence for two distinct thrust sheets in the 'Main Central thrust zone', the Main Central thrust and Ramgarh–Munsiari thrust: implications for upper crustal shortening in central Nepal, *in* Mukherjee, S., Carosi, R., van der Beek, P. A., Mukherjee, B. K., and Robinson, D. M., eds., Tectonics of the Himalaya, Geological Society, London, Special Publications, 412, p. 221-245, doi:10.1144/SP412.2.

Kimbrough, D. L., Grove, M., and Morton, D. M., 2015, Timing and significance of gabbro emplacement within two distinct plutonic domains of the Peninsular Ranges batholith, southern and Baja California: Geological Society of America Bulletin, v. 127, p. 19-37, doi:10.1130/B30914.1.

Klootwijk, C. T., and Bingham, D. K., 1980, The extent of greater India, III. Palaeomagnetic data from the Tibetan sedimentary series, Thakkhola region, Nepal Himalaya: Earth and Planetary Science Letters, v. 51, p. 381-405, doi:10.1016/0012-821X(80)90219-8.

Klootwijk, C. T., Shah, S. K., Gergan, J., Sharma, M. L., Tirkey, B., and Gupta, B. K., 1983, A palaeomagnetic reconnaissance of Kashmir, northwestern Himalaya, India: Earth and Planetary Science Letters, v. 63, p. 305-324, doi:10.1016/0012-821X(83)90044-4.

Kohn, M. J., 2014, Himalayan metamorphism and its tectonic implications: Annual Review of Earth and Planetary Sciences, v. 42, p. 381-419, doi:10.1146/annurev-earth-060313-055005.

Kohn, M. J., Paul, S. K., and Corrie, S. L., 2010, The lower Lesser Himalayan sequence: a Paleoproterozoic arc on the northern margin of the Indian plate: Geological Society of America Bulletin, v. 122, p. 323-335, doi:10.1130/B26587.1.

Kohn, M. J., Wieland, M., Parkinson, C. D., and Upreti, B. N., 2004, Miocene faulting at plate tectonic velocity in the Himalaya of central Nepal: Earth and Planetary Science Letters, v. 228, p. 299-310, doi:10.1016/j.epsl.2004.10.007.

Kouketsu, Y., Hattori, K., and Guillot, S., 2017, Protolith of the Stak eclogite in the northwestern Himalaya: Italian Journal of Geosciences, v. 136, p. 64–72, doi: 10.3301/IJG.2015.41.

Kolodner, K., Avigad, D., McWilliams, M., Wooden, J. L., Weissbrod, T., and Feinstein, S., 2006, Provenance of north Gondwana Cambrian–Ordovician sandstone: U–Pb SHRIMP dating of detrital zircons from Israel and Jordan: Geological Magazine, v. 143, p. 367-391, doi:10.1017/S0016756805001640

Kominz, M. A., Browning, J. V., Miller, K. G., Sugarman, P. J., Mizintseva, S., and Scotese, C. R., 2008, Late Cretaceous to Miocene sea-level estimates from the New Jersey and Delaware coastal plain coreholes: an error analysis: Basin Research, v. 20, p. 211-226, doi:10.1111/j.1365-2117.2008.00354.x.

Kumar, A., Mitra, S., and Suresh, G., 2015, Seismotectonics of the eastern Himalayan and indo-burman plate boundary systems: Tectonics, v. 34, p. 2279–2295, doi:10.1002/2015TC003979.

Larson, K.P., Kellett, D.A., Cottle, J.M., King, J., Lederer, G., and Rai, S.M., 2016, Anatexis, cooling, and kinematics during orogenesis: Miocene development of the Himalayan metamorphic core, east-central Nepal: Geosphere, v. 12, p. 1575–1593, doi: 10.1130/GES01293.1.

Larson, K. P., Ambrose, T. K., Webb, A. A. G., Cottle, J. M., and Shrestha, S., 2015, Reconciling Himalayan midcrustal discontinuities: the Main Central Thrust system: Earth and Planetary Science Letters, v. 429, p. 139-146, doi:10.1016/j.epsl.2015.07.070.

Larson, K. P., and Cottle, J. M., 2014, Midcrustal discontinuities and the assembly of the Himalayan midcrust: Tectonics, v. 33, p. 718–740, doi:10.1002/2013TC003452.

Larson, K. P., Godin, L., and Price, R. A., 2010, Relationships between displacement and distortion in orogens: linking the Himalayan foreland and hinterland in central Nepal: Geological Society of America Bulletin, v. 122, p. 1116-1134, doi:10.1130/B30073.1.

Le Fort, P., 1975, Himalayas: the collided range. Present knowledge of the continental arc: American Journal of Science, v. 275-a, p. 1-44.

Lee, J., Hacker, B. R., Dinklage, W. S., Wang, Y., Gans, P., Calvert, A., Wan, J. L., Chen, W., Blythe, A. E., and McClelland, W., 2000, Evolution of the Kangmar Dome, southern Tibet: structural, petrologic, and thermochronologic constraints: Tectonics, v. 19, p. 872-895, doi:10.1029/1999TC001147.

Leger, R. M., Webb, A. A. G., Henry, D. J., Craig, J. A., and Dubey, P., 2013, Metamorphic field gradients across the Himachal Himalaya, northwest India: implications for the emplacement of the Himalayan crystalline core: Tectonics, v. 32, p. 540–557, doi:10.1002/tect.20020.

Li, X.-h., Li, Z.-X., Zhou, H., Liu, Y., and Kinney, P. D., 2002, U–Pb zircon geochronology, geochemistry and Nd isotopic study of Neoproterozoic bimodal volcanic rocks in the Kangdian Rift of South China: implications for the initial rifting of Rodinia: Precambrian Research, v. 113, p. 135-154, doi:10.1016/S0301-9268(01)00207-8.

Li, Z.X., Bogdanova, S.V., Collins, A.S., Davidson, A., De Waele, B., Ernst, R.E., Fitzsimons, I.C.W., Fuck, R.A., Gladkochub, D.P., Jacobs, J., Karlstrom, K.E., Lu, S., Natapov, L.M., Pease, V., et al., 2008, Assembly, configuration, and break-up history of Rodinia: A synthesis: Precambrian Research, v. 160, p. 179–210, doi:10.1016/j.precamres.2007.04.021.

Liu, G., and Einsele, G., 1994, Sedimentary history of the Tethyan basin in the Tibetan Himalayas: Geologische Rundschau (International Journal of Earth Sciences), v. 83, p. 32-61, doi:10.1007/BF00211893.

Liu, Y., Siebel, W., Theye, T., and Massonne, H.-J., 2011, Isotopic and structural constraints on the late Miocene to Pliocene evolution of the Namche Barwa area, eastern Himalayan syntaxis, SE Tibet: Gondwana Research, v. 19, p. 894–909, doi: 10.1016/j.gr.2010.11.005.

Long, S., McQuarrie, N., Tobgay, T., and Grujic, D., 2011a, Geometry and crustal shortening of the Himalayan fold-thrust belt, eastern and central Bhutan: Geological Society of America Bulletin, v. 123, p. 1427-1447, doi:10.1130/B30203.1.

Long, S., McQuarrie, N., Tobgay, T., Rose, C., Gehrels, G., and Grujic, D., 2011b, Tectonostratigraphy of the Lesser Himalaya of Bhutan: implications for the along-strike stratigraphic continuity of the northern Indian margin: Geological Society of America Bulletin, v. 123, p. 1406-1426, doi:10.1130/B30202.1.

Long, S. P., McQuarrie, N., Tobgay, T., Coutand, I., Cooper, F. J., Reiners, P. W., Wartho, J.-A., and Hodges, K. V., 2012, Variable shortening rates in the eastern Himalayan thrust belt, Bhutan: insights from multiple thermochronologic and geochronologic data sets tied to kinematic reconstructions: Tectonics, v. 31, TC5004, doi:10.1029/2012TC003155.

Luais, B., Duchene, S., and de Sigoyer, J., 2001, Sm–Nd disequilibrium in high-pressure, low-temperature Himalayan and Alpine rocks: Tectonophysics, v. 342, p. 1–22, doi: 10.1016/S0040-1951(01)00154-8.

Ma, Y., Yang, T., Yang, Z., Zhang, S., Wu, H., Li, H., Li, H., Chen, W., Zhang, J., and Ding, J., 2014, Paleomagnetism and U-Pb zircon geochronology of Lower Cretaceous lava flows from the western Lhasa terrane: new constraints on the India-Asia collision process and intracontinental deformation within Asia: Journal of Geophysical Research, v. 119, p. 7404-7424, doi:10.1002/2014JB011362.

Mamani, M., Worner, G., and Sempere, T., 2009, Geochemical variations in igneous rocks of the Central Andean orocline (13°S to 18°S): tracing crustal thickening and magma generation through time and space: Geological Society of America Bulletin, v. 122, p. 162-182, doi:10.1130/B26538.1.

Mandal, S., Robinson, D.M., Kohn, M.J., Khanal, S., Das, O., and Bose, S., 2016, Zircon U-Pb ages and Hf isotopes of the Askot klippe, Kumaun, northwest India: Implications for Paleoproterozoic tectonics, basin evolution and associated metallogeny of the northern Indian cratonic margin: Tectonics, v. 35, p. 965–982, doi:10.1002/2015TC004064.

Markwitz, V., Kirkland, C.L., and Evans, N.J., 2017, Early Cambrian metamorphic zircon in the northern Pinjarra Orogen: Implications for the structure of the West Australian Craton margin: Lithosphere, v. 9, p. 3–13, doi:10.1130/L569.1.

Martin, A.J., 2016, A review of definitions of the Himalayan Main Central Thrust: International Journal of Earth Sciences, doi: 10.1007/s00531-016-1419-8.

Martin, A. J., Copeland, P., and Benowitz, J. A., 2015, Muscovite $^{40}Ar/^{39}Ar$ ages help reveal the Neogene tectonic evolution of the southern Annapurna Range, central Nepal, *in* Mukherjee, S., Carosi, R., van der Beek, P. A., Mukherjee, B. K., and Robinson, D. M., eds., Tectonics of the Himalaya, Geological Society, London, Special Publications, 412, p. 199-220, doi:10.1144/SP412.5.

Martin, A. J., Ganguly, J., and DeCelles, P. G., 2010, Metamorphism of Greater and Lesser Himalayan rocks exposed in the Modi Khola valley, central Nepal: Contributions to Mineralogy and Petrology, v. 159, p. 203-223, doi:10.1007/s00410-009-0424-3.

Martin, A. J., Gehrels, G. E., and DeCelles, P. G., 2007, The tectonic significance of (U,Th)/Pb ages of monazite inclusions in garnet from the Himalaya of central Nepal: Chemical Geology, v. 244, p. 1-24, doi:10.1016/j.chemgeo.2007.05.003.

Mazzotti, S., and Hyndman, R. D., 2002, Yakutat collision and strain transfer across the northern Canadian Cordillera: Geology, v. 30, p. 495-498, doi:10.1130/0091-7613(2002)030<0495:YCASTA>2.0.CO;2.

McElroy, R., Cater, J., Roberts, I., Peckham, A., and Bond, M., 1990, The structure and stratigraphy of SE Zanskar, Ladakh Himalaya: Journal of the Geological Society of London, v. 147, p. 989-997, doi:10.1144/gsjgs.147.6.0989.

McKenzie, N. R., Hughes, N. C., Myrow, P. M., Xiao, S., and Sharma, M., 2011a, Correlation of Precambrian–Cambrian sedimentary successions across northern India and the utility of isotopic signatures of Himalayan lithotectonic zones: Earth and Planetary Science Letters, v. 312, p. 471-483, doi:10.1016/j.epsl.2011.10.027.

McKenzie, N. R., Hughes, N. C., Myrow, P. M., Choi, D. K., and Park, T.-Y., 2011b, Trilobites and zircons link north China with the eastern Himalaya during the Cambrian: Geology, v. 39, p. 591-594, doi:10.1130/G31838.1.

McQuarrie, N., Long, S. P., Tobgay, T., Nesbit, J. N., Gehrels, G., and Ducea, M. N., 2013, Documenting basin scale, geometry and provenance through detrital geochemical data: Lessons from the Neoproterozoic to Ordovician Lesser, Greater, and Tethyan Himalayan strata of Bhutan: Gondwana Research, v. 23, p. 1491-1510, doi:10.1016/j.gr.2012.09.002.

McQuarrie, N., Tobgay, T., Long, S. P., Reiners, P. W., and Cosca, M. A., 2014, Variable exhumation rates and variable displacement rates: documenting recent slowing of Himalayan shortening in western Bhutan: Earth and Planetary Science Letters, v. 386, p. 161-174, doi:10.1016/j.epsl.2013.10.045.

Medlicott, H. B., 1865, IV.—On the geological structure and relations of the southern portion of the Himalayan range between the rivers Ganges and Ravee: Memoirs of the Geological Survey of India, v. 3, p. 1-206.

Medlicott, H. B., and Blanford, W. T., 1879, A manual of the geology of India: Calcutta, Geological Survey of India, 817 p.

Meert, J. G., Pandit, M. K., Pradhan, V. R., Banks, J., Sirianni, R., Stroud, M., Newstead, B., and Gifford, J., 2010, Precambrian crustal evolution of peninsular India: a 3.0 billion year odyssey: Journal of Asian Earth Sciences, v. 39, p. 483-515, doi:10.1016/j.jseaes.2010.04.026.

Mezger, K., and Cosca, M. A., 1999, The thermal history of the Eastern Ghats Belt (India) as revealed by U–Pb and ^{40}Ar/^{39}Ar dating of metamorphic and magmatic minerals: implications for the SWEAT correlation: Precambrian Research, v. 94, p. 251-271, doi:10.1016/S0301-9268(98)00118-1.

Middlemiss, C. S., 1890, Physical geology of the sub-Himalaya of Garhwal and Kumaun: Memoirs of the Geological Survey of India, v. 24, part 2, p. 1-142.

Miller, C., Thoni, M., Frank, W., Grasemann, B., Klotzli, U., Guntli, P., and Draganits, E., 2001, The early Palaeozoic magmatic event in the Northwest Himalaya, India: source, tectonic setting and age of emplacement: Geological Magazine, v. 138, p. 237-251, doi:10.1017/S0016756801005283.

Mishra, D. C., Gupta, S. B., Rao, M. B. S. V., and Venkatrayudu, M., 1996, Crustal structure and basement tectonics under Vindhyan Basin: gravity-magnetic study: Memoir of the Geological Society of India, v. 36, p. 213-224.

Monsalve, G., Sheehan, A., Schulte-Pelkum, V., Rajaure, S., Pandey, M. R., and Wu, F., 2006, Seismicity and one-dimensional velocity structure of the Himalayan collision zone: Earthquakes in the crust and upper mantle: Journal of Geophysical Research, v. 111, B10301, doi:10.1029/2005JB004062.

Montomoli, C., Iaccarino, S., Carosi, R., Langone, A., and Visona, D., 2013, Tectonometamorphic discontinuities within the Greater Himalayan Sequence in Western Nepal (Central Himalaya): insights on the exhumation of crystalline rocks: Tectonophysics, v. 608, p. 1349-1370, doi:10.1016/j.tecto.2013.06.006.

Mory, A.J., Iasky, R.P., and Ghori, K.A.R., 2003, A summary of the geological evolution and petroleum potential of the Southern Carnarvon Basin, Western Australia: Perth, Geological Survey of Western Australia, Report 86, 26 p.

Mottram, C. M., Argles, T. W., Harris, N. B. W., Parrish, R. R., Horstwood, M. S. A., Warren, C. J., and Gupta, S., 2014, Tectonic interleaving along the Main Central Thrust, Sikkim Himalaya: Journal of the Geological Society of London, v. 171, p. 255-268, doi:10.1144/jgs2013-064.

Mugnier, J. L., and Huyghe, P., 2006, Ganges basin geometry records a pre-15 Ma isostatic rebound of Himalaya: Geology, v. 34, p. 445-448, doi:10.1130/G22089.1.

Mukherjee, S., 2013, Higher Himalaya in the Bhagirathi section (NW Himalaya, India): its structures, backthrusts and extrusion mechanism by both channel flow and critical taper mechanisms: International Journal of Earth Sciences, v. 102, p. 1851-1870, doi:10.1007/s00531-012-0861-5.

Mukherjee, S., 2015, A review on out-of-sequence deformation in the Himalaya, *in* Mukherjee, S., Carosi, R., van der Beek, P.A., Mukherjee, B.K., and Robinson, D.M. eds., Tectonics of the Himalaya, London, Geological Society, Special Publication, v. 412, p. 67–109, doi:10.1144/SP412.13.

Mukhopadhyay, G., Mukhopadhyay, S. K., Roychowdhury, M., and Parui, P. K., 2010, Stratigraphic correlation between different Gondwana basins of India: Journal of the Geological Society of India, v. 76, p. 251-266, doi:10.1007/s12594-010-0097-6.

Mukhopadhyay, M., 1984, Seismotectonics of transverse lineaments in the eastern Himalaya and its foredeep: Tectonophysics, v. 109, p. 227-240, doi:10.1016/0040-1951(84)90142-2.

Muller, R. D., Sdrolias, M., Gaina, C., Steinberger, B., and Heine, C., 2008, Long-term sea-level fluctuations driven by ocean basin dynamics: Science, v. 319, p. 1357-1362, doi:10.1126/science.1151540.

Munteanu, I., Willingshofer, E., Matenco, L., Sokoutis, D., and Cloetingh, S., 2014, Far-field contractional polarity changes in models and nature: Earth and Planetary Science Letters, v. 395, p. 101-115, doi:10.1016/j.epsl.2014.03.036.

Murphy, M. A., and Yin, A., 2003, Structural evolution and sequence of thrusting in the Tethyan fold-thrust belt and Indus-Yalu suture zone, Southwest Tibet: Geological Society of America Bulletin, v. 115, p. 21-34, doi:10.1130/0016-7606(2003)115<0021:SEASOT>2.0.CO;2.

Myrow, P. M., Hughes, N. C., Paulsen, T. S., Williams, I. S., Parcha, S. K., Thompson, K. R., Bowring, S. A., Peng, S. C., and Ahluwalia, A. D., 2003, Integrated tectonostratigraphic analysis of the Himalaya and implications for its tectonic reconstruction: Earth and Planetary Science Letters, v. 212, p. 433-441, doi:10.1016/S0012-821X(03)00280-2.

Myrow, P. M., Snell, K. E., Hughes, N. C., Paulsen, T. S., Heim, N. A., and Parcha, S. K., 2006a, Cambrian depositional history of the Zanskar valley region of the Indian Himalaya: tectonic implications: Journal of Sedimentary Research, v. 76, p. 364-381, doi:10.2110/jsr.2006.020.

Myrow, P.M., Thompson, K.R., Hughes, N.C., Paulsen, T.S., Sell, B.K., and Parcha, S.K., 2006b, Cambrian stratigraphy and depositional history of the northern Indian Himalaya, Spiti Valley, north-central India: Geological Society of America Bulletin, v. 118, p. 491–510, doi: 10.1130/B25828.1.

Myrow, P.M., Hughes, N.C., Goodge, J.W., Fanning, C.M., Williams, I.S., Peng, S., Bhargava, O.N., Parcha, S.K., and Pogue, K.R., 2010, Extraordinary transport and mixing of sediment across Himalayan central Gondwana during the Cambrian-Ordovician: Geological Society of America Bulletin, v. 122, p. 1660–1670, doi:10.1130/B30123.1.

Myrow, P. M., Hughes, N. C., Derry, L. A., McKenzie, N. R., Jiang, G., Webb, A. A. G., Banerjee, D. M., Paulsen, T. S., and Singh, B. P., 2015, Neogene marine isotopic evolution and the erosion of Lesser Himalayan strata: implications for Cenozoic tectonic history: Earth and Planetary Science Letters, v. 417, p. 142-150, doi:10.1016/j.epsl.2015.02.016.

Myrow, P.M., Hughes, N.C., McKenzie, N.R., Pelgay, P., Thomson, T.J., Haddad, E.E., and Fanning, C.M., 2016, Cambrian–Ordovician orogenesis in Himalayan equatorial Gondwana: Geological Society of America Bulletin, v. 128, p. 1679–1695, doi: 10.1130/B31507.1.

Najman, Y., and Garzanti, E., 2000, Reconstructing early Himalayan tectonic evolution and paleogeography from Tertiary foreland basin sedimentary rocks, northern India: Geological Society of America Bulletin, v. 112, p. 435-449, doi:10.1130/0016-7606(2000)112<435:REHTEA>2.0.CO;2.

Najman, Y., Clift, P., Johnson, M. R. W., and Robertson, A. H. F., 1993, Early stages of foreland basin evolution in the Lesser Himalaya, N India, *in* Treloar, P. J., and Searle, M. P., eds., Himalayan tectonics: Geological Society Special Publication 74, p. 541-558, doi10.1144/GSL.SP.1993.074.01.36.

Najman, Y., Carter, A., Oliver, G., and Garzanti, E., 2005, Provenance of Eocene foreland basin sediments, Nepal: constraints to the timing and diachroneity of early Himalayan orogenesis: Geology, v. 33, p. 309-312, doi:10.1130/G21161.1.

Najman, Y., Appel, E., Boudagher-Fadel, M., Brown, P., Carter, A., Garzanti, E., Godin, L., Han, J., Liebke, U., Oliver, G., Parrish, R., and Vezzoli, G., 2010, Timing of India-Asia collision: geological, biostratigraphic, and palaeomagnetic constraints: Journal of Geophysical Research, v. 115, B12416, doi:10.1029/2010JB007673.

Najman, Y., Jenks, D., Godin, L., Boudagher-Fadel, M., Millar, I., Garzanti, E., Horstwood, M., and Bracciali, L., 2017, The Tethyan Himalayan detrital record shows that India–Asia terminal collision occurred by 54 Ma in the Western Himalaya: Earth and Planetary Science Letters, v. 459, p. 301–310, doi: 10.1016/j.epsl.2016.11.036.

Nakata, T., 1972, Geomorphic history and crustal movements of the foot-hills of the Himalayas, The science reports of the Tohoku University, 7th series (Geography): Sendai, Faculty of Science, Tohoku University, p. 39-177.

-, 1975, On Quaternary tectonics around the Himalayas, The science reports of the Tohoku University, 7th series (Geography): Sendai, Faculty of Science, Tohoku University, p. 111-118.

Neumayer, J., Wiesmayr, G., Janda, C., Grasemann, B., and Draganits, E., 2004, Eohimalayan fold and thrust belt in the NW-Himalaya (Lingti-Pin valleys): shortening and depth to detachment calculation: Austrian Journal of Earth Sciences, v. 95/96, p. 28-36.

Oldham, R. D., 1893, A manual of the geology of India, 2nd edition: Calcutta, Geological Survey of India, 543 p.

Orme, D.A., and Laskowski, A.K., 2016, Basin analysis of the Albian–Santonian Xigaze forearc, Lazi region, south-central Tibet: Journal of Sedimentary Research, v. 86, p. 894–913, doi: 10.2110/jsr.2016.59.

Orme, D.A., Carrapa, B., and Kapp, P., 2015, Sedimentology, provenance and geochronology of the upper Cretaceous-lower Eocene western Xigaze forearc basin, southern Tibet: Basin Research, v. 27, p. 387–411, doi: 10.1111/bre.12080.

Pandit, D., and Panigrahi, M. K., 2012, Comparative petrogenesis and tectonics of Paleoproterozoic Malanjkhand and Dongargarh granitoids, Central India: Journal of Asian Earth Sciences, v. 50, p. 14-26, doi:10.1016/j.jseaes.2012.01.017.

Panien, M., Buiter, S. J. H., Schreurs, G., and Pfiffner, O. A., 2006, Inversion of a symmetric basin: insights from a comparison between analogue and numerical experiments, *in* Buiter, S. J. H., and Schreurs, G., eds., Analogue and numerical modelling of crustal-scale processes, Geological Society, London, Special Publications, 253, p. 253-270, doi:10.1144/GSL.SP.2006.253.01.13.

Panien, M., Schreurs, G., and Pfiffner, A., 2005, Sandbox experiments on basin inversion: testing the influence of basin orientation and basin fill: Journal of Structural Geology, v.

27, p. 433-445, doi:10.1016/j.jsg.2004.11.001.

Papritz, K., and Rey, R., 1989, Evidence for the occurrence of Permian Panjal Trap basalts in the Lesser- and Higher-Himalayas of the Western Syntaxis area, NE Pakistan: Eclogae Geologicae Helvetiae, v. 82, p. 603–627, doi: 10.5169/seals-166392.

Patel, R. C., Singh, S., Asokan, A., Manickavasagam, R. M., and Jain, A. K., 1993, Extensional tectonics in the Himalayan orogen, Zanskar, NW India, *in* Treloar, P. J., and Searle, M. P., eds., Himalayan Tectonics, Geological Society, London, Special Publications, 74, p. 445-459, doi:10.1144/GSL.SP.1993.074.01.30.

Pearce, J. A., Harris, N. B. W., and Tindle, A. G., 1984, Trace element discrimination diagrams for the tectonic interpretation of granitic rocks Journal of Petrology, v. 25, p. 956-983, doi:10.1093/petrology/25.4.956.

Pearson, O. N., and DeCelles, P. G., 2005, Structural geology and regional tectonic significance of the Ramgarh thrust, Himalayan fold-thrust belt of Nepal: Tectonics, v. 24, TC4008, doi:10.1029/2003TC001617.

Philippon, M., Willingshofer, E., Sokoutis, D., Corti, G., Sani, F., Bonini, M., and Cloetingh, S., 2015, Slip re-orientation in oblique rifts: Geology, v. 43, p. 147-150, doi:10.1130/G36208.1.

Pinto, L., Munoz, C., Nalpas, T., and Charrier, R., 2010, Role of sedimentation during basin inversion in analogue modelling: Journal of Structural Geology, v. 32, p. 554-565, doi:10.1016/j.jsg.2010.03.001.

Platt, J. P., and Behr, W. M., 2011, Lithospheric shear zones as constant stress experiments: Geology, v. 39, p. 127-130, doi:10.1130/G31561.1.

Pogue, K. R., Wardlaw, B. R., Harris, A. G., and Hussain, A., 1992, Paleozoic and Mesozoic stratigraphy of the Peshawar basin, Pakistan: correlations and implications: Geological Society of America Bulletin, v. 104, p. 915-927, doi:10.1130/0016-7606(1992)104<0915:PAMSOT>2.3.CO;2.

Pollock, J. C., Hibbard, J. P., and van Staal, C. R., 2012, A paleogeographical review of the peri-Gondwanan realm of the Appalachian orogen: Canadian Journal of Earth Sciences, v. 49, p. 259-288, doi:10.1139/E11-049.

Powell, C.M., and Conaghan, P.J., 1973, Plate tectonics and the Himalayas: Earth and Planetary Science Letters, v. 20, p. 1–12, doi:10.1016/0012-821X(73)90134-9.

Prasad, B. R., Klemperer, S. L., Rao, V. V., Tewari, H. C., and Khare, P., 2011, Crustal structure beneath the Sub-Himalayan fold–thrust belt, Kangra recess, northwest India, from seismic reflection profiling: implications for Late Paleoproterozoic orogenesis and modern earthquake hazard: Earth and Planetary Science Letters, v. 308, p. 218-228, doi:10.1016/j.epsl.2011.05.052.

Pullen, A., Ibanez-Mejia, M., Gehrels, G.E., Ibanez-Mejia, J.C., and Pecha, M., 2014, What happens when n=1000? Creating large-n geochronological datasets with LA-ICP-MS for geologic investigations: Journal of Analytical Atomic Spectrometry, v. 29, p. 971–980, doi:10.1039/c4ja00024b.

Quigley, M. C., Liangjun, Y., Gregory, C., Corvino, A., Sandiford, M., Wilson, C. J. L., and Xiaohan, L., 2008, U–Pb SHRIMP zircon geochronology and T–t–d history of the Kampa Dome, southern Tibet: Tectonophysics, v. 446, p. 97-113, doi:10.1016/j.tecto.2007.11.004.

Quinn, M. J., Wright, J. E., and Wyld, S. J., 1997, Happy Creek igneous complex and tectonic evolution of the early Mesozoic arc in the Jackson Mountains, northwest Nevada:

Geological Society of America Bulletin, v. 109, p. 461-482, doi:10.1130/0016-7606(1997)109<0461:HCICAT>2.3.CO;2.

Raiverman, V., Chugh, M. L., Srivastava, A. K., Prasad, D. N., and Das, S. K., 1994, Cenozoic tectonics of the fold belt of Himalaya and the Indo-Gangetic foredeep with pointers towards hydrocarbon prospects, *in* Biswas, S. K., et al., ed., Proceedings of the second seminar on petroliferous basins of India, volume 3: Dehra Dun, Indian Petroleum Publishers, p. 25-54.

Raiverman, V., Srivastava, A. K., and Prasad, D. N., 1993, On the foothill thrust of northwestern Himalaya: Journal of Himalayan Geology, v. 4, p. 237-256.

Ram, J., Shukla, S. N., Pramanik, A. G., Varma, B. K., Chandra, G., and Murty, M. S. N., 1996, Recent investigations in the Vindhyan Basin: implications for the basin tectonics: Memoir of the Geological Society of India, v. 36, p. 267-286.

Rameshwar Rao, D., and Sharma, R., 2011, Arc magmatism in eastern Kumaun Himalaya, India: a study based on geochemistry of granitoid rocks: Island Arc, v. 20, p. 500-519, doi:10.1111/j.1440-1738.2011.00781.x.

Ran, B., Wang, C., Zhao, X., Li, Y., Meng, J., Cao, K., and Wang, P., 2012, Dimension of Greater India in the early Mesozoic: paleomagnetic constraints from Triassic sediments in the Tethyan Himalaya: Journal of Asian Earth Sciences, v. 53, p. 15-24, doi:10.1016/j.jseaes.2011.11.006.

Rao, M. B. R., 1973, The subsurface geology of the Indo-Gangetic plains: Journal of the Geological Society of India, v. 14, p. 217-242.

Ratschbacher, L., Frisch, W., Liu, G., and Chen, C., 1994, Distributed deformation in southern and western Tibet during and after the India-Asia collision: Journal of Geophysical Research, v. 99, p. 19917-19945, doi:10.1029/94JB00932.

Raza, M., Khan, A., and Khan, M. S., 2009, Origin of Late Palaeoproterozoic Great Vindhyan basin of north Indian shield: geochemical evidence from mafic volcanic rocks: Journal of Asian Earth Sciences, v. 34, p. 716-730, doi:10.1016/j.jseaes.2008.10.011.

Reddy, S. M., Searle, M. P., and Massey, J. A., 1993, Structural evolution of the High Himalayan gneiss sequence, Langtang Valley, Nepal, *in* Treloar, P. J., and Searle, M. P., eds., Himalayan tectonics: Geological Society Special Publication 74: London, p. 375-389, doi:10.1144/GSL.SP.1993.074.01.25.

Reid, A., Hand, M., Jagodzinski, E., Kelsey, D., and Pearson, N., 2008, Paleoproterozoic orogenesis in the southeastern Gawler Craton, South Australia: Australian Journal of Earth Sciences, v. 55, p. 449-471, doi:10.1080/08120090801888594.

Renne, P.R., Sprain, C.J., Richards, M.A., Self, S., Vanderkluysen, L., and Pande, K., 2015, State shift in Deccan volcanism at the Cretaceous-Paleogene boundary, possibly induced by impact: Science, v. 350, p. 76–78, doi:10.1126/science.aac7549.

Rennie, S. F., Fagereng, A., and Diener, J. F. A., 2013, Strain distribution within a km-scale, mid-crustal shear zone: the Kuckaus Mylonite Zone, Namibia: Journal of Structural Geology, v. 56, p. 57-69, doi:10.1016/j.jsg.2013.09.001.

Richards, A., Argles, T., Harris, N. B. W., Parrish, R. R., Ahmad, T., Darbyshire, F., and Draganits, E., 2005, Himalayan architecture constrained by isotopic tracers from clastic sediments: Earth and Planetary Science Letters, v. 236, p. 773-796, doi:10.1016/j.epsl.2005.05.034.

Robinson, D. M., DeCelles, P. G., Garzione, C. N., Pearson, O. N., Harrison, T. M., and Catlos, E. J., 2003, Kinematic model for the Main Central Thrust in Nepal: Geology, v. 31, p.

359-362, doi:10.1130/0091-7613(2003)031<0359:KMFTMC>2.0.CO;2.

Robinson, D. M., DeCelles, P. G., and Copeland, P., 2006, Tectonic evolution of the Himalayan thrust belt in western Nepal: Implications for channel flow models: Geological Society of America Bulletin, v. 118, p. 865-885, doi:10.1130/B25911.1.

Robinson, D. M., and Martin, A. J., 2014, Reconstructing the Greater Indian margin: a balanced cross section in central Nepal focusing on the Lesser Himalayan duplex: Tectonics, v. 33, p. 2143-2168, doi:10.1002/2014TC003564.

Rogers, J. J. W., and Santosh, M., 2009, Tectonics and surface effects of the supercontinent Columbia: Gondwana Research, v. 15, p. 373-380, doi:10.1016/j.gr.2008.06.008.

Roure, F., 2008, Foreland and hinterland basins: what controls their evolution?: Swiss Journal of Geosciences, v. 101, p. 5-29, doi:10.1007/s00015-008-1285-x.

Roy, T. K., 1990, Structural styles in southern Cambay Basin India and role of Narmada Geofracture in formation of giant hydrocarbon accumulations: Bulletin of the Oil and Natural Gas Commission, v. 27, p. 15-56.

Rubatto, D., Chakraborty, S., and Dasgupta, S., 2013, Timescales of crustal melting in the Higher Himalayan Crystallines (Sikkim, Eastern Himalaya) inferred from trace element-constrained monazite and zircon chronology: Contributions to Mineralogy and Petrology, v. 165, p. 349-372, doi:10.1007/s00410-012-0812-y.

Rubatto, D., Hermann, J., and Buick, I. S., 2006, Temperature and bulk composition control on the growth of monazite and zircon during low-pressure anatexis (Mount Stafford, central Australia): Journal of Petrology, v. 47, p. 1973-1996, doi:10.1093/petrology/egl033.

Saha, D., and Mazumder, R., 2012, An overview of the Palaeoproterozoic geology of Peninsular India, and key stratigraphic and tectonic issues, *in* Mazumder, R., and Saha, D., eds., Palaeoproterozoic of India, Geological Society, London, Special Publications, 365, p. 5-29, doi:10.1144/SP365.2.

Sakai, H., 1983, Geology of the Tansen Group of the Lesser Himalaya in Nepal: Memoirs of the Faculty of Science, Kyushu University, Series D, Geology, v. 25, no. 1, p. 27-74.

Sakai, H., Iwano, H., Danhara, T., Takigami, Y., Rai, S. M., Upreti, B. N., and Hirata, T., 2013, Rift-related origin of the Paleoproterozoic Kuncha Formation, and cooling history of the Kuncha nappe and Taplejung granites, eastern Nepal Lesser Himalaya: a multichronological approach: Island Arc, v. 22, p. 338-360, doi:10.1111/iar.12021.

Sastri, V. V., Bhandari, L. L., Raju, A. T. R., and Datta, K., 1971, Tectonic framework and subsurface stratigraphy of the Ganga basin: Journal of the Geological Society of India, v. 12, p. 222-233.

Saxena, M. N., 1971, The crystalline axis of the Himalaya: Indian shield and continental drift: Tectonophysics, v. 12, p. 443-447, doi:10.1016/0040-1951(71)90044-8.

Scharer, U., Xu, R.-H., and Allegre, C. J., 1986, U-(Th)-Pb systematics and ages of Himalayan leucogranites, south Tibet: Earth and Planetary Science Letters, v. 77, p. 35-48, doi:10.1016/0012-821X(86)90130-5.

Schelling, D., and Arita, K., 1991, Thrust tectonics, crustal shortening, and the structure of the far-eastern Nepal Himalaya: Tectonics, v. 10, p. 851–862, doi: 10.1029/91TC01011.

Schill, E., Appel, E., Gautam, P., and Dietrich, P., 2002, Thermo-tectonic history of the Tethyan Himalayas deduced from the palaeomagnetic record of metacarbonates from Shiar Khola (central Nepal): Journal of Asian Earth Sciences, v. 20, p. 203-210, doi:10.1016/S1367-9120(01)00023-2.

Schoene, B., Samperton, K. M., Eddy, M. P., Keller, G., Adatte, T., Bowring, S. A., Khadri, S. F.

R., and Gertsch, B., 2015, U-Pb geochronology of the Deccan Traps and relation to the end-Cretaceous mass extinction: Science, v. 347, p. 182-184, doi:10.1126/science.aaa0118.

Schultz, M.H., Hodges, K.V., Ehlers, T.A., van Soest, M., and Wartho, J.-A., 2017, Thermochronologic constraints on the slip history of the South Tibetan detachment system in the Everest region, southern Tibet: Earth and Planetary Science Letters, v. 459, p. 105–117, doi: 10.1016/j.epsl.2016.11.022.

Searle, M., Corfield, R. I., Stephenson, B., and McCarron, J., 1997, Structure of the North Indian continental margin in the Ladakh–Zanskar Himalayas: implications for the timing of obduction of the Spontang ophiolite, India–Asia collision and deformation events in the Himalaya: Geological Magazine, v. 134, p. 297-316.

Searle, M. P., 1986, Structural evolution and sequence of thrusting in the High Himalayan, Tibetan—Tethys and Indus suture zones of Zanskar and Ladakh, Western Himalaya: Journal of Structural Geology, v. 8, p. 923-936, doi:10.1016/0191-8141(86)90037-4.

-, 2010, Low-angle normal faults in the compressional Himalayan orogen; Evidence from the Annapurna–Dhaulagiri Himalaya, Nepal: Geosphere, v. 6, p. 296-315, doi:10.1130/GES00549.1.

Searle, M. P., Law, R. D., Godin, L., Larson, K., Streule, M. J., Cottle, J. M., and Jessup, M. J., 2008, Defining the Himalayan Main Central thrust in Nepal: Journal of the Geological Society of London, v. 165, p. 523-534, doi:10.1144/0016-76492007-081.

Searle, M. P., Waters, D. J., Rex, D. C., and Wilson, R. N., 1992, Pressure, temperature and time constraints on Himalayan metamorphism from eastern Kashmir and western Zanskar: Journal of the Geological Society of London, v. 149, p. 753-773, doi:10.1144/gsjgs.149.5.0753.

Seeber, L., and Armbruster, J., 1979, Seismicity of the Hazara arc in northern Pakistan: decollement vs. basement faulting, *in* Farah, A., and DeJong, K. A., eds., Geodynamics of Pakistan: Quetta, Geological Survey of Pakistan, p. 131-142.

Seeber, L., and Armbruster, J. G., 1981, Great detachment earthquakes along the Himalayan arc and long-term forecasting, *in* Simpson, D. W., and Richards, P. G., eds., Earthquake Prediction–An International Review: Washington, D.C., American Geophysical Union, p. 259-277, doi:10.1029/ME004p0259.

Seton, M., Muller, R. D., Zahirovic, S., Gaina, C., Torsvik, T., Shepard, G., Talsma, M., Gurnis, M., Turner, M., Maus, S., and Chandler, M., 2012, Global continental and ocean basin reconstructions since 200 Ma: Earth-Science Reviews, v. 113, p. 212-270, doi:10.1016/j.earscirev.2012.03.002.

Shellnutt, J. G., Bhat, G. M., Wang, K.-L., Yeh, M.-W., Brookfield, M. E., and Jahn, B.-M., 2015, Multiple mantle sources of the Early Permian Panjal Traps, Kashmir, India: American Journal of Science, v. 315, p. 589-619, doi:10.2475/07.2015.01.

Sheppard, S., Griffin, T. J., Tyler, I. M., and Page, R. W., 2001, High- and low-K granites and adakites at a Palaeoproterozoic plate boundary in northwestern Australia: Journal of the Geological Society of London, v. 158, p. 547-560, doi:10.1144/jgs.158.3.547.

Simmat, R., and Raith, M. M., 2008, U–Th–Pb monazite geochronometry of the Eastern Ghats Belt, India: timing and spatial disposition of poly-metamorphism: Precambrian Research, v. 162, p. 16-39, doi:10.1016/j.precamres.2007.07.016.

Sinclair, H. D., 1997, Tectonostratigraphic model for underfilled peripheral foreland basins: an Alpine perspective: Geological Society of America Bulletin, v. 109, p. 324-346, doi:10.1130/0016-7606(1997)109<0324:TMFUPF>2.3.CO;2.

Singh, I. B., 1996, Geological evolution of Ganga plain – an overview: Journal of the Palaeontological Society of India, v. 41, p. 99-137.

Singh, S., Kumar, R., Barley, M. E., and Jain, A. K., 2007, SHRIMP U–Pb ages and depth of emplacement of Ladakh Batholith, Eastern Ladakh, India: Journal of Asian Earth Sciences, v. 30, p. 490-503, doi:10.1016/j.jseaes.2006.12.003.

Sinha-Roy, S., 1976, A possible Himalayan microcontinent: Nature, v. 263, p. 117–120, doi:10.1038/263117a0.

Slama, J., and Kosler, J., 2012, Effects of sampling and mineral separation on accuracy of detrital zircon studies: Geochemistry, Geophysics, Geosystems, v. 13, Q05007, doi:10.1029/2012GC004106.

Sorcar, N., Hoppe, U., Dasgupta, S., and Chakraborty, S., 2014, High-temperature cooling histories of migmatites from the High Himalayan Crystallines in Sikkim, India: rapid cooling unrelated to exhumation?: Contributions to Mineralogy and Petrology, v. 167:957, doi:10.1007/s00410-013-0957-3.

Soto, R., Martinod, J., and Odonne, F., 2007, Influence of early strike-slip deformation on subsequent perpendicular shortening: an experimental approach: Journal of Structural Geology, v. 29, p. 59-72, doi:10.1016/j.jsg.2006.08.001.

Spencer, C. J., Harris, R. A., Sachan, H. K., and Saxena, A., 2011, Depositional provenance of the Greater Himalayan Sequence, Garhwal Himalaya, India: implications for tectonic setting: Journal of Asian Earth Sciences, v. 41, p. 344-354, doi:10.1016/j.jseaes.2011.02.001.

Spencer, D.A., Tonarini, S., and Pognante, U., 1995, Geochemical and Sr-Nd characterisation of Higher Himalayan eclogites (and associated metabasites): European Journal of Mineralogy, v. 7, p. 89–102.

Spring, L., and Crespo-Blanc, A., 1992, Nappe tectonics, extension, and metamorphic evolution in the Indian Tethys Himalaya (Higher Himalaya, SE Zanskar and NW Lahul): Tectonics, v. 11, p. 978-989, doi:10.1029/92TC00338.

Srinivasan, S., and Khar, B. M., 1996, Status of hydrocarbon exploration in northwest Himalaya and foredeep–contributions to stratigraphy and structure, Proceedings, symposium on recent advances in geological studies of northwest Himalaya and the foredeep, Geological Survey of India Special Publication 21, p. 295-405.

Srinivasan, V., 2003, Stratigraphy and structure of Siwaliks in Arunachal Pradesh: a reappraisal through remote sensing techniques: Journal of the Geological Society of India, v. 62, p. 139-151.

Srivastava, D. C., and Sahay, A., 2003, Brittle tectonics and pore-fluid conditions in the evolution of the Great Boundary Fault around Chittaurgarh, northwestern India: Journal of Structural Geology, v. 25, p. 1713-1733, doi:10.1016/S0191-8141(03)00012-9.

Srivastava, P., and Mitra, G., 1994, Thrust geometries and deep structure of the outer and lesser Himalaya, Kumaon and Garhwal (India): Implications for evolution of the Himalayan fold-and-thrust belt: Tectonics, v. 13, p. 89–109, doi: 10.1029/93TC01130.

Srivastava, V., Mukul, M., and Barnes, J.B., 2016, Main Frontal thrust deformation and topographic growth of the Mohand Range, northwest Himalaya: Journal of Structural Geology, v. 93, p. 131–148, doi: 10.1016/j.jsg.2016.10.009.

Steck, A., 2003, Geology of the NW Indian Himalaya: Eclogae Geologicae Helvetiae, v. 96, p. 147-196, doi:10.5169/seals-169014.

Stephenson, R., Egholm, D. L., Nielsen, S. B., and Stovba, S. M., 2009, Role of thermal refraction in localizing intraplate deformation in southeastern Ukraine: Nature Geoscience, v. 2, p. 290-293, doi:10.1038/ngeo479.

Stern, R. J., 2004, Subduction initiation: spontaneous and induced: Earth and Planetary Science Letters, v. 226, p. 275-292, doi:10.1016/j.epsl.2004.08.007.

Stern, R. J., and Johnson, P., 2010, Continental lithosphere of the Arabian Plate: a geologic, petrologic, and geophysical synthesis: Earth-Science Reviews, v. 101, p. 29-67, doi:10.1016/j.earscirev.2010.01.002.

Strachey, R., 1851, On the geology of part of the Himalaya Mountains and Tibet: Quarterly Journal of the Geological Society, v. 7, p. 292-310, doi:10.1144/GSL.JGS.1851.007.01-02.54.

Sullivan, W. A., Boyd, A. S., and Monz, M. E., 2013, Strain localization in homogeneous granite near the brittle–ductile transition: a case study of the Kellyland fault zone, Maine, USA: Journal of Structural Geology, v. 56, p. 70-88, doi:10.1016/j.jsg.2013.09.003.

Surpless, B. E., 2010, Geologic map of the central Wassuk Range, W. NV: Geological Society of America Map Series, MCH098, scale 1:24,000.

-, 2012, Cenozoic tectonic evolution of the central Wassuk Range, western Nevada, USA: International Geology Review, v. 54, p. 547-571, doi:10.1080/00206814.2010.548117.

Talwani, M., Desa, M.A., Ismaiel, M., and Sree Krishna, K., 2016, The tectonic origin of the Bay of Bengal and Bangladesh: Journal of Geophysical Research: Solid Earth, v. 121, p. 4836–4851, doi: 10.1002/2015JB012734.

Tangri, S. K., and Pande, A. C., 1995, Tethyan Sequence, *in* Bhargava, O. N., ed., The Bhutan Himalaya: a geological account: Calcutta, Geological Survey of India Special Publication 39, p. 109-141.

Thakur, V. C., 2013, Active tectonics of Himalayan Frontal Fault system: International Journal of Earth Sciences, v. 102, p. 1791-1810, doi:10.1007/s00531-013-0891-7.

Thanh, N. X., Rajesh, V. J., Itaya, T., Windley, B., Kwon, S., and Park, C.-S., 2012, A Cretaceous forearc ophiolite in the Shyok suture zone, Ladakh, NW India: implications for the tectonic evolution of the Northwest Himalaya: Lithos, v. 155, p. 81-93, doi:10.1016/j.lithos.2012.08.016.

Thomas, W. A., 2006, Tectonic inheritance at a continental margin: GSA Today, v. 16, p. 4-11.

Thorarinsson, S. B., Holm, P. M., Duprat, H., and Tegner, C., 2011, Silicic magmatism associated with Late Cretaceous rifting in the Arctic Basin—petrogenesis of the Kap Kane sequence, the Kap Washington Group volcanics, North Greenland: Lithos, v. 125, p. 65-85, doi:10.1016/j.lithos.2011.01.013.

Torsvik, T. H., and Cocks, L. R. M., 2013, Gondwana from top to base in space and time: Gondwana Research, v. 24, p. 999-1030, doi:10.1016/j.gr.2013.06.012.

Torsvik, T. H., Paulsen, T. S., Hughes, N. C., Myrow, P. M., and Ganerod, M., 2009, The Tethyan Himalaya: palaeogeographical and tectonic constraints from Ordovician palaeomagnetic data: Journal of the Geological Society of London, v. 166, p. 679-687, doi:10.1144/0016-76492008-123.

Torsvik, T.H., Van der Voo, R., Preeden, U., Mac Niocaill, C., Steinberger, B., Doubrovine, P.V., van Hinsbergen, D.J.J., Domeier, M., Gaina, C., Tohver, E., Meert, J.G., McCausland, P.J.A., and Cocks, L.R.M., 2012, Phanerozoic polar wander, palaeogeography and dynamics: Earth-Science Reviews, v. 114, p. 325–368, doi:10.1016/j.earscirev.2012.06.007.

Trivedi, J.R., Gopalan, K., and Valdiya, K.S., 1984, Rb-Sr ages of granitic rocks within Lesser Himalayan nappes, Kumaun, India: Journal of the Geological Society of India, v. 25, p. 641–654.

Turner, J. P., and Williams, G. A., 2004, Sedimentary basin inversion and intra-plate shortening: Earth-Science Reviews, v. 65, p. 277–304, doi:10.1016/j.earscirev.2003.10.002.

Upadhyay, D., Gerdes, A., and Raith, M. M., 2009, Unraveling sedimentary provenance and tectonothermal history of high-temperature metapelites, using zircon and monazite chemistry: a case study from the Eastern Ghats Belt, India: The Journal of Geology, v. 117, p. 665-683, doi:10.1086/606036.

Upreti, B. N., 1996, Stratigraphy of the western Nepal Lesser Himalaya: a synthesis: Journal of Nepal Geological Society, v. 13, p. 11-28.

Valdiya, K. S., 1976, Himalayan transverse faults and folds and their parallelism with subsurface structures of north Indian plains: Tectonophysics, v. 32, p. 353-386, doi:10.1016/0040-1951(76)90069-X.

-, 1981, Tectonics of the central sector of the Himalaya, *in* Gupta, H. K., and Delany, F. M., eds., Zagros Hindu Kush Himalaya Geodynamic Evolution: Washington, D.C., American Geophysical Union, p. 87-110.

-, 2003, Reactivation of Himalayan Frontal Fault: implications: Current Science, v. 85, p. 1031-1040.

van Hinsbergen, D. J. J., Lippert, P. C., Dupont-Nivet, G., McQuarrie, N., Doubrovine, P. V., Spakman, W., and Torsvik, T. H., 2012, Greater India Basin hypothesis and a two-stage Cenozoic collision between India and Asia: Proceedings of the National Academy of Sciences of the United States of America, v. 109, p. 7659-7664, doi:10.1073/pnas.1117262109.

van Lente, B., Ashwal, L.D., Pandit, M.K., Bowring, S.A., and Torsvik, T.H., 2009, Neoproterozoic hydrothermally altered basaltic rocks from Rajasthan, northwest India: Implications for late Precambrian tectonic evolution of the Aravalli Craton: Precambrian Research, v. 170, p. 202–222, doi:10.1016/j.precamres.2009.01.007.

Vannay, J.-C., and Grasemann, B., 2001, Himalayan inverted metamorphism and syn-convergence extension as a consequence of a general shear extrusion: Geological Magazine, v. 138, p. 253-276, doi:10.1017/S0016756801005313.

Vannay, J. C., and Hodges, K. V., 1996, Tectonometamorphic evolution of the Himalayan metamorphic core between the Annapurna and Dhaulagiri, central Nepal: Journal of Metamorphic Geology, v. 14, no. 5, p. 635-656, doi:10.1046/j.1525-1314.1996.00426.x.

Vannay, J. C., and Spring, L., 1993, Geochemistry of the continental basalts within the Tethyan Himalaya of Lahul-Spiti and SE Zanskar, northwest India, *in* Treloar, P. J., and Searle, M. P., eds., Geological Society, London, Special Publications, 74, p. 237-249, doi:10.1144/GSL.SP.1993.074.01.17.

Vannay, J. C., and Steck, A., 1995, Tectonic evolution of the High Himalaya in Upper Lahul (NW Himalaya, India): Tectonics, v. 14, p. 253-263, doi:10.1029/94TC02455.

Vannay, J.-C., Sharp, Z.D., and Grasemann, B., 1999, Himalayan inverted metamorphism constrained by oxygen isotope thermometry: Contributions to Mineralogy and Petrology, v. 137, p. 90–101, doi:10.1007/s004100050584.

Veevers, J. J., 2000, Antarctic Beardmore-Ross and Mirny provenances saturate Paleozoic-Mesozoic East Gondwanaland with 0.6-0.5 Ga zircons, *in* Veevers, J. J., ed., Billion-year earth history of Australia and neighbours in Gondwanaland: Sydney, GEMOC Press, p.

110-130.

-, 2012, Reconstructions before rifting and drifting reveal the geological connections between Antarctica and its conjugates in Gondwanaland: Earth-Science Reviews, v. 111, p. 249-318, doi:10.1016/j.earscirev.2011.11.009.

Verma, R. K., and Banerjee, P., 1992, Nature of continental crust along the Narmada—Son Lineament inferred from gravity and deep seismic sounding data: Tectonophysics, v. 202, p. 375-397, doi:10.1016/0040-1951(92)90121-L.

Vernant, P., Bilham, R., Szeliga, W., Drupka, D., Kalita, S., Bhattacharyya, A.K., Gaur, V.K., Pelgay, P., Cattin, R., and Berthet, T., 2014, Clockwise rotation of the Brahmaputra Valley relative to India: Tectonic convergence in the eastern Himalaya, Naga Hills, and Shillong Plateau: Journal of Geophysical Research: Solid Earth, v. 119, p. 6558–6571, doi: 10.1002/2014JB011196.

Visona, D., Rubatto, D., and Villa, I. M., 2010, The mafic rocks of Shao La (Kharta, S. Tibet): Ordovician basaltic magmatism in the greater himalayan crystallines of central-eastern Himalaya: Journal of Asian Earth Sciences, v. 38, p. 14-25, doi:10.1016/j.jseaes.2009.12.004.

Wadia, D. N., 1919, Geology of India: London, Macmillan and Company, 398 p.

-, 1939, Geology of India, 2nd edition: London, Macmillan and Company, 460 p.

Walker, C. B., Searle, M. P., and Waters, D. J., 2001, An integrated tectonothermal model for the evolution of the High Himalaya in western Zanskar with constraints from thermobarometry and metamorphic modeling: Tectonics, v. 20, p. 810-833, doi:10.1029/2000TC001249.

Wang, W., Qiao, X., Yang, S., and Wang, D., 2017, Present-day velocity field and block kinematics of Tibetan Plateau from GPS measurements: Geophysical Journal International, v. 208, p. 1088–1102, doi: 10.1093/gji/ggw445.

Wang, X., Zhang, J., Santosh, M., Liu, J., Yan, S., and Guo, L., 2012, Andean-type orogeny in the Himalayas of south Tibet: implications for early Paleozoic tectonics along the Indian margin of Gondwana: Lithos, v. 154, p. 248-262, doi:10.1016/j.lithos.2012.07.011.

Wang, Y., Zeng, L., Gao, L.-E., Guo, C., Hou, K., Zhang, L., Wang, W., and Sun, H., 2017, Neoproterozoic magmatism in eastern Himalayan terrane: Science Bulletin, v. 62, p. 415–424, doi: 10.1016/j.scib.2017.02.003.

Webb, A. A. G., 2013, Preliminary balanced palinspastic reconstruction of Cenozoic deformation across the Himachal Himalaya (northwestern India): Geosphere, v. 9, p. 572-587, doi:10.1130/GES00787.1.

Webb, A. A. G., Yin, A., Harrison, T. M., Celerier, J., Gehrels, G. E., Manning, C. E., and Grove, M., 2011a, Cenozoic tectonic history of the Himachal Himalaya (northwestern India) and its constraints on the formation mechanism of the Himalayan orogen: Geosphere, v. 7, p. 1013-1061, doi:10.1130/GES00627.1.

Webb, A. A. G., Schmitt, A. K., He, D., and Weigand, E. L., 2011b, Structural and geochronological evidence for the leading edge of the Greater Himalayan Crystalline complex in the central Nepal Himalaya: Earth and Planetary Science Letters, v. 304, p. 483-495; doi:10.1016/j.epsl.2011.02.024.

Webb, A. A. G., Yin, A., and Dubey, C. S., 2013, U-Pb zircon geochronology of major lithologic units in the eastern Himalaya: implications for the origin and assembly of Himalayan rocks: Geological Society of America Bulletin, v. 125, p. 499-522, doi:10.1130/B30626.1.

Webb, A. A. G., Yin, A., Harrison, T. M., Celerier, J., and Burgess, W. P., 2007, The leading edge of the Greater Himalayan Crystalline complex revealed in the NW Indian Himalaya: implications for the evolution of the Himalayan orogen: Geology, v. 35, p. 955–958, doi:10.1130/G23931A.1.

Wegert, D., Parker, D., and Ren, M., 2013, The Nathrop Domes, Colorado: geochemistry and petrogenesis of a topaz rhyolite: Rocky Mountain Geology, v. 48, p. 1-14, doi:10.2113/gsrocky.48.1.1.

Wesnousky, S.G., Kumahara, Y., Chamlagain, D., Pierce, I.K., Karki, A., and Gautam, D., 2017, Geological observations on large earthquakes along the Himalayan frontal fault near Kathmandu, Nepal: Earth and Planetary Science Letters, v. 457, p. 366–375, doi: 10.1016/j.epsl.2016.10.006.

White, L. T., Ahmad, T., Ireland, T. R., Lister, G. S., and Forster, M. A., 2011, Deconvolving episodic age spectra from zircons of the Ladakh Batholith, northwest Indian Himalaya: Chemical Geology, v. 289, p. 179-196, doi:10.1016/j.chemgeo.2011.07.024.

Whitehouse, M. J., Windley, B. F., Stoeser, D. B., Al-Khirbash, S., Ba-Bttat, M. A. O., and Haider, A., 2001, Precambrian basement character of Yemen and correlations with Saudi Arabia and Somalia: Precambrian Research, v. 105, p. 357-369, doi:10.1016/S0301-9268(00)00120-0.

Wiesmayr, G., and Grasemann, B., 2002, Eohimalayan fold and thrust belt: implications for the geodynamic evolution of the NW-Himalaya (India): Tectonics, v. 21, 1058, doi:10.1029/2002TC001363.

Will, T. M., Zeh, A., Gerdes, A., Frimmel, H. E., Millar, I. L., and Schmadicke, E., 2009, Palaeoproterozoic to Palaeozoic magmatic and metamorphic events in the Shackleton Range, East Antarctica: constraints from zircon and monazite dating, and implications for the amalgamation of Gondwana: Precambrian Research, v. 172, p. 25-45, doi:10.1016/j.precamres.2009.03.008.

Xu, W.-C., Zhang, H.-F., Parrish, R., Harris, N., Guo, L., and Yuan, H.-L., 2010, Timing of granulite-facies metamorphism in the eastern Himalayan syntaxis and its tectonic implications: Tectonophysics, v. 485, p. 231–244, doi: 10.1016/j.tecto.2009.12.023.

Xu, W., Dong, Y., Zhang, X., Deng, M., and Zhang, L., 2016, Petrogenesis of high-Ti mafic dykes from Southern Qiangtang, Tibet: Implications for a ca. 290 Ma large igneous province related to the early Permian rifting of Gondwana: Gondwana Research, v. 36, p. 410–422, doi: 10.1016/j.gr.2015.07.016.

Xu, Yajun, Cawood, P. A., Du, Y., Hu, L., Yu, W., Zhu, Y., and Li, W., 2013, Linking south China to northern Australia and India on the margin of Gondwana: constraints from detrital zircon U-Pb and Hf isotopes in Cambrian strata: Tectonics, v. 32, p. 1547–1558, doi:10.1002/tect.20099.

Yang, S.-Y., Jiang, S.-Y., Zhao, K.-D., Jiang, Y.-H., Ling, H.-F., and Luo, L., 2012, Geochronology, geochemistry and tectonic significance of two Early Cretaceous A-type granites in the Gan-Hang Belt, Southeast China: Lithos, v. 150, p. 155-170, doi:10.1016/j.lithos.2012.01.028.

Yang, Y., 2011, Tectonically-driven underfilled–overfilled cycles, the middle Cretaceous in the northern Cordilleran foreland basin: Sedimentary Geology, v. 233, p. 15-27, doi:10.1016/j.sedgeo.2010.10.002.

Yang, Y., and Miall, A. D., 2010, Migration and stratigraphic fill of an underfilled foreland basin: Middle–Late Cenomanian Belle Fourche Formation in southern Alberta, Canada:

Sedimentary Geology, v. 227, p. 51-64, doi:10.1016/j.sedgeo.2010.03.005.

Yeats, R. S., and Thakur, V. C., 2008, Active faulting south of the Himalayan front: establishing a new plate boundary: Tectonophysics, v. 453, p. 63-73, doi:10.1016/j.tecto.2007.06.017.

Yin, A., 2006, Cenozoic tectonic evolution of the Himalayan orogen as constrained by along-strike variation of structural geometry, exhumation history, and foreland sedimentation: Earth Science Reviews, v. 76, p. 1-131, doi:10.1016/j.earscirev.2005.05.004.

Yin, A., Dubey, C. S., Kelty, T. K., Webb, A. A. G., Harrison, T. M., Chou, C. Y., and Celerier, J., 2010a, Geologic correlation of the Himalayan orogen and Indian craton: Part 2. Structural geology, geochronology, and tectonic evolution of the Eastern Himalaya: Geological Society of America Bulletin, v. 122, p. 360-395, doi:10.1130/B26461.1.

Yin, A., Dubey, C. S., Webb, A. A. G., Kelty, T. K., Grove, M., Gehrels, G. E., and Burgess, W. P., 2010b, Geologic correlation of the Himalayan orogen and Indian craton: Part 1. Structural geology, U-Pb zircon geochronology, and tectonic evolution of the Shillong Plateau and its neighboring regions in NE India: Geological Society of America Bulletin, v. 122, p. 336-359, doi:10.1130/B26460.1.

Yoshida, M., and Upreti, B. N., 2006, Neoproterozoic India within East Gondwana: constraints from recent geochronologic data from Himalaya: Gondwana Research, v. 10, p. 349-356, doi:10.1016/j.gr.2006.04.011.

Yu, H., Webb, A. A. G., and He, D., 2015, Extrusion vs. duplexing models of Himalayan mountain building 1: discovery of the Pabbar thrust confirms duplex-dominated growth of the northwestern Indian Himalaya since Mid-Miocene: Tectonics, v. 34, p. 313-333, doi:10.1002/2014TC003589.

Zeumann, S., and Hampel, A., 2015, Deformation of erosive and accretive forearcs during subduction of migrating and non-migrating aseismic ridges: Results from 3-D finite element models and application to the Central American, Peruvian, and Ryukyu margins: Tectonics, v. 34, p. 1769–1791, doi:10.1002/2015TC003867.

Zhai, W., Sun, X., Yi, J., Zhang, X., Mo, R., Zhou, F., Wei, H., and Zeng, Q., 2014, Geology, geochemistry, and genesis of orogenic gold–antimony mineralization in the Himalayan Orogen, south Tibet, China: Ore Geology Reviews, v. 58, p. 68-90, doi:10.1016/j.oregeorev.2013.11.001.

Zhang, Z.M., Zhao, G.C., Santosh, M., Wang, J.L., Dong, X., and Liou, J.G., 2010, Two stages of granulite facies metamorphism in the eastern Himalayan syntaxis, south Tibet: petrology, zircon geochronology and implications for the subduction of Neo-Tethys and the Indian continent beneath Asia: Journal of Metamorphic Geology, v. 28, p. 719–733, doi: 10.1111/j.1525-1314.2010.00885.x.

Zhang, Z., Dong, X., Santosh, M., Liu, F., Wang, W., Yiu, F., He, Z., and Shen, K., 2012, Petrology and geochronology of the Namche Barwa Complex in the eastern Himalayan syntaxis, Tibet: constraints on the origin and evolution of the north-eastern margin of the Indian Craton: Gondwana Research, v. 21, p. 123-137, doi:10.1016/j.gr.2011.02.002.

Zhou, H., Xiao, L., Dong, Y., Wang, C., Wang, F., and Ni, P., 2009, Geochemical and geochronological study of the Sanshui basin bimodal volcanic rock suite, China: implications for basin dynamics in southeastern China: Journal of Asian Earth Sciences, v. 34, p. 178-189, doi:10.1016/j.jseaes.2008.05.001.

Zhu, D., Mo, X., Pan, G., Zhao, Z., Dong, G., Shi, Y., Liao, Z., Wang, L., and Zhou, C., 2008, Petrogenesis of the earliest Early Cretaceous mafic rocks from the Cona area of the eastern Tethyan Himalaya in south Tibet: interaction between the incubating Kerguelen plume and the eastern Greater India lithosphere?: Lithos, v. 100, p. 147-173, doi:10.1016/j.lithos.2007.06.024.

Zhuang, G., Najman, Y., Guillot, S., Roddaz, M., Antoine, P.-O., Metais, G., Carter, A., Marivaux, L., and Solangi, S.H., 2015, Constraints on the collision and the pre-collision tectonic configuration between India and Asia from detrital geochronology, thermochronology, and geochemistry studies in the lower Indus basin, Pakistan: Earth and Planetary Science Letters, v. 432, p. 363–373, doi:10.1016/j.epsl.2015.10.026.

Zou, G., Pan, Z., Zhuang, Z., Zhu, T., Li, J., and Feng, X., 2013, Phanerozoic paleomagnetism characteristics of the Qomolangma area in Tibet: Acta Geologica Sinica, v. 87, p. 517-527, doi:10.1111/1755-6724.12065.

FIGURE CAPTIONS

1. The geography of the Himalaya and surrounding regions. The Himalayan Orogen is bounded by the Main Frontal Thrust, Indus-Yarlung Suture/Main Mantle Thrust, Chaman Fault, and Sagaing Fault. The Shillong Plateau and Mikir Hills area is also part of the Himalayan Orogen. Brown text indicates mountains and green text labels geographical areas. Other symbols are defined in Figure 5. Modified from Dasgupta et al. (2000) and Balakrishnan et al. (2009).
2. Geologic map of the Himalayan Orogen. Listed ages are depositional or igneous crystallization ages. Cenozoic intrusions, chiefly in Assemblage B, are not shown. The array of modern microplates at the eastern edge of the map is not shown (Vernant et al., 2014; Talwani et al., 2016; W. Wang et al., 2017). K-Kathmandu. Modified from Webb (2013).
3. Deformed-state cross-sections across the Himalaya. The gross structural architecture is consistent along the orogen. Cross-section locations shown in Figure 2. Sections A, B, and D were balanced, section C is schematic. Cross-sections modified from: A: Webb (2013), B: Khanal and Robinson (2013), C: He et al. (2015), D: McQuarrie et al. (2014).
4. Comparison of salients, recesses, and oroclines in some Phanerozoic orogens. (A) Western Canadian Cordillera. (B) Andes. (C) Himalaya. The red arrow points to the largest salient and recess pair in the Main Frontal Thrust between the syntaxes. The white arrow points to the Kangra Recess in the Main Central Thrust. (D) Appalachians. Himalayan salients and recesses between the eastern and western syntaxes have much smaller amplitudes and wavelengths than those in the other orogens. Parts A, B, and C

modified from GeoMapApp (www.geomapapp.org). Part D modified from Thomas (2006).

5. Map of high strain zones in the foreland of the Himalayan Orogen as well as some geologic elements north of the Himalaya. Most northeast-trending foreland normal-sense high strain zones were active in the Paleoproterozoic Era, but some northwest trending high strain zones may not have been active at that time. Depositional strike of the Paleoproterozoic sedimentary rocks filling the basins produced by the northeast-trending high strain zones was at a high angle to the strike of Cenozoic frontal structures in the western Himalaya; this angle decreased eastward. The positions of the foreland high strain zones, including the Main Frontal Thrust, were taken from Dasgupta et al. (2000). Jain and Sinha (2005) provided the senses of motion on the faults near Patna. The Kopili Fault was taken from Kayal et al. (2006). The base map and other faults were modified from Balakrishnan et al. (2009).
6. Options for the disposition of Himalayan Assemblage A and Himalayan Assemblage B prior to Paleocene time. (A) Geosyncline Model (Wadia, 1939). The location of the Paleoproterozoic part of Assemblage A is not specified in the model, but presumably it would lie depositionally below the younger Assemblage A rocks. (B) In the Contiguous Deposition Outboard of India Model, Assemblage B sediment was deposited adjacent to and directly outboard of Assemblage A (Frank et al., 1973; Colchen et al., 1982). Variations of this model have no major high strain zones (Myrow et al., 2003); a Carboniferous normal-sense high strain zone with modest slip, perhaps 10-20 km (Yin, 2006); or many Cretaceous normal-sense high strain zones that accommodated approximately 2500 km of extension (Fuchs and Willems, 1990). The normal-sense high

strain zone is shown schematically, multiple normal-sense high strain zones could be present in this model. A convergent margin in middle Cambrian to Middle Ordovician time is a necessary modification to the model. (C) In the Noncontiguous Deposition Outboard of India Model, Neoproterozoic to Cretaceous Assemblage B sediment was deposited at least 5000 km outboard of Assemblage A (Jain and Kanwar, 1970). Accretion occurred during the Cenozoic Era. Jain and Kanwar (1970) did not specify whether Assemblage B was deposited on oceanic or continental crust. The thrust is shown schematically; accretion actually would take place on multiple thrusts. (D) Assemblage B Deposition and Intrusion East of India Model (amplified from Brookfield, 1993). Part (D) shows that Assemblage B was located east of northern India and Assemblage A during Neoproterozoic to Middle Jurassic time. Some other circum-Gondwana blocks are shown for reference but it is beyond the scope of this paper to discuss the locations of other blocks in Gondwana. Paleoproterozoic deposition of Assemblage A on the northern margin of India is not depicted to save space. The top reconstruction, in a paleomagnetic reference frame, was modified from Figure 17 (280 Ma) in Torsvik and Cocks (2013). The sediment transport arrows schematically indicate ultimate sediment sources, not actual sediment transport pathways at the time of deposition. I placed the Qiangtang terrane astride the Plume Generation Zone because of the presence of Permian plume-related mafic dikes (Xu et al., 2016). The bottom reconstruction, in the paleomagnetic reference frame of Torsvik et al. (2012), was produced using GPlates, a reconstruction time of 135 Ma, and a 3D orthographic projection. The bottom reconstruction depicts the position of Assemblage B after completion of left-handed transcurrent motion. A – Assemblage A, B – Assemblage B, GHS – Greater Himalayan Sequence, LHS – Lesser Himalayan Sequence, MCT – Main Central Thrust, THS – Tethyan Himalayan Sequence. Different parts of the figure are not at the same scale.

7. Legend for Figures 8, 9, and 10.
8. Along-strike correlation of Assemblage A. GG is the Gondwana Group. Units for which the formal stratigraphic rank is not shown are formations. References for the lithologies and the depositional and igneous crystallization ages are given in Appendix A.
9. Along-strike correlation of Assemblage B. Sha+UK+So is the combined Shahkot, Utch Khattak, and Sobrah formations, MG is the Mansehra granitic gneiss, Chu+Panj+Ku is the combined Chumik Formation, Panjal Traps, and Kuling Formation, TK+Han+Zoz is the combined Tamba Kurkur, Hanse, and Zozar formations, Laptal+FO is the combined Laptal and Ferruginous Oolite formations, Stu+Dib is the combined Stumpata and Dibling formations, L+FO+D is the combined Laptal, Ferruginous Oolite, and Dangar formations, Phulch Gp. is the Phulchauki Group, H+S is the combined Hongshantou and Shiqipo formations, Kd+Qub+Qbrig+Sh+Bg is the combined Kadong, Qubu, Quburiga, Shengmi, and Baga formations, De+Qul+Yaz is the combined Derirong, Qulonggongba, and Yazhi formations, NH+Lala is the combined Niehnieh Hsionla and Lalongla formations. Units for which the formal stratigraphic rank is not shown are formations. References for the lithologies and the depositional and igneous crystallization ages are given in Appendix B.
10. Comparison of Himalayan Assemblage A, Himalayan Assemblage B, and some nearby rock packages. References for the lithologies and the depositional and igneous crystallization ages are given in Appendix C.

11. Neoproterozoic-Jurassic sediment sources in the context of the Contiguous Deposition Outboard of India Model. Compare to Figure 6D. Provenance analysis of Assemblage B deposits cannot distinguish between the Contiguous Deposition Outboard of India and the Assemblage B Deposition and Intrusion East of India models because both models explain equally well the derivation of Assemblage B sediment from all major sectors of East Gondwana. The sediment transport arrows schematically indicate ultimate sediment sources, not actual sediment transport pathways at the time of deposition. The reconstruction, in a paleomagnetic reference frame, was modified from Figure 17 (280 Ma) in Torsvik and Cocks (2013). A – Assemblage A, B – Assemblage B.
12. Part of Gondwana at Triassic-Jurassic boundary time with Himalayan Assemblage B reconstructed to a position consistent with the Assemblage B Deposition and Intrusion East of India Model. In this reconstruction, Himalayan Assemblage B sits at approximately the same latitude as the northern part of cratonal India during Triassic time, satisfying Triassic paleomagnetic paleolatitude data. Reconstructed in the paleomagnetic reference frame of Torsvik et al. (2012) using GPlates, a reconstruction time of 200 Ma, and a 3D orthographic projection.
13. Plot of Triassic paleolatitude versus present longitude for sites in Himalayan Assemblage B. Colored bands depict paleolatitude predictions from the two indicated models at 200 Ma using the reconstruction in figure 12. The available data rule out neither the Contiguous Deposition Outboard of India Model nor the Assemblage B Deposition and Intrusion East of India Model. Data point error bars shown at the 95% confidence level. The large scatter in the data probably results from incorrect interpretations about the origins of the remnant magnetism in the analyzed samples. The large uncertainty on the

paleolatitude prediction for the Assemblage B Deposition and Intrusion East of India Model stems from uncertainty on how far offshore of western Australia Assemblage B was located prior to the Early Cretaceous Epoch.

TABLES

1. Himalayan nomenclature.
2. Definitions of Himalayan rock units and high strain zones.
3. Paleolatitude of Himalayan Assemblage B sites during the Triassic Period.

Figure 1

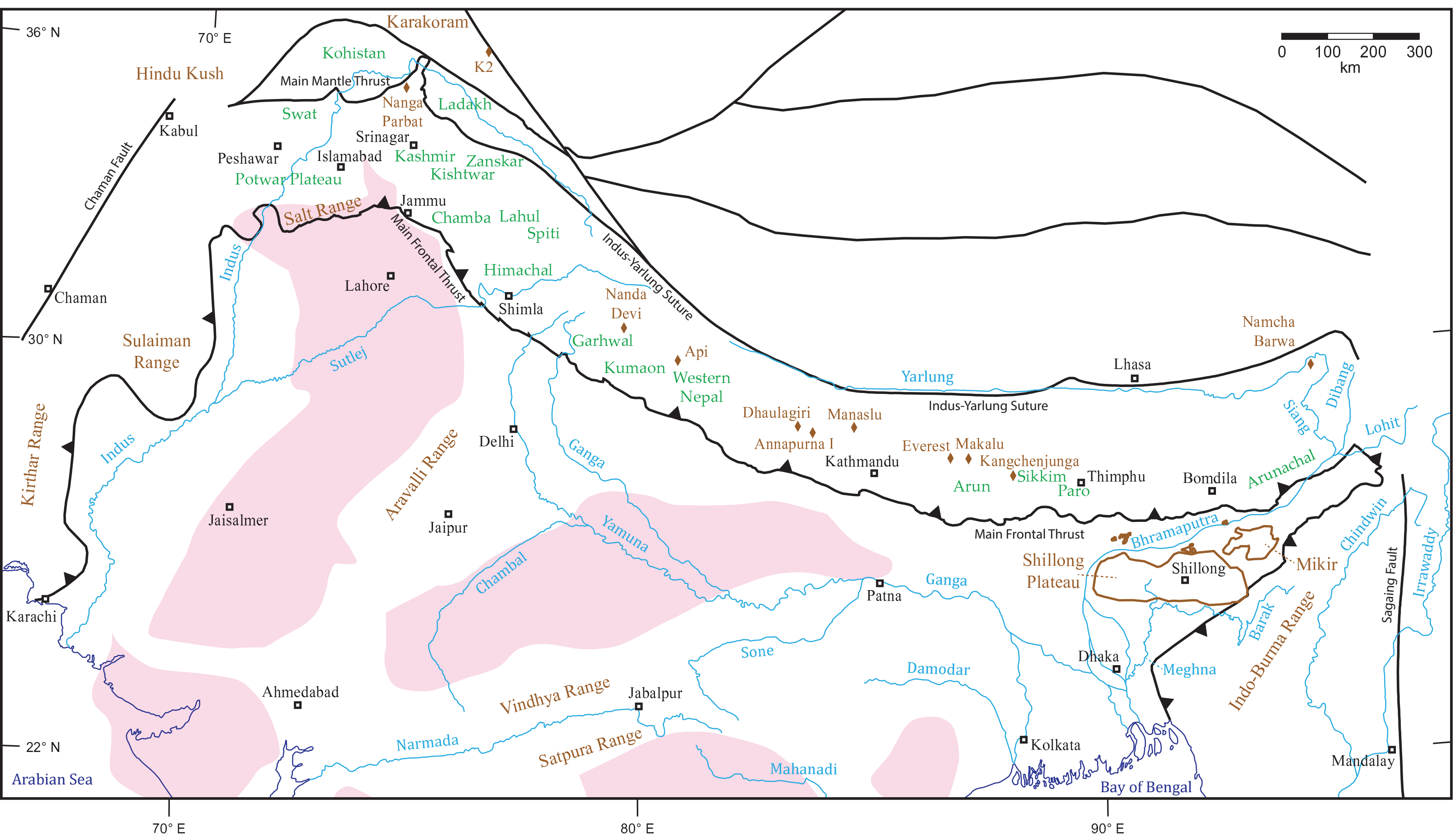

Fig. 1 (Martin)

Figure 2

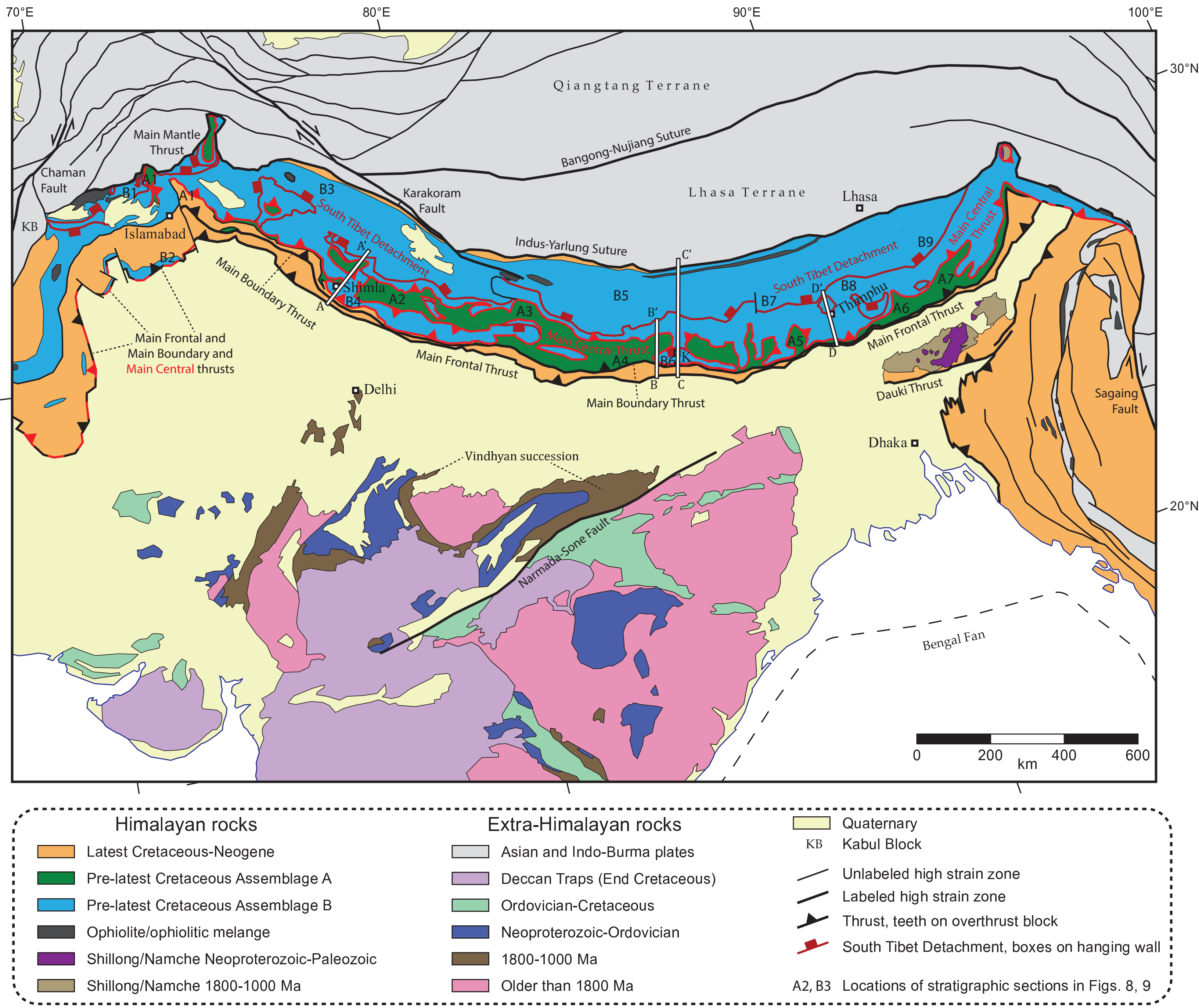

Fig. 2 (Martin)

Figure 3

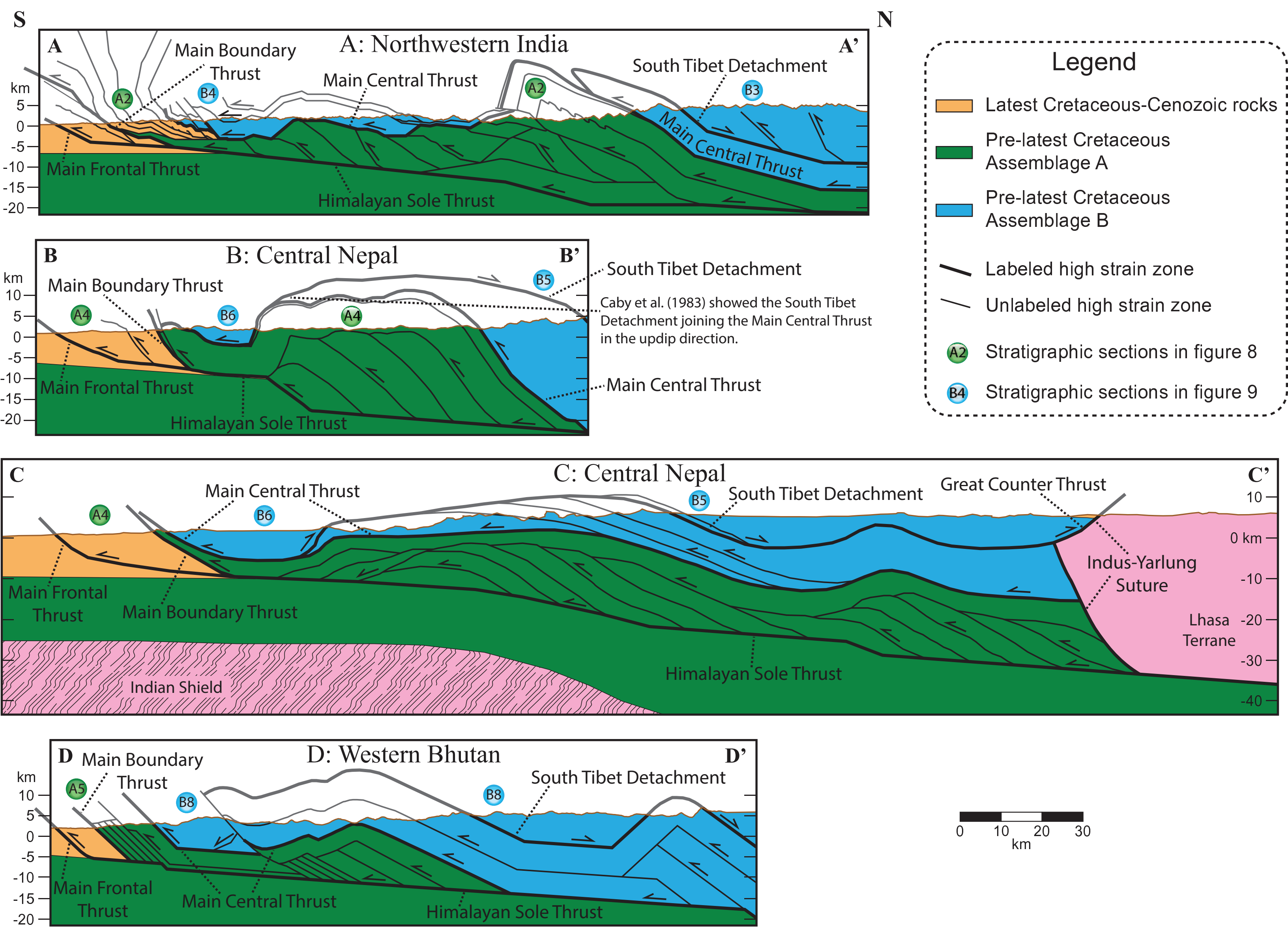

Fig. 3 (Martin)

Figure 4

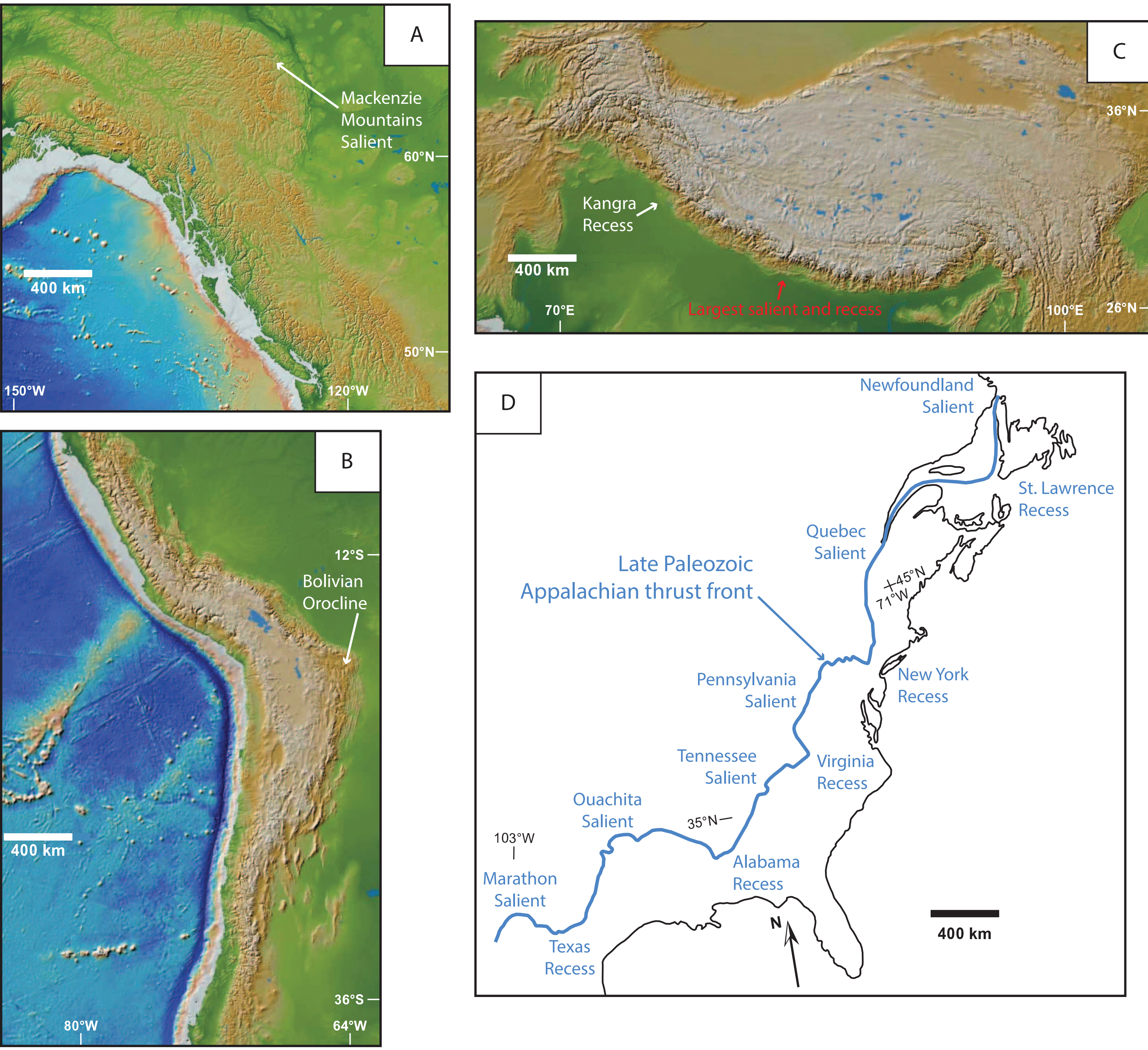

Figure 4 (Martin)

Figure 5

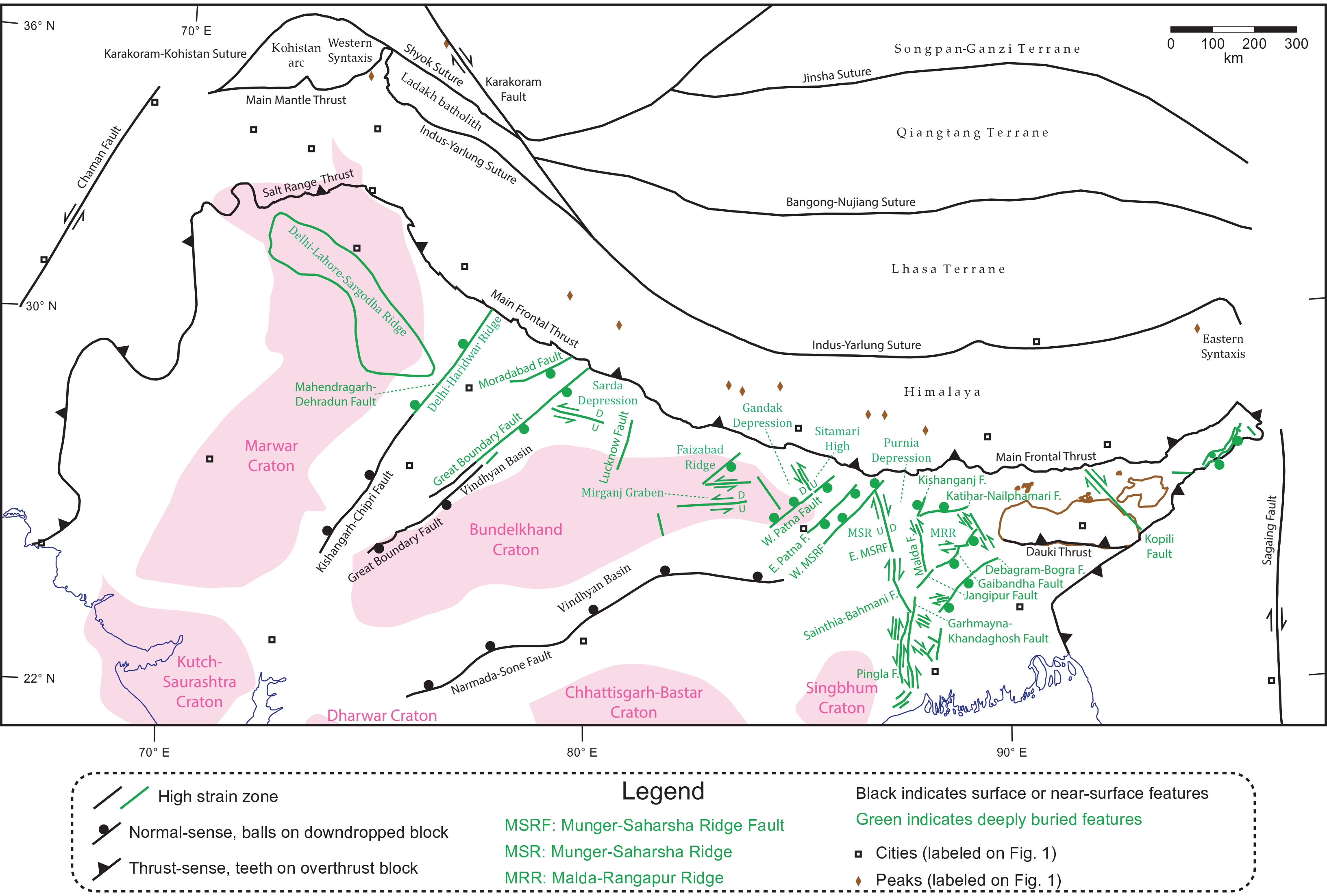

Fig. 5 (Martin)

Figure 6 page 1

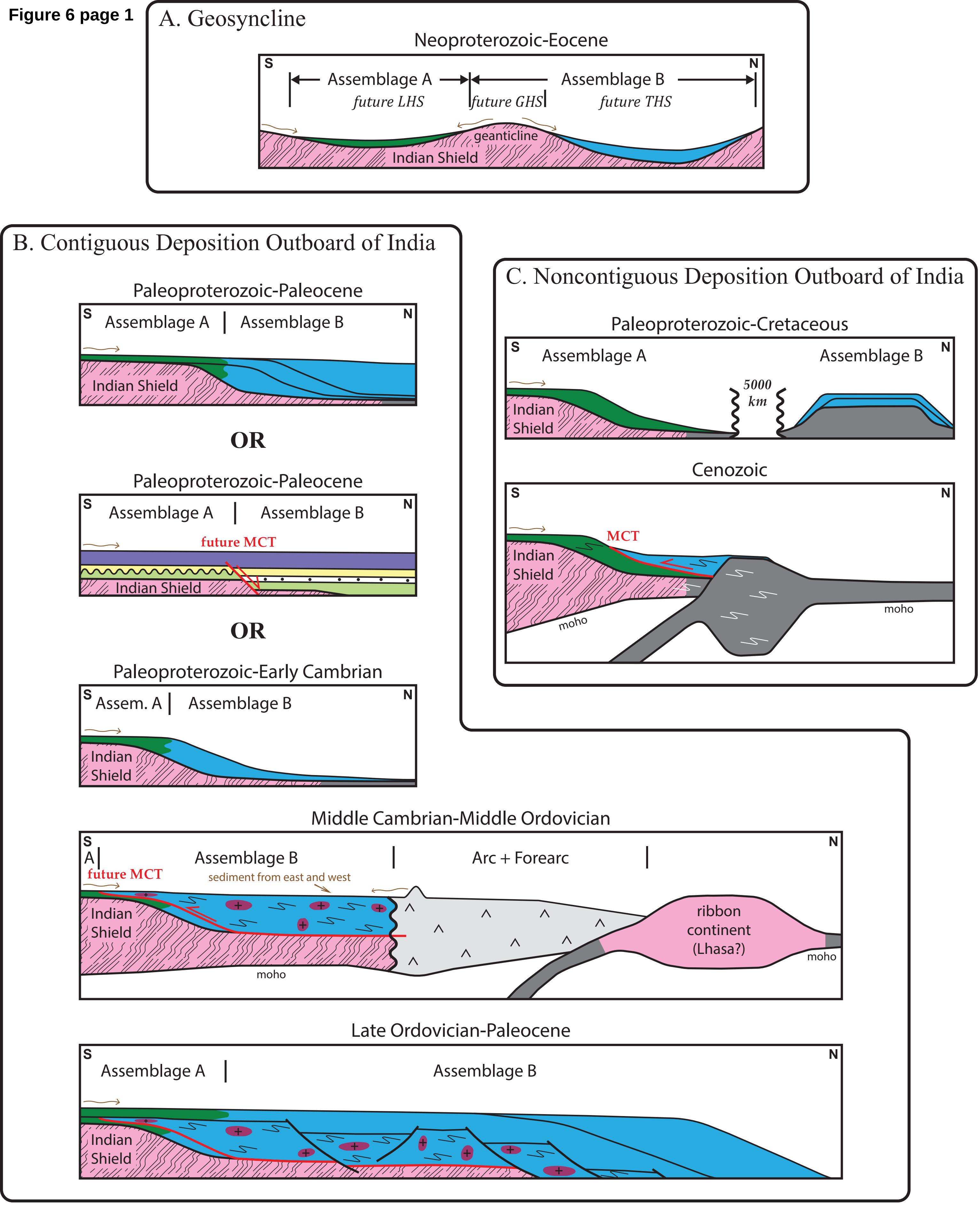

Fig. 6 Page 1 (Martin)

Figure 6 page 2

D. Assemblage B Deposition and Intrusion East of India

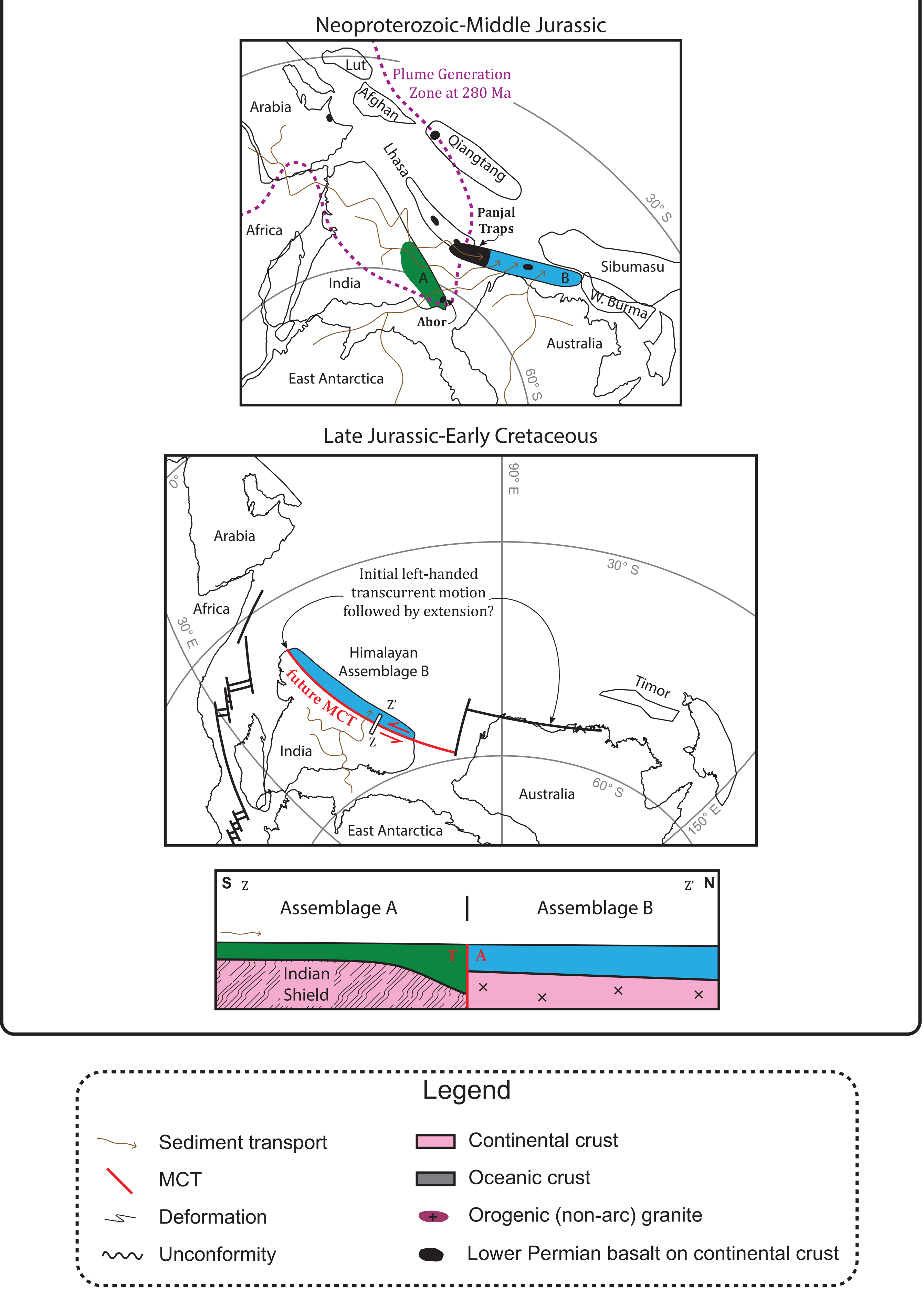

Fig. 6 Page 2 (Martin)

Figure 7

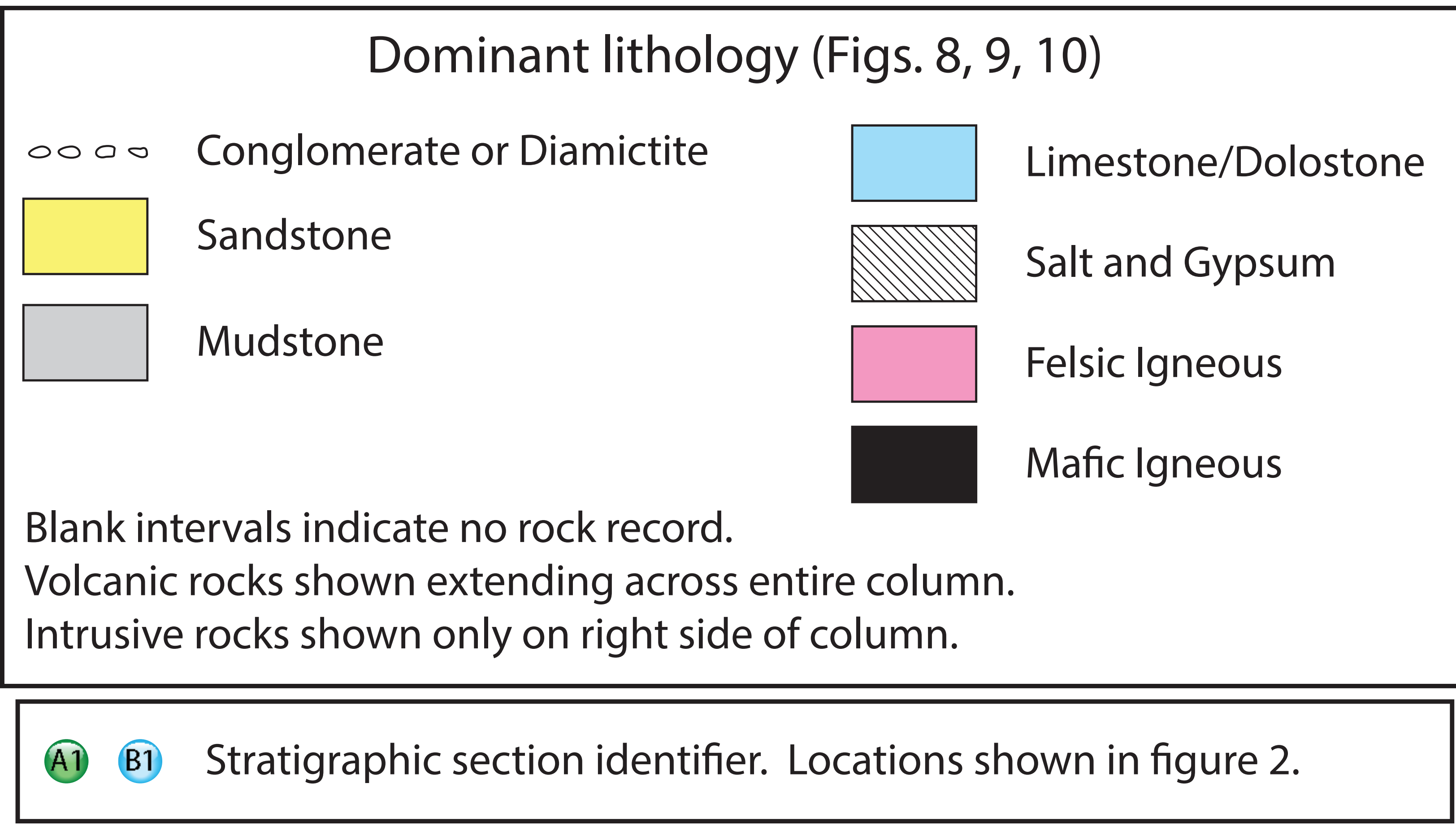

Figure 7 (Martin)

Figure 8

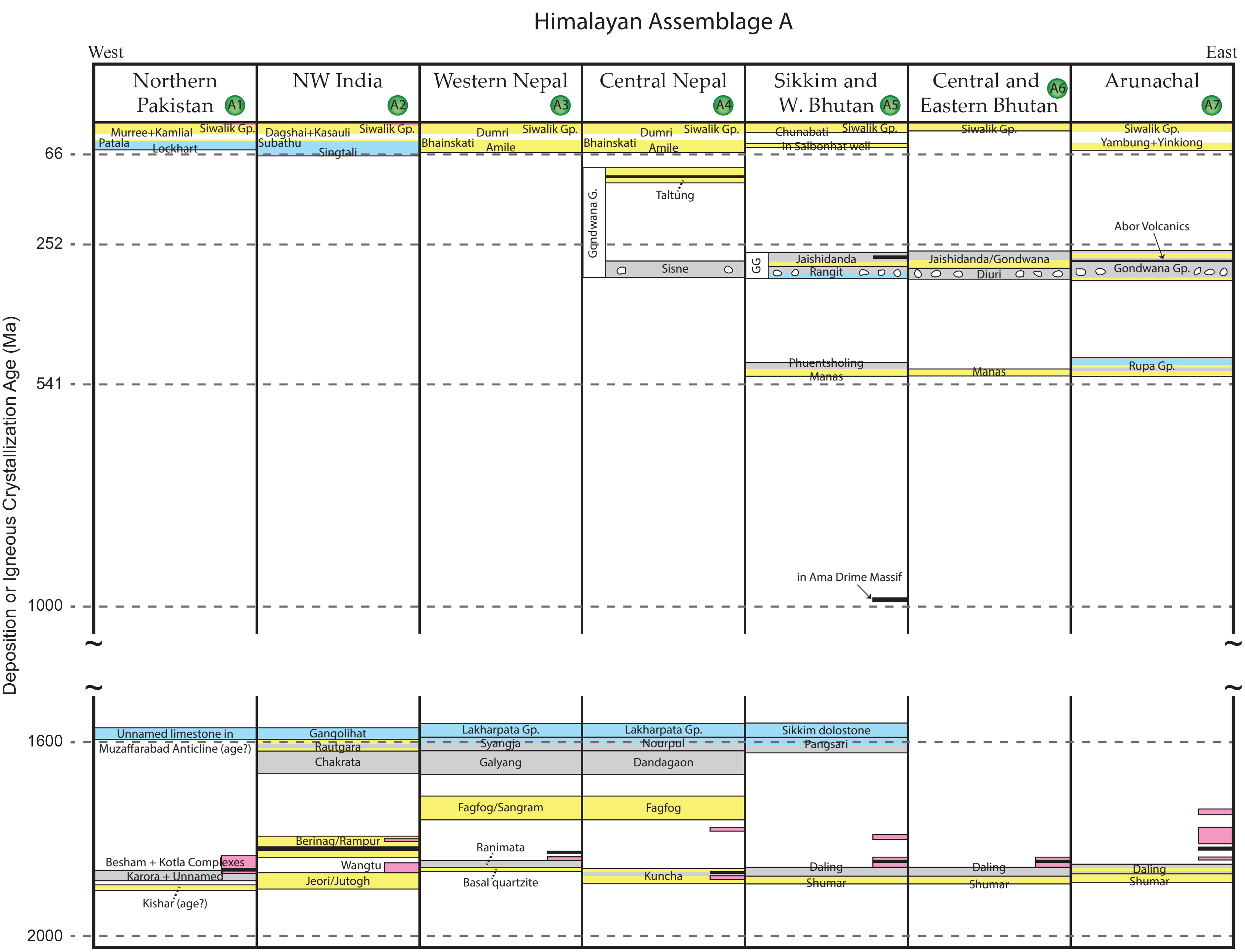

Figure 8 (Martin)

Figure 9

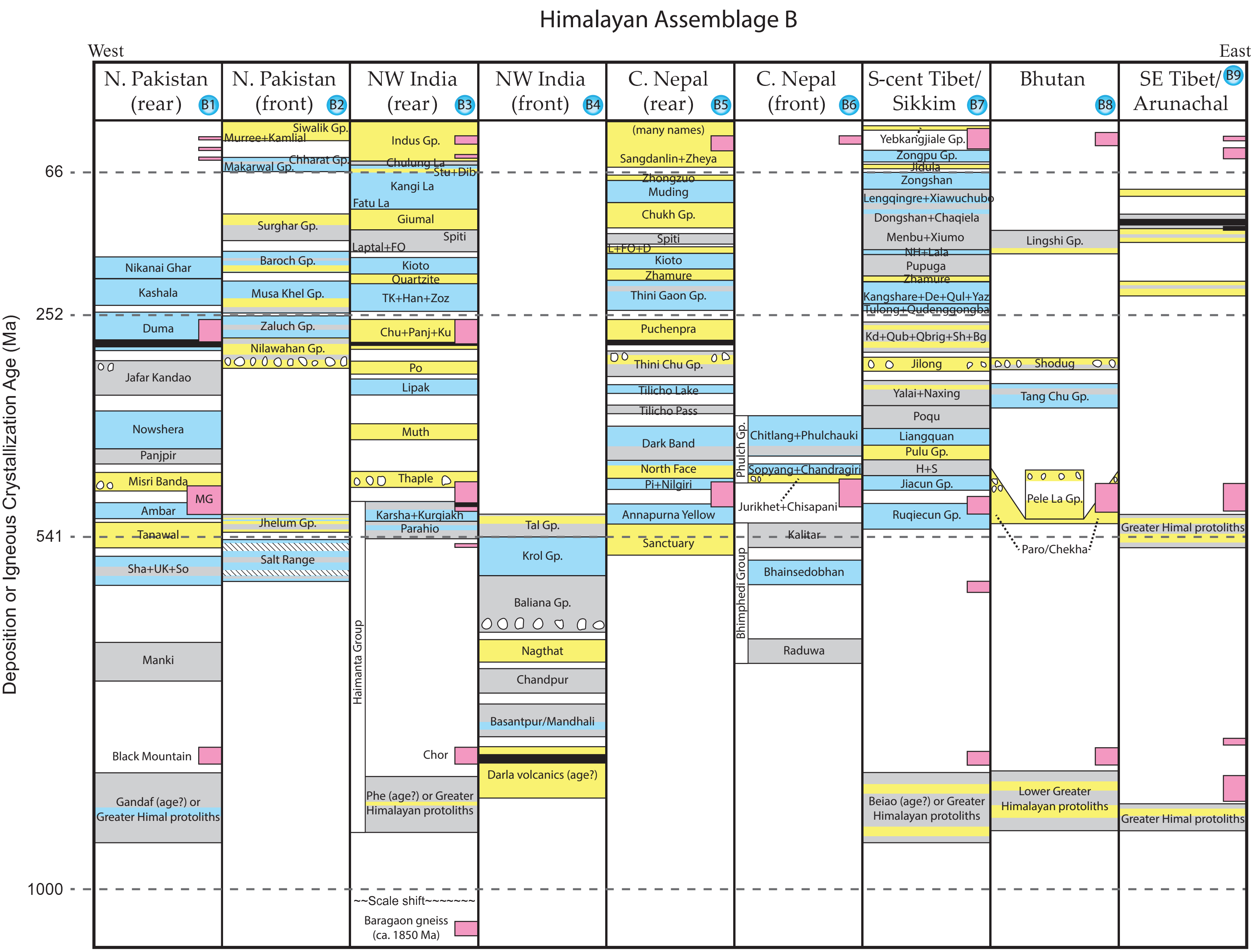

Figure 9 (Martin)

Figure 10

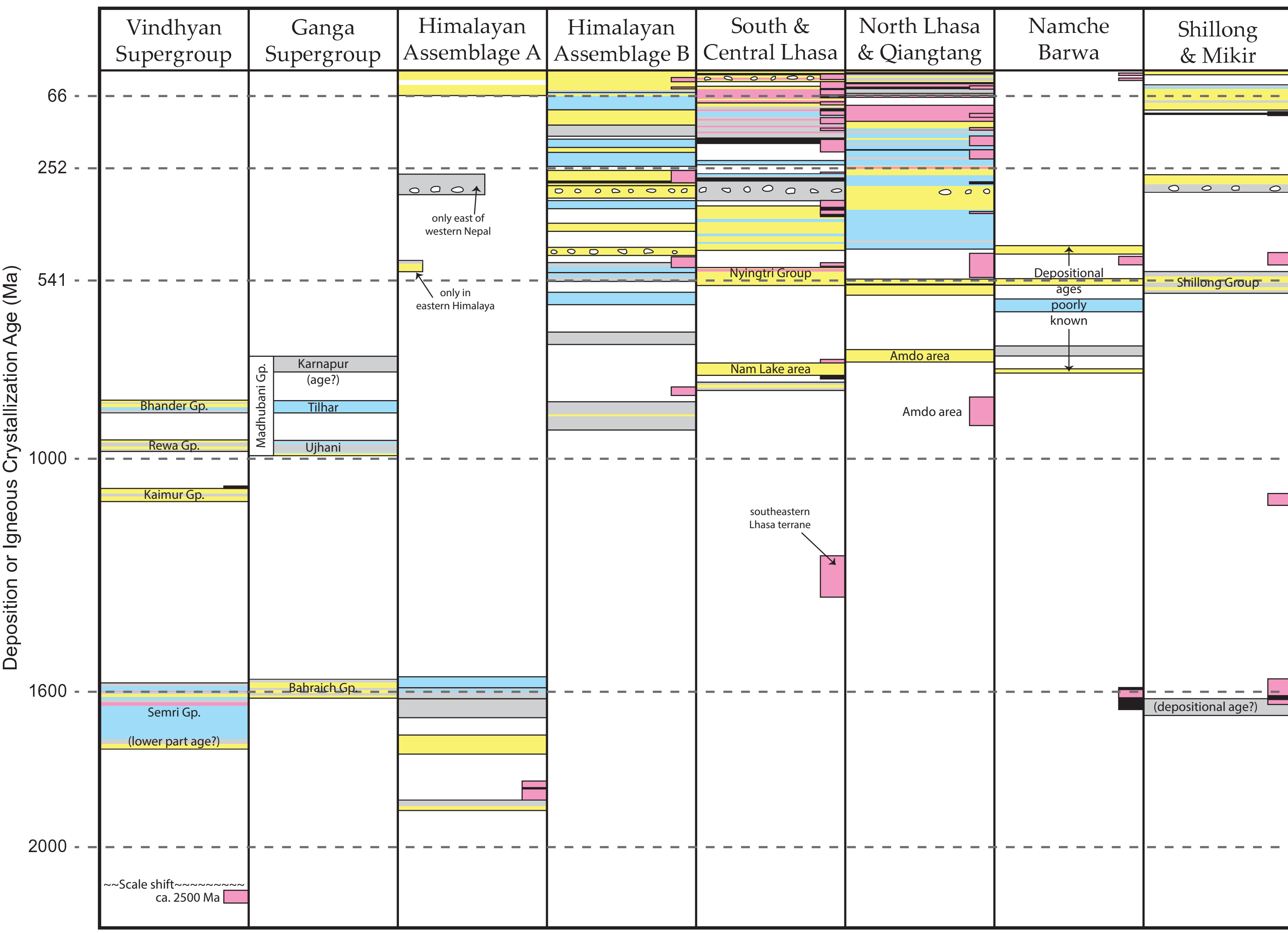

Figure 10 (Martin)

Figure 11

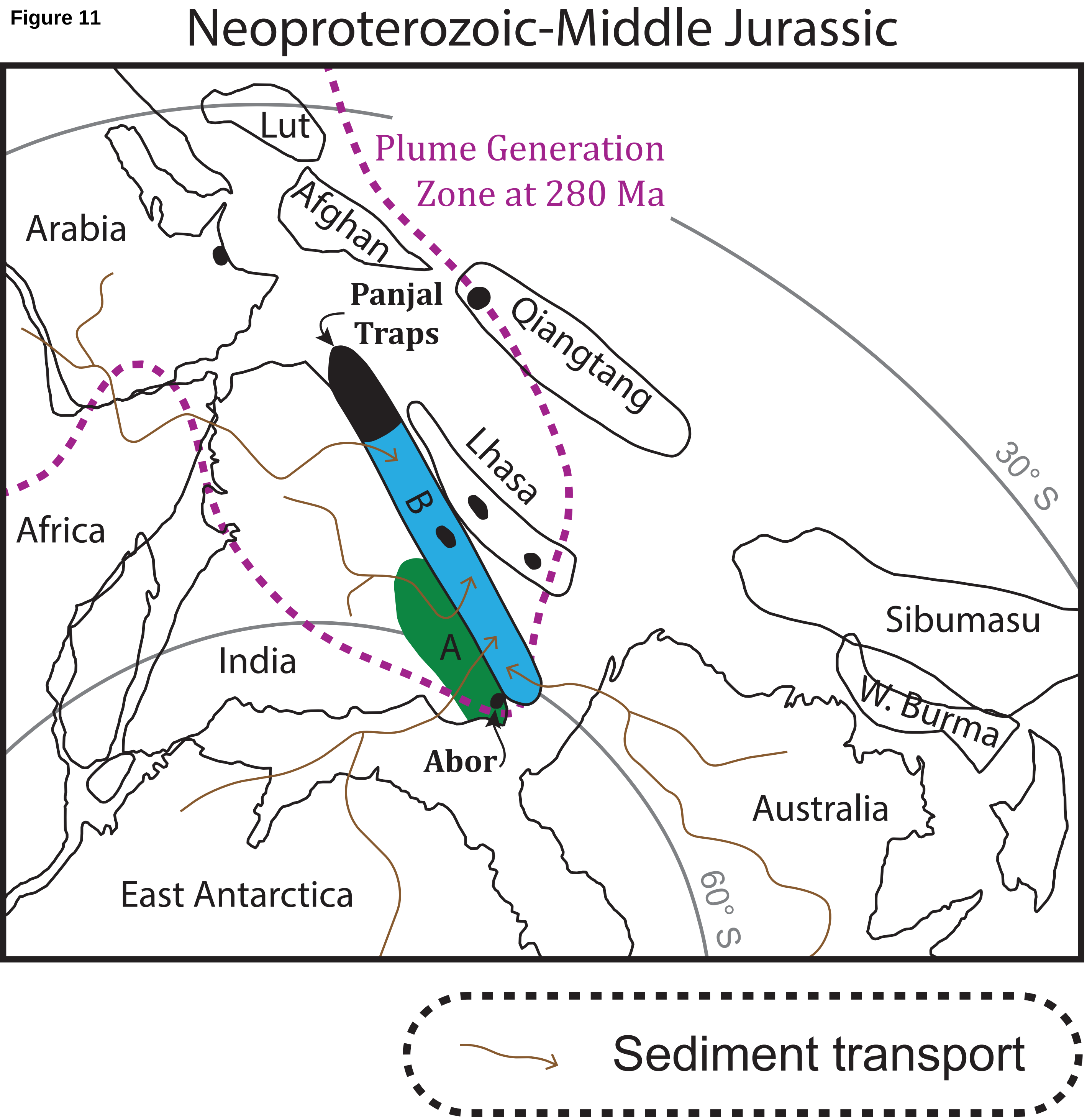

Fig. 11 (Martin)

Figure 12

200 Ma

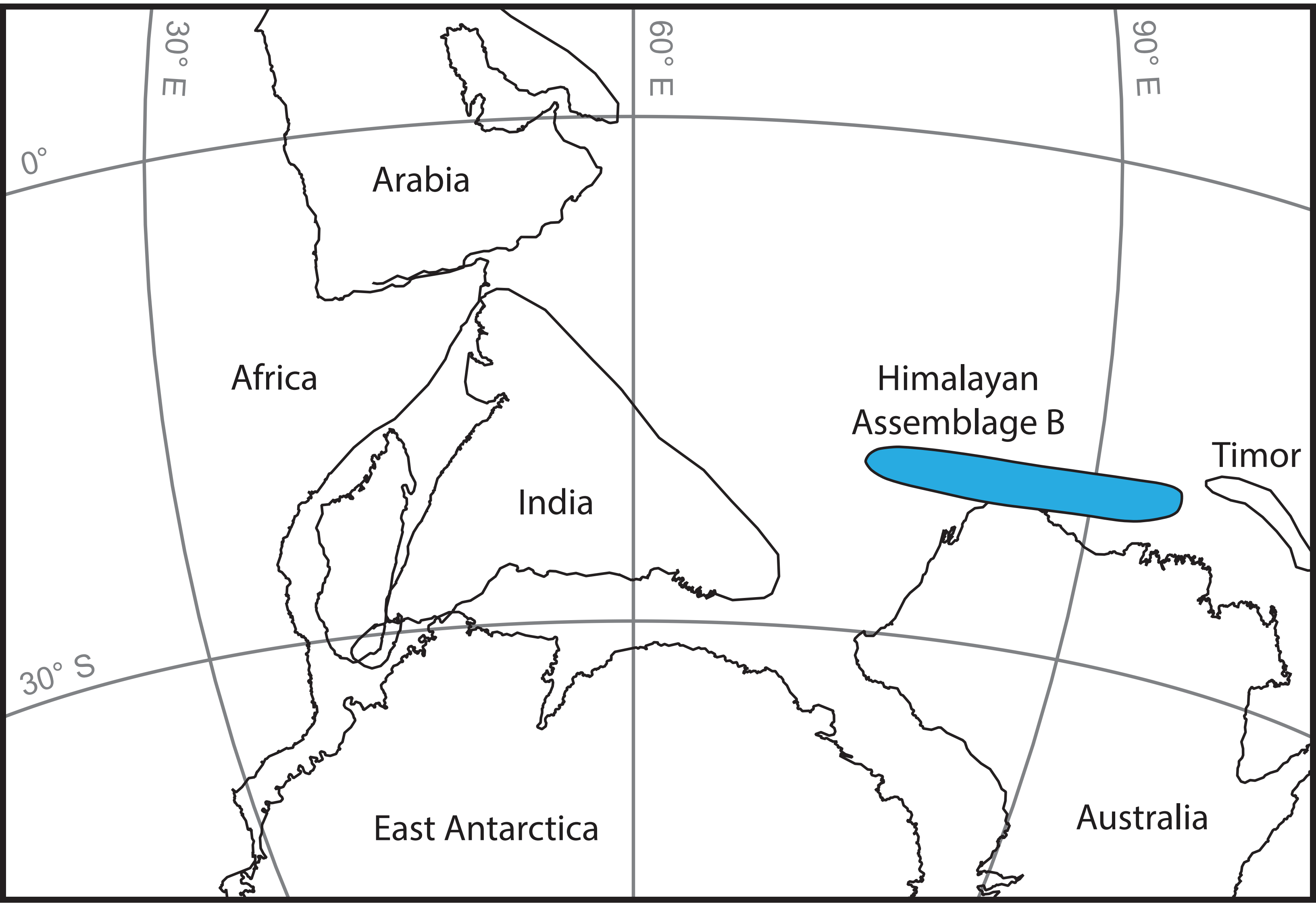

Figure 12 (Martin)

Figure 13

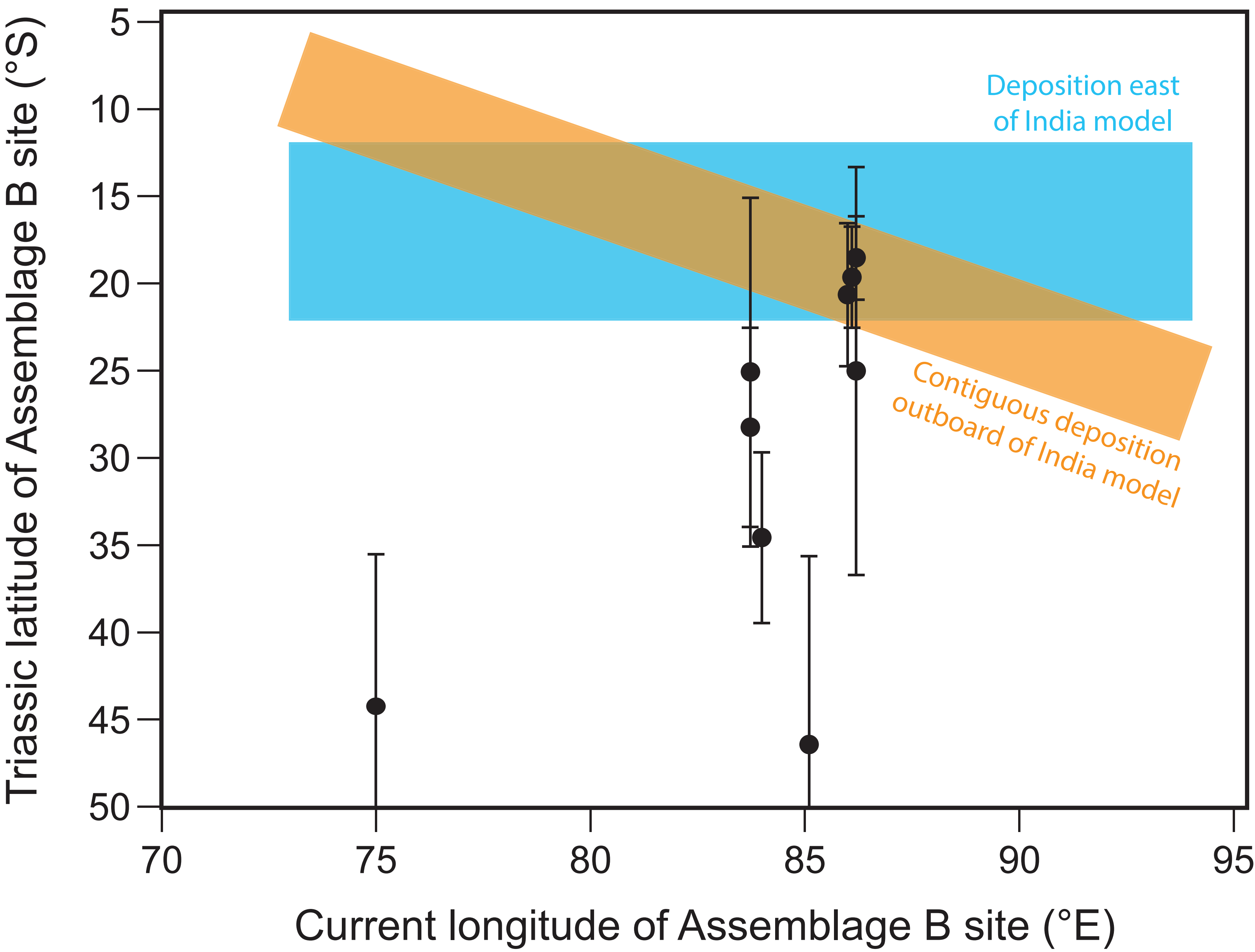

Figure 13 (Martin)

Table 1

Table 1: Himalayan nomenclature

Classification Category	Name 1	Name 2	Name 3	Name 4
Current Elevation[a]	Low	Midlands or Intermediate	High	High
Cenozoic structural position (plus Cenozoic metamorphic grade for Greater vs. Tethyan)	Sub	Lesser	Greater	Tethyan
Depositional or intrusive relationships	Assemblage A	Assemblage A	Assemblage B	Assemblage B

[a]The columns indicate typical relationships to elevation but the rocks in all columns also can be found at low and intermediate elevations.

Table 2

Table 2: Himalayan rock unit and high strain zone definitions

ORIGINAL ROCK RELATIONSHIPS

Name	Definition
Himalayan Assemblage A	depositional or intrusive contiguity between adjacent members of the assemblage at the time of rock formation.
Himalayan Assemblage B	depositional or intrusive contiguity between adjacent members of the assemblage at the time of rock formation.

HIGH STRAIN ZONES

Name	Classification type	Definition[a]
Himalayan Sole Thrust	structural	structurally lowest throughgoing thrust
Main Frontal Thrust	structural	most frontal foreland-vergent thrust[b]
Main Boundary Thrust	structural plus stratigraphic	most frontal foreland-vergent thrust that carried pre-Cenozoic rocks in its hanging wall[c]
Main Central Thrust	structural plus stratigraphic	foreland-vergent thrust that juxtaposed Assemblage B against Indian Shield rocks; between the syntaxes these Indian Shield rocks are Assemblage A
South Tibet Detachment	structural plus metamorphic	(1) more than 10 km top-to-hinterland displacement and (2) juxtaposed high- and low-grade rocks (600 °C cutoff)
Indus-Yarlung Suture	structural plus stratigraphic	juxtaposed continental rocks formerly part of the Indian vs. a northern lithospheric plate

[a]The definition of each high strain zone additionally includes Cenozoic displacement.

[b]Excludes the high strain zones that bound the Shillong Plateau and Mikir Hills.

[c]Excludes the Himalayan Sole Thrust as well as the high strain zones that bound the Shillong Plateau and Mikir Hills.

ROCK UNITS DEFINED BY CENOZOIC OROGENIC EFFECTS

Name	Classification type	Definition
Sub-Himalayan Sequence	structural position	rocks located between the Main Frontal and Main Boundary thrusts
Lesser Himalayan Sequence	structural position	rocks located between the Main Boundary and Main Central thrusts
Greater Himalayan Sequence	structural position plus metamorphic	rocks located in the hanging wall of the MCT and high-grade (Cenozoic peak >600 °C)
Tethyan Himalayan Sequence	structural position plus metamorphic	rocks located in the hanging wall of the MCT and low-grade (Cenozoic peak ≤600 °C)

Table 3

Table 3: Triassic paleolatitude determinations for Himalayan Assemblage B

Location	Site current latitude (°N)	Site current longitude (°N)	Paleomagnetic pole latitude (°N)	Paleomagnetic pole longitude (°E)	A95 (°)	Site paleolatitude (°N)	Paleolatitude ± (°)	Reference
Kashmir	34.0	75.0	24.1[a]	126.7	8.7	-44.2	8.7	Klootwijk et al., 1983
Thakkhola	28.8	83.7	25.7[a]	294.0	5.7	-28.2	5.7	Klootwijk and Bingham, 1980
Thakkhola	28.8	83.7	26.0[a]	300.0	10.0	-25.1	10.0	Klootwijk and Bingham, 1980
Manang	28.7	84.0	22.2[a]	286.8	4.9	-34.6	4.9	Appel et al., 1991
Shiar (c. Nepal)	28.6	85.1	14.1[a]	256.3	10.8	-46.4	10.8	Schill et al., 2002
Tingri	28.6	86.0	-38.1	106.3	4.1	-20.6	4.1	Zou et al., 2013
Tingri	28.4	86.1	-37.6	112.1	2.9	-19.6	2.9	Zou et al., 2013
Tingri	28.5	86.2	-40.4	106.6	2.4	-18.5	2.4	Zou et al., 2013
Tingri	28.7	86.2	34.5	282.2	11.7	-25.0	11.7	Ran et al., 2012

[a]Paleomagnetic pole positions for these five sites taken from recalculated locations in van Hinsbergen et al. (2012).